HIGHWAY RESEARCH RECORD

Number 373

Design of Culverts, Energy Dissipators, and Filter Systems

8 Reports

Subject Areas

23 Highway Drainage
34 General Materials
63 Mechanics (Earth Mass)

HIGHWAY RESEARCH BOARD
DIVISION OF ENGINEERING NATIONAL RESEARCH COUNCIL
NATIONAL ACADEMY OF SCIENCES—NATIONAL ACADEMY OF ENGINEERING
WASHINGTON, D.C. 1971

ISBN 0-309-01987-7

Price: $3.60

Available from

Highway Research Board
National Academy of Sciences
2101 Constitution Avenue
Washington, D.C. 20418

CONTENTS

HYDRAULICS OF RIGID BOUNDARY BASINS

Frederick J. Watts and Daryl B. Simons 1

ANALYSIS OF RIGID OUTFALL BASINS WITH HIGH TAILWATER

Frederick J. Watts, Daryl B. Simons, and Michael A. Stevens 11

RIPRAPPED BASINS FOR CULVERT OUTFALLS

Michael A. Stevens, Daryl B. Simons, and Frederick J. Watts 24

DESIGN CRITERIA FOR CONTROLLED SCOUR AND ENERGY DISSIPATION AT CULVERT OUTLETS USING ROCK AND A SILL

Donald A. Thorson, Arunprakash M. Shirole, and Mansour Karim 39

EVALUATION OF THREE ENERGY DISSIPATORS FOR STORM DRAIN OUTLETS

John L. Grace, Jr., and Glenn A. Pickering 52

ROUGHNESS ELEMENTS AS ENERGY DISSIPATORS OF FREE-SURFACE FLOW IN CIRCULAR PIPES

James M. Wiggert, Paul D. Erfle, and Henry M. Morris 64

PERFORMANCE OF PLASTIC FILTER CLOTHS AS A REPLACEMENT FOR GRANULAR FILTER MATERIALS

Charles C. Calhoun, Jr., Joseph R. Compton, and William E. Strohm, Jr. 74

RESPONSE OF CORRUGATED STEEL PIPE TO EXTERNAL SOIL PRESSURES

Reynold K. Watkins and Alma P. Moser 86

Discussion

M. G. Spangler 96

Richard A. Parmelee 109

Authors' Closure 111

FOREWORD

The papers in this RECORD discuss energy dissipators at culvert outlets, use of roughness elements within a circular pipe to dissipate energy in free surface flow, use of plastic filter cloths to replace granular filter materials, and full-scale external load testing of buried corrugated steel pipes. The papers will be of interest to those concerned with erosion prevention at culvert and drain outlets, riprap protection of erodible soil, and loads on buried corrugated pipe.

The paper by Watts and Simons represents a study of the mechanics of flow in a rectangular basin with artificial roughness elements to induce a hydraulic jump. Both a circular and a rectangular culvert outfall were tested, and the invert of the culvert was placed high enough that the tailwater did not submerge the culvert outlet. The necessary coefficients were developed experimentally so that the designer is equipped to analyze a proposed basin and to have flexibility in his choice of dimensions.

The paper by Watts, Simons, and Stevens gives a method for the analysis and design of energy-dissipator basins at culvert outlets where high tailwater prevails. Sample designs, including one basin with low tailwater, are given.

The paper on riprapped basins by Stevens, Simons, and Watts gives a method for the design of rock-riprapped, energy-dissipator basins at culvert outfalls. Three types of basins were investigated: the nonscouring basin, the hybrid basin (slight scour but not enough to provide efficient dissipation), and the scoured basin. The scoured basin forms its own scour hole to dissipate energy, but the basin must be sized correctly because the mound of scoured riprap is an intergral part of the basin.

The paper by Thorson, Shirole, and Karim gives criteria for the design of rock-basin energy dissipators with or without a transverse sill. The study concludes that rock basin should have a width of at least 3 pipe diameters and divergence angles of 1:3 when no sill is used and 1:1.75 when a sill is used. Criteria permit design for no-scour or for controlled scour depth.

Grace and Pickering evaluate 3 energy dissipators: the stilling well, the Bureau of Reclamation impact dissipator, and the St. Anthony Falls dissipator. Charts are given to show the maximum recommended discharge that will result in good performance for given conditions. With these curves and other parameters, the designer can select the type of dissipator best suited to protect the outlet.

The paper by Wiggert, Erfle, and Morris tested the effect of peripheral roughness elements in a smooth circular pipe to dissipate energy in free surface flow. It was found that roughness elements of proper relative size and spacing and of square cross section will cause considerable reduction of exit velocity in pipes on steep slopes flowing partly full. The exit Froude number can be reduced to nearly unity. Gravel and silt were placed in the pipe barrel and were washed out by the flow. An 18-in. concrete pipe was used as a prototype to verify the model results.

The paper by Calhoun, Compton, and Strohn described an investigation of the performance of 8 plastic filter cloths used to replace granular filter materials under riprap and similar applications. Laboratory tests were conducted on 7 of the 8 cloths to determine their chemical and physical

properties and their filtering abilities. Information on uses and performance of filter cloths at Corps of Engineers projects is given.

The paper by Watkins and Moser presents the results of full-scale external load testing of buried corrugated steel pipe and gives the structural performance limits of the soil-pipe system. The 3 most important factors influencing performance were found to be the yield-point strength of the pipe wall, the soil compressibility determined primarily by soil density, and the ring flexibility of the pipe. A design graph is given that incorporates the empirical relationship of these 3 factors. Significant discussions by Spangler and Parmelee of test procedures and results are included.

—James R. Searcy

SPONSORSHIP OF THIS RECORD

GROUP 2—DESIGN AND CONSTRUCTION OF TRANSPORTATION FACILITIES
John L. Beaton, California Division of Highways, chairman

Committee on Surface Drainage of Highways
Lester A. Herr, Federal Highway Administration, chairman
Alvin G. Anderson, Harry H. Barnes, Jr., Mike Bealey, Allen L. Cox, Charles R. Edgerton, Kenneth S. Eff, Samuel V. Fox, Harry C. Green, John G. Hendrickson, Jr., Stifel W. Jens, Frank L. Johnson, Robert A. Norton, Byron Maurice Parker, Ralph M. Peterson, A. L. Pond, Jr., W. O. Ree, Brian M. Reich, James K. Searcy, Roy E. Smith, William P. Somers, F. W. Thorstenson, Adrianus Van Kampen, A. Mainard Wacker

Committee on Subsurface Structures Design
Kenneth S. Eff, U. S. Department of the Army, chairman
Roger L. Brockenbrough, T. F. deCapiteau, Paul D. Doubt, W. B. Drake, C. Raymond Hanes, Paul M. Heffern, John G. Hendrickson, Jr., L. R. Lawrence, F. Dwayne Nielson, Eric F. Nordlin, Richard A. Parmelee, A. J. Reed, M. G. Spangler, Robert S. Standley, Harold V. Swanson, James D. Washington, Reynold K. Watkins, Howard L. White

Committee on Subsurface Drainage
Glen L. Martin, Department of Civil Engineering and Engineering Mechanics, Montana State University, Bozeman, chairman
Reginald A. Barron, Mike Bealey, Paul J. Brudy, Harry R. Cedergren, Hsai-Yang Fang, Kenneth F. Ferrari, David S. Gedney, John G. Hendrickson, Jr., W. R. Lovering, Alfred W. Maner, Lyndon H. Moore, William B. Nern, Carl I. Olsen, Travis W. Smith, W. T. Spencer, R. S. Standley

Lawrence F. Spaine, Highway Research Board staff

The sponsoring committee is identified by a footnote on the first page of each report.

HYDRAULICS OF RIGID BOUNDARY BASINS

Frederick J. Watts, University of Idaho; and
Daryl B. Simons, Colorado State University

The mechanics of flow in a particular type of energy dissipator is investigated from a basic point of view. The dissipator uses artificial roughness elements to induce a hydraulic jump. A comprehensive test program was conducted to determine the energy and momentum coefficients and the drag coefficients necessary to analyze the basins analytically. The method outlined is general and allows the designer flexibility in his choice of dimensions. The test program included studies of flow from both circular and rectangular culvert outfalls. Discharges ranging from 6.75 to 23.5 ft^3/sec were investigated in a 1.45-ft diameter circular pipe and a 1.25- by 1.25-ft rectangular box.

•THIS PAPER presents a design procedure for a particular type of energy-dissipating basin at culvert outfalls. The basin features a simple geometrical design, readily adaptable to field construction methods. It utilizes roughness elements to induce a hydraulic jump that enhances the dissipation of energy. The necessary coefficients have been developed in an experimental program so that the designer is equipped to analyze a proposed basin by using fundamental hydraulic principles.

When tailwater submerges a culvert outlet section, the jet of water emerging from the conduit has the characteristics of a submerged jet. When low tailwater occurs and the conduit walls terminate abruptly but the floor continues at the same slope, the efflux has the characteristics of flow at an abrupt expansion. Most culverts function somewhere between these two extremes. This report is concerned with the case where the inverts of culverts are set so that flow at the outfall has the characteristics of flow at an abrupt expansion; i. e., the inverts are set sufficiently high so that the flow will plunge and spread in a predictable manner.

The basin investigated is shown in plan and section in Figure 1. It features an optional width and roughness elements of selected height and spacing.

The basic equations used in the analysis are the continuity equation and momentum equation with an appropriate drag term. The procedure requires the use of the following design aids developed during this study: momentum equation correction coefficients for nonhydrostatic pressure and nonuniform distribution of velocity at the outfall section; dimensionless water surface contours and relative velocities for the rapidly varied flow region downstream of the outfall; and suitable drag coefficients for a particular size and grouping of roughness elements placed on the floor of the basin.

In the interest of brevity, only one each of the design aids and only a brief description of the experimental programs required to develop the design aids are presented. The number of references cited is also limited by length considerations. The notation used is given at the end of the paper.

METHOD OF ANALYSIS

Basic Equations

With reference to Figure 1, the momentum equation written in the direction of flow for the control volume between station 0.0 and station B is

$$\beta_2\rho V_o Q + \beta_1\gamma(y_o^2/2)W_o = F_T + F_R + \beta_4\rho V_2 Q + \beta_3\gamma(y_2^2/2)W_2 \qquad (1)$$

Sponsored by Committee on Surface Drainage of Highways and presented at the 50th Annual Meeting.

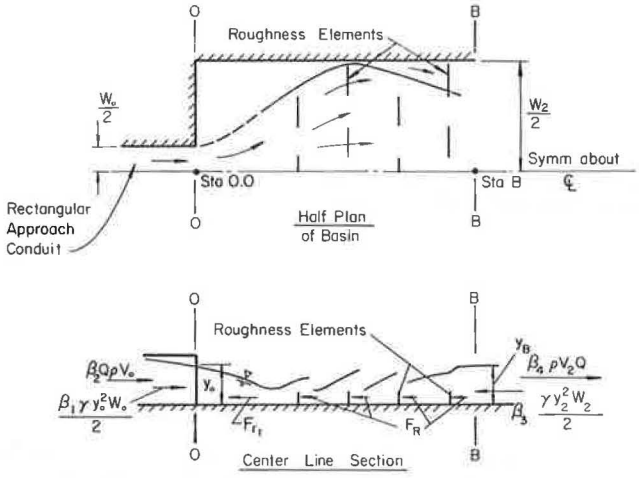

Figure 1. Energy-dissipating basin.

The drag force F_R is defined as

$$F_R = C_D A_F N \rho(V_a^2/2) \tag{2}$$

V_a is the approach velocity at the first row of roughness elements, defined as the average velocity 2 pipe diameters downstream of the outlet. F_T, the shear force exerted by the floor on the flow in the area upstream of the roughness elements and downstream of the outlet, is small and henceforth is included in the F_R term.

Making use of the continuity equation, we obtain

$$y_2 = Q/V_2W_2 \tag{3}$$

Inserting the value of y_2 and F_R (Eq. 2) into Eq. 1 and assuming $\beta_3 = \beta_4 = 1$ yield the following relationship

$$\beta_2\rho V_oQ + \beta_1\gamma(y_o^2/2)\,W_o = C_D A_F N \rho(V_a^2/2) + \rho Q V_2 + (\gamma Q^2/2V_2^2W_2) \tag{4}$$

This is the design equation. For a given discharge, depth of flow at the outfall section, approach pipe width, β_1, β_2, a particular set of roughness elements, C_D, and V_a, and estimate of V_2 the exit velocity from the basin is readily obtained.

The following sections describe the experimental program conducted for the purpose of developing design aids that provide suitable values of β_1, β_2, V_a, and C_D.

ENERGY AND MOMENTUM CORRECTION FACTORS

Theoretical Development

At any cross section, the amount of energy per pound of water at any point is

$$H = \alpha_1[(P/\gamma) + y] + \alpha_2(V^2/2g) \tag{5}$$

Where nonuniform steady-flow conditions prevail, it is convenient to evaluate the power of the flow at a section by multiplying the quantity of energy per pound of water by the number of pounds of water per second that pass through the incremental area surrounding the point; i. e.,

$$\Delta P_T = \{[(P/\gamma) + y] + (V^2/2g)\}\,\gamma\Delta Q \tag{6}$$

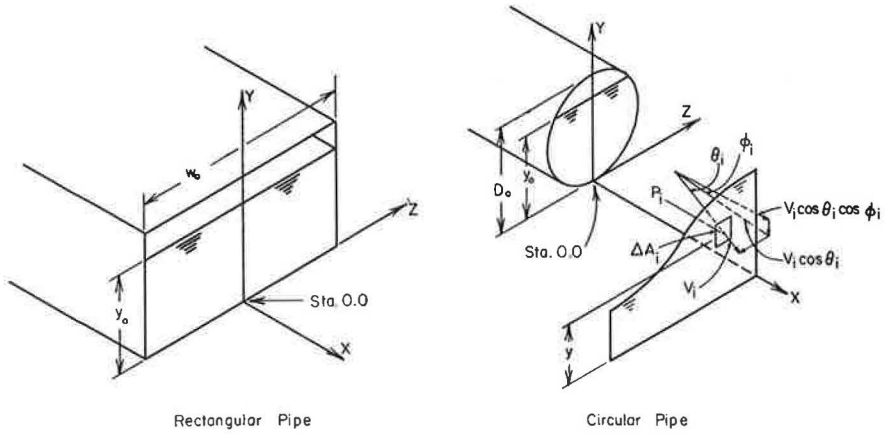

Figure 2. Outfall definition.

Referring to Figure 2, we have

$$\Delta Q_i = V_i \cos\theta_i \cos\phi_i \Delta A_i \tag{7}$$

At any cross section, the total power available is

$$P_T = \sum_i \{[(P/\gamma) + y]_i + (V_i^2/2g)\} \gamma V_i \cos\theta_i \cos\phi_i \Delta A_i \tag{8}$$

where the sum is taken over the entire section in question.

The specific energy equation that is the most convenient is made up of gross flow quantities.

$$H = \alpha_1 y + \alpha_2 [(Q/A)^2/2g] \tag{9}$$

This is converted to power by multiplying H by γQ.

$$P_T = HQ\gamma = \{\alpha_1 y + \alpha_2 [(Q/A)^2/2g]\} \gamma Q \tag{10}$$

Equating Eqs. 8 and 10 yields

$$\sum_i \{[(P/\gamma) + y]_i + (V_i^2/2g)\} (\gamma V_i \cos\theta_i \cos\phi_i) \Delta A_i = \{\alpha_1 y + \alpha_2 [(Q/A)^2/2g]\} \gamma Q \tag{11}$$

Canceling out γ, equating the like terms from each side, and solving for α_1 and α_2, we obtain

$$\alpha_1 = \frac{\sum_i \{[(P/\gamma) + y]_i (V_i \cos\theta_i \cos\phi_i \Delta A_i)\}}{yQ} \tag{12}$$

and

$$\alpha_2 = \frac{\sum_i (V_i^3 \cos\theta_i \cos\phi_i \Delta A_i)}{Q^3/A^2} \tag{13}$$

Utilizing the impulse and momentum principle and similar reasoning, we can show in differential form that the external force and momentum flux at any cross section in the x-direction are

$$F = \sum_i P_i \, \Delta A_i + \sum_i \rho V_i^2 \cos^2\theta_i \cos^2\phi_i \, \Delta A_i \tag{14}$$

The convenient expression for momentum and pressure force in terms of gross flow quantities is

$$F = \beta_1 (\gamma y^2 W/2) + \beta_2 Q \rho V \tag{15}$$

Equating Eqs. 14 and 15 and sorting out similar terms easily shows that

$$\beta_1 = \sum_i P_i \Delta A_i / [\gamma (yA/2)] \tag{16}$$

and

$$\beta_2 = \frac{\sum_i (V_i^2 \cos^2\theta_i \cos^2\phi_i \, \Delta A_i)}{Q^2/A} \tag{17}$$

where A = wetted area at the outfall section for either circular or rectangular conduits.

Equations 8 and 14 are general. There are no limiting assumptions; i. e., if the quantities can be measured precisely and if the incremental areas are taken small enough so that the summation is a good approximation of the integral, the quantities are correct for that particular cross section.

The procedure used to evaluate these quantities was to divide each cross section into a grid; measure the velocity, total head, and elevation at the centroid of each incremental area; deduce the pressure at the centroid by subtracting the sum of the velocity head and elevation head from the measured total head; and perform the various summations. Yaw and pitch probes were used in combination to obtain the yaw (horizontal) angle and pitch (vertical) angle of the velocity vector simultaneously with the measurements of total head and velocity magnitude at each grid point. The measured data were used to evaluate Eqs. 12, 13, 16, and 17. (Basic data are not presented in this paper but can be obtained at cost from Colorado State University.)

Sufficient data were also gathered at downstream sections for the purpose of plotting dimensionless water surface contours and relative velocities.

Test Facility

A rectangular basin with a horizontal aluminum floor 10 ft wide by 14 ft long with 1-ft vertical walls was positioned symmetrically downstream of a 20-ft length of approach pipe. The entire assembly was constructed within a large (185 ft long by 20 ft wide by 8 ft deep) outdoor flume. Data were collected for 2 approach pipes: a 1.45-ft diameter circular pipe and a 1.25- by 1.25-ft rectangular box. Both culverts had smooth walls. The pipe invert was horizontal and was carefully matched to the top surface of the basin floor. A rectangular, sharp-crested weir at the lower end of the large flume was used to check the discharges that were obtained by integration of experimental data. Tailwater effects from the weir were avoided by installing the floor of the test basin 2 ft above the concrete floor of the large flume. A variable-height dam for the purpose of tailwater control was constructed 35 ft downstream of the pipe outlet. The crest of the dam was maintained at the elevation of the top surface of the basin floor for all runs.

The measuring probes and supporting equipment were mounted on a large instrument carriage spanning the large flume.

Test Program and Range of Parameters

Seven discharges varying from 9.77 to 23.5 ft^3/sec were examined for the 1.45-ft circular approach pipe. The relative depth ratio y_o/D_o ranged from 0.75 to 1.00. The parameter $Q/D_o^{5/2}$ varied from 3.87 to 9.28. This encompasses the usual range of these parameters in highway culvert operation. Velocity data were taken at stations 0.0 and 2.9, and water surface contours were obtained at stations 0.0, 1.45, 2.9, and 4.35. In this paper, the station number indicates the distance downstream from the outfall section.

For the rectangular approach pipe, 6 discharges varying from 6.75 to 21.3 ft^3/sec were examined. The relative depth ratio y_o/W_o (depth of flow divided by pipe width) ranged from 0.61 to 0.94, and the Froude number $V_o/\sqrt{gy_o}$ varied from 1.44 to 2.35, the usual range of culvert operation. Velocity and water surface data were collected at stations 0.0, 2.5, 5.0, and 10.0.

Energy and momentum coefficients for circular and rectangular outfall sections are shown in Figures 3 and 4. One typical plot of dimensionless water surface contours and relative velocities is shown in Figure 5. Measurement apparatus, measuring procedures, analysis of data, and additional plots for the range of Froude numbers and relative depths mentioned earlier are included in other reports (5, 6, 7).

COEFFICIENTS OF DRAG

Problem Analysis

It has been shown by previous studies (2, 3, 4) that, for both supercritical and subcritical flow, an important correlating parameter with respect to the drag exerted by a roughness element on the flow is the relative depth, y/a, the ratio of the depth of flow striking the element to the height of the element. In the energy-dissipating basin where the water is diverted upward by the element, it is obvious that, up to a limiting point at least, the deeper the flow over the element is, the larger the quantity of water disturbed by the element will be and, consequently, the larger the apparent coefficient of drag will be.

The depth of flow at a point 2 pipe diameters downstream of the outlet (the approximate location of the first row of elements) was chosen as the scaling length y. For design purposes, this length is readily obtained from an appropriate plot of dimensionless water surface contours (Fig. 5 shows an example). Because the width of the expanding jet is not controlled by the walls at this point (station 2 D_o), this height is significant for a basin of any width when only the first 2 rows of elements are considered. This is not the case for the remaining rows of elements; i. e., the wider the basin is, the shallower the flow for a given discharge will be. For this reason, an additional correlating factor W_2/W_o, the basin width divided by the conduit width, is necessary.

The longitudinal spacing of the elements, J, is significant. Because of the complexity of the flow, it does not appear practical to include this factor as a density term. Instead, the ratio J/a is included as a geometric ratio and accompanies each design curve.

The lateral spacing of the element, 2M, is not considered critical. The important point is that the elements in each row occupy half the width of the channel and that the elements be staggered in successive rows. This ensures that there will be no smooth longitudinal corridors through the basin. In order that the elements will serrate the flow and not act as a long sill, it is recommended that the ratio M/a be restricted to a range of 2 to 8.

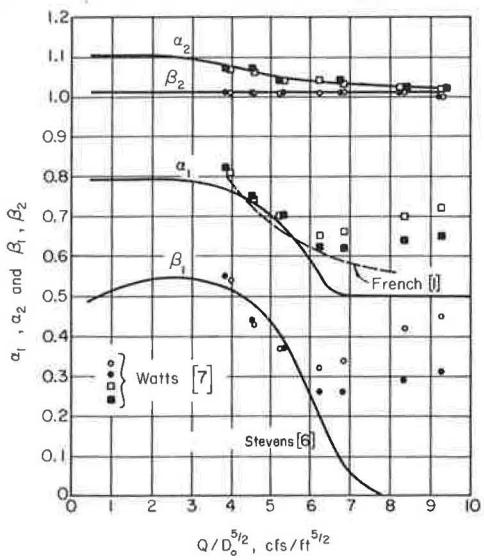

Figure 3. Energy and momentum coefficients for circular approach pipe.

Experimental Procedure for Obtaining Coefficients of Drag

Equation 4 with slight modification was used to evaluate C_D. The procedure was as follows:

1. A basin of known dimensions and pattern of roughness elements was subjected to a specific discharge;

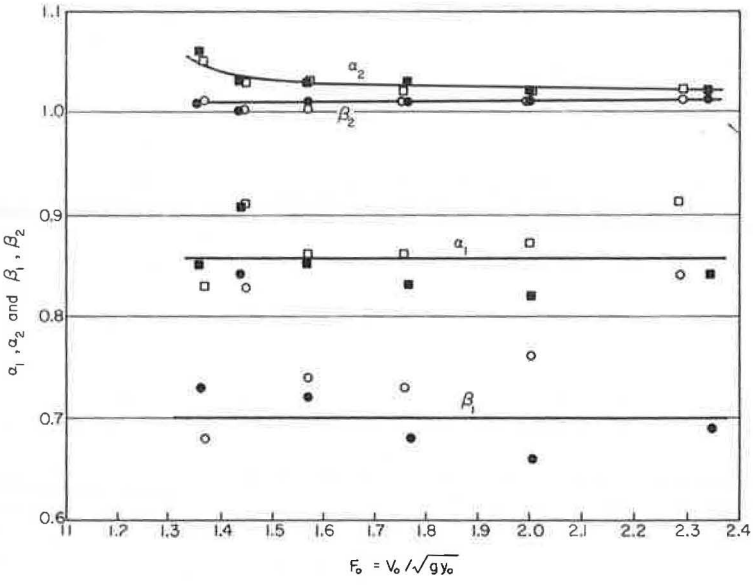

Figure 4. Energy and momentum coefficients for rectangular approach pipe.

2. At a section downstream of the last row of roughness elements, the yaw probe was used to measure the flow quantities, velocity, and pressure;

3. Equation 14 and the measured quantities from step 2 were used to evaluate the quantity $\sum_i P_1 \Delta A_1 + \sum_i \rho V_1^2 \cos^2\theta_1 \cos^2\phi_1 \Delta A_1$, which is equal to $\beta_4 \rho V_2 Q + (\beta_3 \gamma Q^2 / 2 V_2^2 W_2)$;

4. The terms $\beta_2 \rho V_o Q + \beta_1 \gamma (y_o^2/2) W_o$ were evaluated (the necessary information was available from the study of flow properties at station 0.0, previously described);

5. The quantity obtained in step 3 was subtracted from the quantity obtained in step 4, and the remaining quantity is the drag force exerted by the group of elements on the flow, F_R;

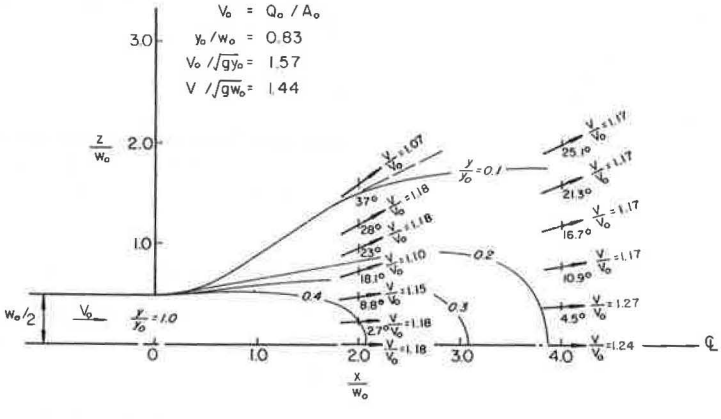

Figure 5. Dimensionless water surface contours and relative velocities for rectangular outfalls.

6. When F_R was known, Eq. 2 was solved for C_D; and
7. C_D was plotted as a function of Y/a, J/a, and W_2/W_o for a particular basin configuration.

Test Program for Evaluating Coefficients of Drag

Fifty-four runs were made to evaluate C_D. For the primary tests, 12 basin and element arrangements were examined. Each basin was subjected to 2 discharges. The lower discharge was approximately the design discharge (based on Wyoming State Highway Department specifications) for the approach pipe. The higher discharge was approximately 50 percent larger.

Two heights of elements were used for each discharge: a = 1¼ in. and a = 2¼ in. A variation of relative depth, y/a, from 1.1 to 2.7 resulted from the combination of 2 discharges and 2 element heights.

One pattern of longitudinal and lateral spacing was used for all runs. With 2 element heights, a two-fold variation of J/a, 6.0 and 12.0, was obtained.

For the 1.25-ft rectangular approach pipe, 2 basin widths, W_2 = 5 ft and W_2 = 10 ft, were tested. One width of basin, W_2 = 10 ft, was used with the 1.45-ft diameter circular approach pipe.

In addition to the primary runs described, 6 special runs were made. The circular approach pipe and 10-ft wide basin were used with two patterns of 4- by 1-in. elements. The significant difference between these basins and those used for the primary runs was the size of the elements. The 4-in. elements were spaced on 18-in. centers laterally; thus, large gaps existed between the elements. As expected, high-speed cores of water were measured downstream of the field of elements. The coefficient of drag deduced for the small, widely spaced elements was somewhat larger than comparable coefficients of drag for the elements 9 in. long. However, because of the probability of high-speed cores of water downstream of the basin, elements spaced laterally at more than twice their length are not recommended.

The 10- by 14-ft basin previously described, with a horizontal aluminum floor, tapped and threaded to accommodate roughness elements anchor bolts, was used for all experiments. False walls were installed for the 5-ft wide basins.

Data from 12 of the runs are shown in Figure 6. Similar figures for other combinations of roughness elements and for basins downstream of circular conduits are presented in other reports (5, 6, 7).

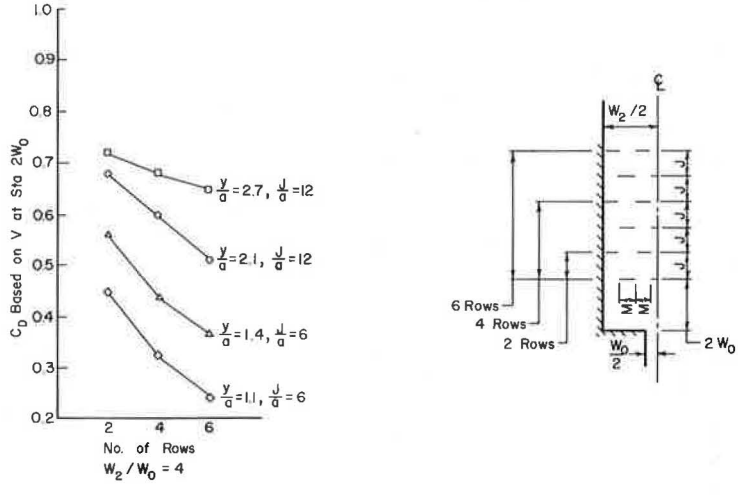

Figure 6. Coefficients of drag for roughness elements in rectangular approach pipe.

BASIN ANALYSIS

The design procedure and use of design aids are most readily explained by the solution of practical problem. A 6- by 6-ft culvert is used as an example, where $Q = 420$ ft^3/sec, $W_o = 6$ ft, and $y_o = 4$ ft. The designer's choice is $W_2/W_o = 4$, $y/a = 1.1$, and 6 rows of elements. Working with one-half of the basin, we have $W_2/W_o = 4$; $W_2 = W_o^4 = (6)(4) = 24$ ft; $Q/2 = 210$ ft^3/sec; $y_o = 4$ ft; $W_o/2 = 3$ ft; $V_o = (Q/2)/\text{area} = 210/[(W_o/2)(y_o)] = 210/[(3)(4)] = 17.5$ ft^3/sec; and $F_o(V_o/\sqrt{gy_o}) = 17.5/\sqrt{(32.2)(4)} = 1.54$.

As shown in Figure 4, $\beta_1 = 0.71$ and $\beta_2 = 1.01$.

The estimate from Figure 5 is $y/y_o = 0.21$; and $y = y_o(0.21) = (4)(0.21) = 0.84$ ft at $x/W_o = 2$, $V_a/V_o = 1.18$, and $V_a = (1.18)V_o = (1.18)(17.5) = 20.6$ ft^3/sec.

The height of element a is obtained by using $y = 0.84$, and $y/a = 1.1$ (designer's choice); therefore, $a = 0.76$ ft or use 0.75 ft.

The length of element m, as shown in Figure 6, is $(W_2/2)/3\frac{1}{2}$ spaces = 3.43 ft. Area of element a = (M)(a) = (3.43) (0.75) = 2.57 sq ft.

The longitudinal spacing of element J, as shown in Figure 6 for $y/a = 1.1$, is $J/a = 6.0$ or $J = (6.0)(0.75) = 4$ ft.

The number of elements N shown in Figure 6 is 10.5.

$C_D = 0.23$ for 6 rows of elements and $y/a = 1.1$ (Fig. 6).

Velocity at outfall of basin V_2 is estimated by using design Eq. 4.

$$\beta_1\gamma(y_o^2/2)(W_o/2) + \beta_2\rho V_o(Q/2) = C_D N A_F \rho (V_a^2/2) + \rho(Q/2)V_2 + [\gamma(Q/2)^2]/(2V_2^2W_2/2)$$

$\gamma = 62.4$ lb/ft^3; $C_D = 0.23$; $\beta_3 = 1$; $V_o = 17.5$ ft^3/sec; $\rho = 1.94$ lb-sec^2/ft^4; $\beta_1 = 0.71$; $\beta_4 = 1$; $y_o = 4$ ft; $\beta_2 = 1.01$; $w_o = 6$ ft; $V_a = 20.6$ ft^3/sec; $W_2 = 24$ ft; and $Q = 420$ ft^3/sec. All values in the equation have been determined except V_2, the unknown. Substituting known values into the equation,

$$(0.71)(62.4)(4^2/2)(6/2) + (1.01)(1.94)(17.5)(210) = (0.23)(10.5)(2.57)(1.94)(20.6^2/2) + (1.94)(210)V_2 + (62.4/2)\{210^2/[V_2^2(24/2)]\}$$

and solving for V_2, we obtain

$$407\,V_2 + (114{,}600/V_2^2) = 5{,}710$$

These are three possible values of V_2: one value is negative and meaningless, and the other two are significant. The lower value is associated with subcritical flow, and the higher value is the conjugate velocity. When the preceding equation is solved, V_2 subcritical = 5.9 ft^3/sec and V_2 supercritical = 12.1 ft^3/sec. The depths of flow at the outfall corresponding to these velocities are $y_2 = (Q/2)/[(W_2/2)V_2]$; y_2 subcritical = $210/[(12)(5.9)] = 3.0$ ft; and y_2 supercritical = $210/[(12)(12.1)] = 1.4$ ft.

If tailwater is less than 1.4 ft, flow will be supercritical and the outfall velocity will be about 12.1 ft^3/sec. If the tailwater is 3.0 ft or higher (it is difficult to imagine a natural channel carrying 420 ft^3/sec at a depth less than this), the exit velocity will be about 5.9 ft^3/sec or less.

If the exit velocity and depths are satisfactory, the basin dimensions are as follows: length = $2W_o + 5J + 1J$ (add J downstream of last row of elements) = (2)(6) + (5)(4) + 4 = 36 ft; width = $(4)(W_o) = (4)(6) = 24$ ft; height of basin walls = y_2 subcritical + freeboard = 3.0 + 1.5 = 4.5 ft; size of element: 0.75 × 3.43; number required: 2 × 10.5 = 21; longitudinal spacing of elements J = 4 ft; and lateral spacing of elements 2M = 6.8 ft.

If V_2 deduced from Eq. 4 is close to critical velocity (this was not the case in the example solved in the preceding) and the tailwater depth downstream of the basin is, coincidentally, near critical depth, an unstable water surface (such as standing waves) is probable. If tailwater depth is near critical, the basin should be redesigned in such a way as to ensure adequate depth. Widening the basin or lowering the downstream portion of the basin are 2 effective means of attaining a suitable depth.

Further explanation of the design procedure and the application to other types of energy basins and a more complete description of the experiments used to develop the design aids are given in other reports (5, 6, 7).

CONCLUSIONS

A method of design for artificially roughened energy basins at culvert outfalls is presented. The momentum and continuity equation used in conjunction with experimentally derived design aids can be used to predict approximate exit velocity from the basin. The procedure is general and is readily applicable to other energy-dissipating structures.

NOTATION

The following notation is used in this paper:

a = height of roughness element, ft;
A = area of wetted cross section, ft^2;
A_F = frontal area of a roughness element, ft^2;
C_D = drag coefficient of roughness element, dimensionless;
D_o = diameter of circular approach pipe, ft;
F = force, lb;
F_R = drag force exerted by roughness elements on the flow, lb;
F_T = shear force exerted by the floor on the flow, lb;
g = acceleration of gravity, ft/sec^2;
H = total energy, ft-lb/lb;
J = longitudinal spacing of roughness elements, ft;
M = width of roughness element, ft;
N = number of elements;
P = pressure intensity at a point, lb/ft^2;
P_T = power, ft-lb/sec;
Q = discharge, ft^3/sec;
V = velocity, ft/sec;
V_a = approach velocity at the first row of roughness elements defined as the average velocity 2-pipe diameters downstream of the outlet, ft/sec;
V_o = average velocity at outfall section, ft/sec;
V_2 = average velocity at section B, ft/sec;
W = width of section, ft;
W_o = width of outfall, ft;
W_2 = width of channel at section B, ft;
x = longitudinal coordinate measured from the outlet section, ft;
y = vertical distance above a datum or depth of flow, ft;
y_o = depth of flow at outfall section, ft;
y_2 = average depth of flow at section B, ft;
z = lateral coordinate measured from the longitudinal centerline, ft;
α_1 = corrective coefficient (energy equation) for nonhydrostatic distribution of pressure, dimensionless;
α_2 = corrective coefficient (energy equation) for nonuniform distribution of velocity, dimensionless;
β_1 = corrective coefficient (momentum equation) for nonhydrostatic distribution of pressure at section 0, dimensionless;
β_2 = corrective coefficient (momentum equation) for nonuniform distribution of velocity at section 0, dimensionless;
β_3 = corrective coefficient (momentum equation) for nonhydrostatic distribution of pressure at section B, dimensionless;
β_4 = corrective coefficient (momentum equation) for nonuniform distribution of velocity at section B, dimensionless;
γ = specific weight of fluid, lb/ft^3; and
ρ = mass density of fluid, $lb\text{-}sec^2/ft^4$.

ACKNOWLEDGMENTS

We are indebted to the Wyoming State Highway Department and the Engineering Experiment Station at Colorado State University, joint sponsors of this project.

REFERENCES

1. French, J. L. Second Progress Report on Hydraulics of Culverts—Pressure and Resistance Characteristics of a Model Pipe Culvert. National Bureau of Standards, U.S. Department of Commerce, No. 4911, Oct. 1956.
2. Herbich, J. B., and Shulits, S. Large-Scale Roughness in Open-Channel Flow. Jour. Hydraulics Div., Proc. ASCE, No. HY6, Paper 4145, Nov. 1964, pp. 203-229.
3. Koloseus, H. J., and Davidian, J. Free-Surface Instability Correlations and Roughness-Concentration Effects on Flow Over Rough Surfaces. U.S. Govt. Printing Office, Washington, D.C., Geological Survey Water Supply Paper 1592-C, D, 1966.
4. Sayre, W. W., and Albertson, M. L. Roughness Spacing in Rigid Open Channels. ASCE Trans., Vol. 128, Part 1, Paper 3417, 1963, pp. 343-372.
5. Simons, D. B., Stevens, M. A., and Watts, F. J. Flood Protection at Culvert Outlets. Colorado State Univ., Fort Collins, Publ. CER 69-70 DBS-MAS-FJW4, 1970.
6. Stevens, M. A. Momentum and Energy Coefficients for the Zero Tailwater Case. Eng. Research Center, Colorado State Univ., Fort Collins, unpublished paper, 1969.
7. Watts, F. J. Hydraulics of Rigid Boundary Basins. Colorado State Univ., Fort Collins, PhD dissertation, 1968.

ANALYSIS OF RIGID OUTFALL BASINS WITH HIGH TAILWATER

Frederick J. Watts, University of Idaho; and
Daryl B. Simons and Michael A. Stevens, Colorado State University

Diffusion characteristics of jets from circular pipes discharging into basins lined with stones were measured under conditions of tailwater either slightly above or slightly below the crown of the pipes. These data together with data from a previous study on culvert outlet protection and with data from orifice jet diffusion studies by others are incorporated into a method for designing stable energy-dissipating basins at culvert outlets where high tailwater exists.

•HIGH TAILWATER is defined as the condition where the water surrounding the high-speed, jet-like core of water discharging from the culvert outlet is as high as or higher than the elevation of the crown of the pipe. This situation occurs at culvert outlets where downstream channel constrictions create backwater or where the culvert discharges into a narrow, low-gradient channel with high banks and a large normal depth.

Unknowns that confront the engineer faced with the problem of designing a stable energy-dissipating basin where high tailwater conditions prevail are the rate of decay of the high-speed velocity core, the rate of lateral expansion of the core, and the probability of the core being diverted off to one side, thus imperiling the banks.

The problem of 2- and 3-dimensional jets discharging into a large volume of quiescent ambient fluid has been studied in detail (1, 2, 3). The purpose of this study was to determine the diffusion characteristics of a jet bounded on the top by a free surface and on the bottom by a rough (rock-lined) essentially rigid boundary. Data obtained during this study correlated well with data presented in another report (1) for the 3-dimensional orifice flow field. The remainder of this report describes the tests conducted and the data collected, presents a comparison of these data with results presented elaswhere (1, 2, 3), and illustrates the application of these results to the solution of practical problems.

EXPERIMENTAL APPARATUS AND PROCEDURE

Three arrangements of culvert and basin configurations were examined. All basins were constructed within a large 185 ft by 20 ft by 8 ft deep outdoor flume equipped with a movable overhead instrument carriage. A smooth circular approach pipe, 1.45 ft in diameter, was used for runs F44 and F45. The basin was approximately 25 ft long with a horizontal floor 6 ft wide and side berms 1 ft high parallel to the centerline and sloping 1 on 2. This condition allowed bank over flow. The basin was constructed of river-rounded rock ranging in size from 4 to 10 in. in diameter with a D_{50} of 7 in. The floor of the basin was placed at approximately the elevation of the pipe invert.

Measurements were taken at 2 discharges: 22.5 ft^3/sec for run F44 and 14.6 ft^3/sec for run F45. The water surface in the basin was maintained about 1.57 ft above the pipe invert; i.e., the crown of the pipe was about 0.12 ft below the average water surface.

Velocity profiles were measured along the centerline of the basin at stations 0.0, 5.0, 10.0, and 20.0. Station number indicates the distance in feet downstream of the culvert outlet. Additional velocity measurements were obtained at stations 15 and 20 for the purpose of constructing isovel plots. This information is shown in Figures 1 and 2.

Sponsored by Committee on Surface Drainage of Highways.

Point velocities were measured with an Ott minor meter. A reliable mean value was obtained by sampling each point for a period of 50 sec. The meter, supported on a point gage, was mounted horizontally with the axis parallel to the longitudinal centerline of the basin. In all runs, the basin was slowly filled to the specified height; the flow was then increased until the desired discharge was obtained.

For runs G56 and G57, a 3-ft diameter smooth pipe was used. The basin was 35 ft long and 20 ft wide with parallel vertical walls 6 ft high. The bed of the basin was constructed with the same rounded rock material as was used for runs F44 and F45. The discharges tested were 65.4 ft^3/sec in run G56 and 84.0 ft^3/sec in run G57. The water surface was maintained at a level 3.05 ft above the pipe invert. A centerline velocity profile was obtained at the outlet, station 0.0. Sufficient velocity data were taken at stations 5.0, 10.0, 15.0, 20.0, and 25.0 to construct the isovel plots shown in Figures 3 and 4.

For runs K70 (20.9 ft^3/sec) and K71 (13.9 ft^3/sec), the 1.45-ft diameter smooth steel approach pipe was used. The basin berms were removed, and the floor was lowered approximately 0.3 ft below the invert. The horizontal floor of the basin was 20 ft wide and 35 ft long, with parallel vertical walls. The rounded material used to construct the basin was much smaller than that used for the previous 4 runs. The D_{50} was slightly under 5 in. with a D_{max} of 7 in.; i.e., the D_{50} rock in this series weighed about one-fourth as much as the rock used for the previous series.

Instead of the tailwater being held at crown elevation or higher as had been the case for the previous runs, the surface was maintained at an elevation approximately 0.2 ft below the crown of the pipe. Velocities were measured at stations 2.5, 5.0, 7.5, 10.0, 12.5, and 15.0, and for run K71 at station 20.0. During run K70, deposition downstream of the scoured region distorted the flow field and, therefore, measurements were not completed at station 20.0. The information collected is shown in Figures 5 and 6.

PRESENTATION OF DATA

Figures 1 through 6 show data collected for the 6 runs. All plots are to scale, with the appropriate scales appearing on the drawings. A section along the longitudinal centerline of the basin is shown on the upper portion of each figure. The water surface elevation, centerline profile of the bed, and the vertical distribution of velocity at the centerline are shown for the various sections. Plots of isovels were constructed from the measured data. The small filled circles indicate points where measurements were taken. The large dotted circle shows the position of the approach pipe relative to the section. The velocity profile in a horizontal plane at an elevation D/2 above the pipe invert is plotted as a solid line directly above each isovel section. The theoretical velocity profile based on the mean exit velocity and the approach pipe diameter is shown as a dashed line. This profile was computed by using data shown in Figures 9 and 10 and the measured mean velocities at each station. Three facts are apparent from the various plots.

1. Lowering the tailwater only one-seventh of the approach pipe diameter allowed the jet to plunge in such a manner as to cause significant scour. How much of this scour resulted from the plunging effect and how much resulted because of the smaller rock are not known; however, the slope of the water surface indicated the jet was directed toward the floor.
2. Where the jet discharged into the low tailwater basin, the location of the core of maximum velocity is at the surface, whereas the location is at mid-depth or lower for the high tailwater basins.
3. The theoretically predicted velocity profiles are in good agreement with measured values for both tailwater conditions. Thus it is apparent that data shown in Figures 9 and 10 used in conjunction with those shown in Figure 8 are adequate criteria for computing transverse velocity distribution.

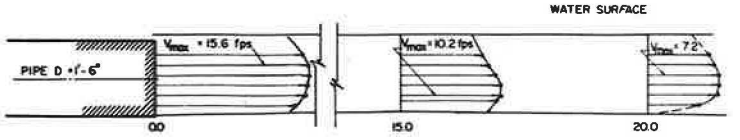

CENTER LINE VELOCITY PROFILES

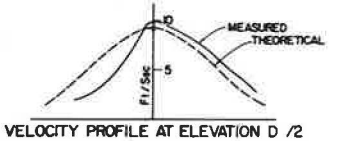

VELOCITY PROFILE AT ELEVATION D /2

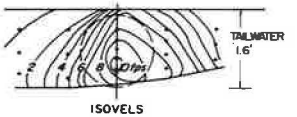

ISOVELS
STATION 15.0 ft.

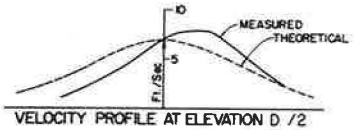

VELOCITY PROFILE AT ELEVATION D /2

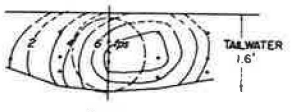

ISOVELS
STATION 20.0 ft.

Q = 22.5 cfs
TAIL WATER — 1.57 ft
PIPE DIAMETER — 1.45 ft.
D_{50} OF ROCK — .7 in.
FLAT BED – 6 ft. BOTTOM- 2:1 BERMS
RUN F44

Figure 1. Centerline velocity profiles, isovels, and transverse velocity profiles for run F44.

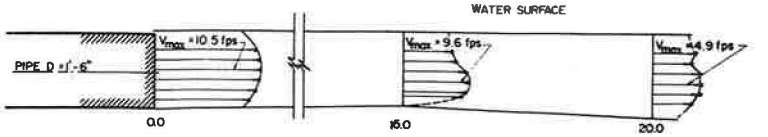

CENTER LINE VELOCITY PROFILES

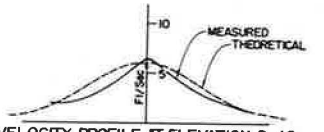

VELOCITY PROFILE AT ELEVATION D / 2

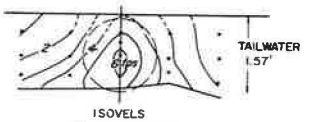

ISOVELS
STATION 15.0 ft.

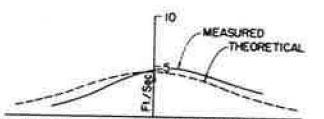

VELOCITY PROFILE AT ELEVATION D /2

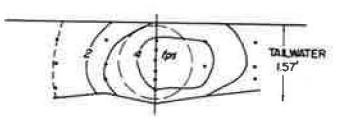

ISOVELS
STATION 20.0 ft.

Q = 14.6 cfs
TAIL WATER --- 1.57 ft.
PIPE DIAMETER — 1.45 ft.
D_{50} OF ROCK — 7 in.
FLAT BED – 6 ft. BOTTOM - 2:1 BERMS
RUN F45

Figure 2. Centerline velocity profiles, isovels, and transverse velocity profiles for run F45.

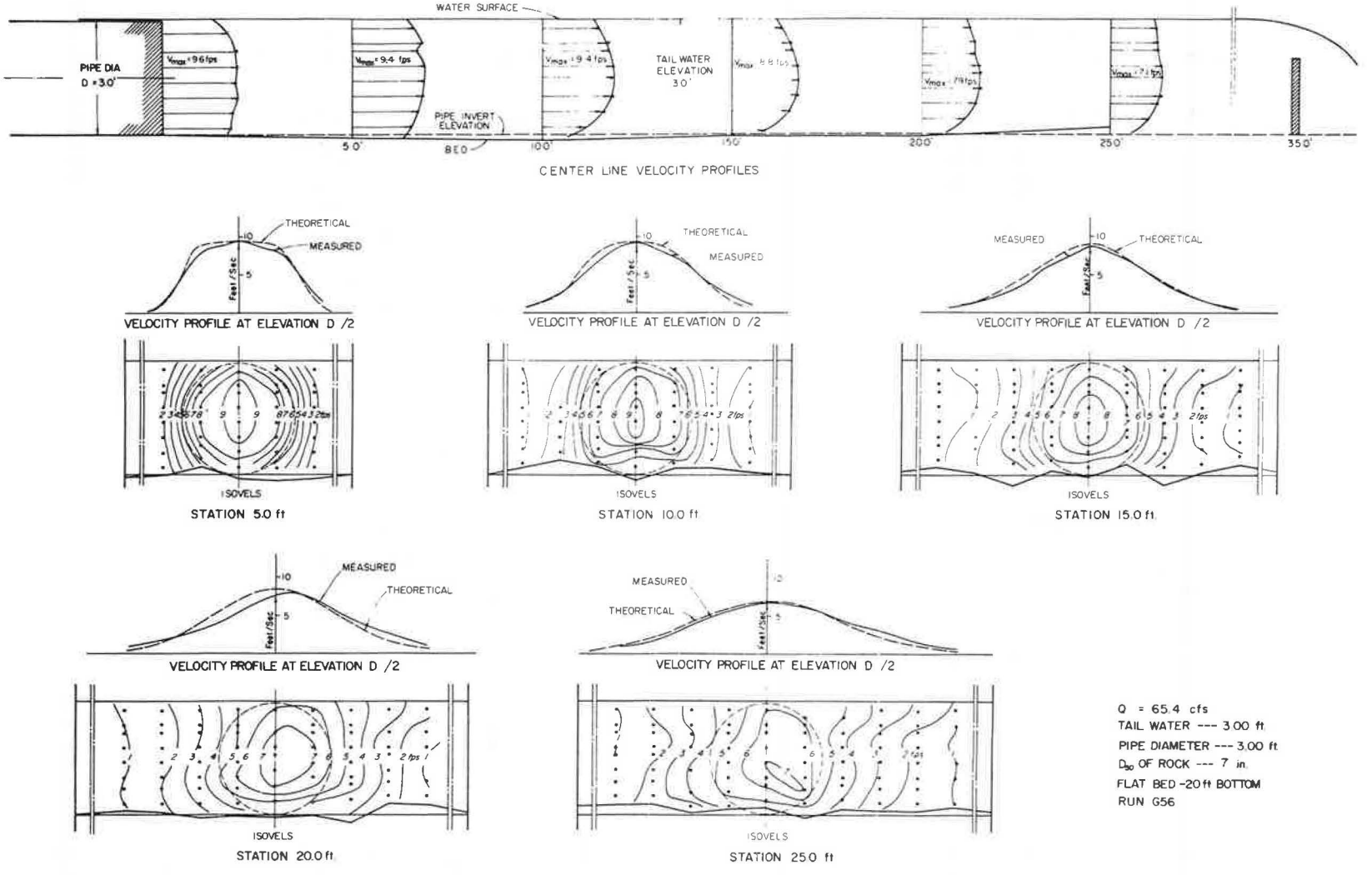

Figure 3. Centerline velocity profiles, isovels, and transverse velocity profiles for run G56.

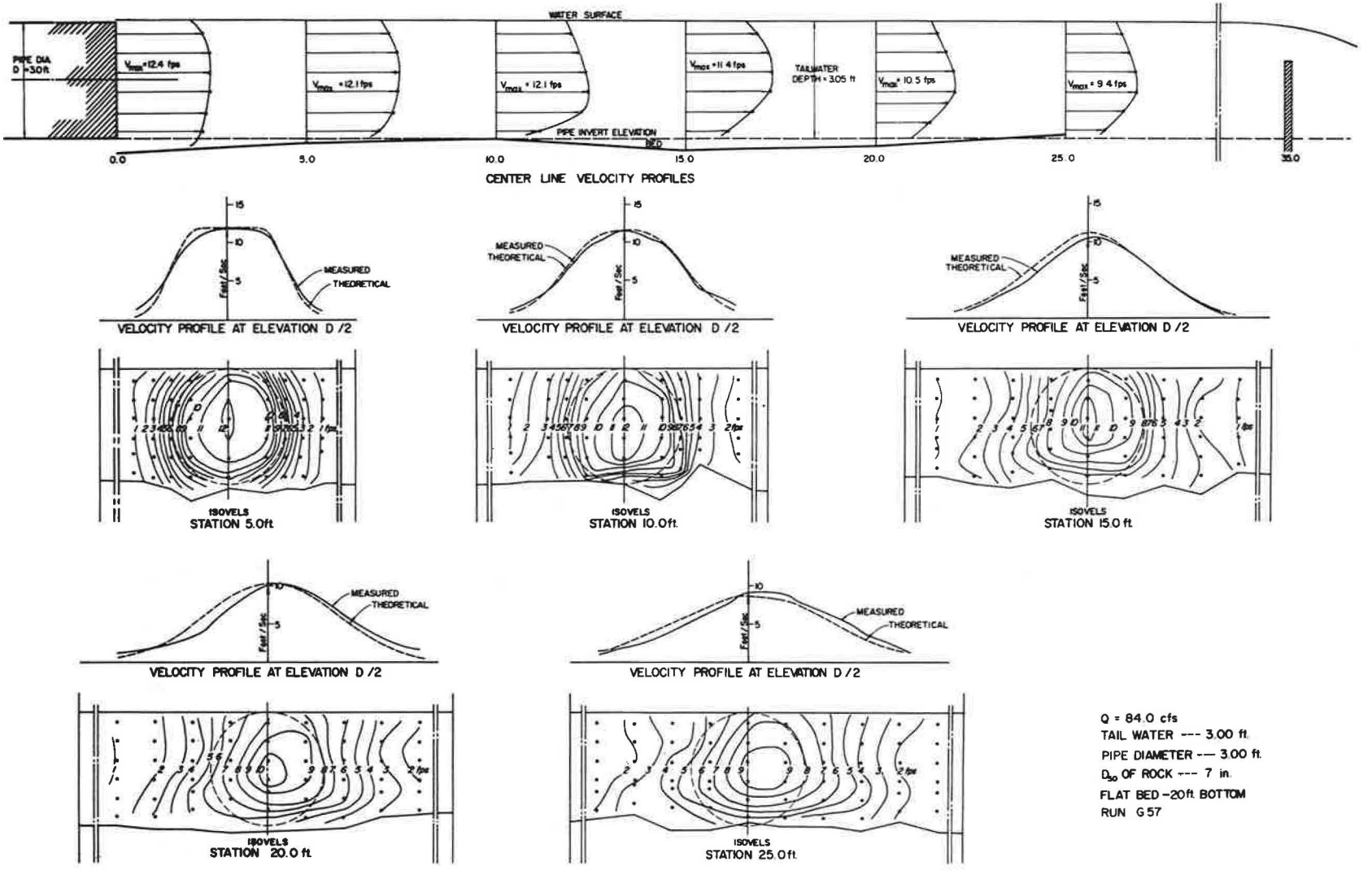

Figure 4. Centerline velocity profiles, isovels, and transverse velocity profiles for run G57.

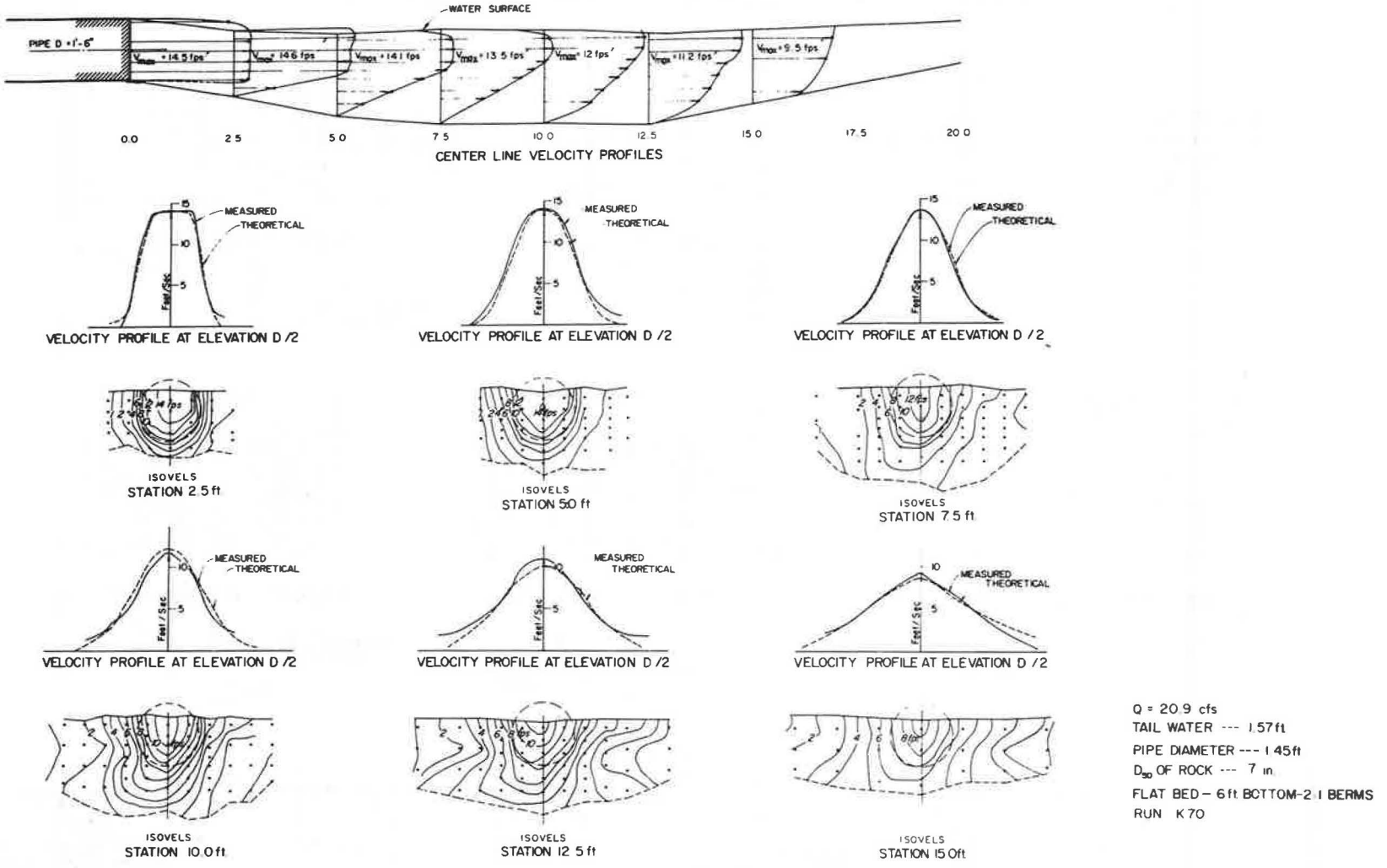

Figure 5. Centerline velocity profiles, isovels, and transverse velocity profiles for run K70.

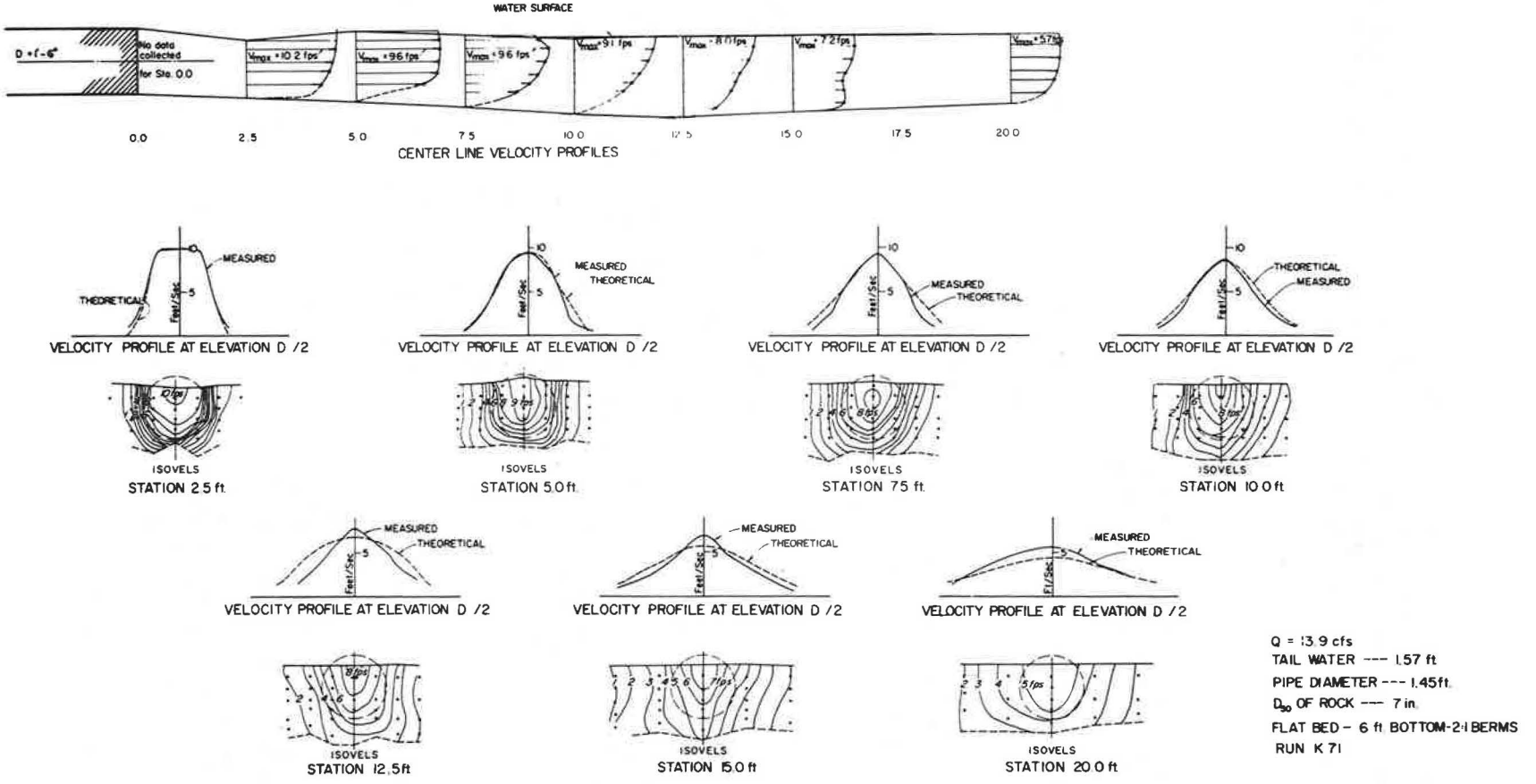

Figure 6. Centerline velocity profiles, isovels, and transverse velocity profiles for run K71.

RESULTS

The data collected downstream of the culverts appeared to correlate closely with the data presented by Albertson et al. for the 3-dimensional orifice flow field (1). The 3-dimensional orifice flow field was divided into 2 zones: the zone of flow establishment adjacent to the outlet and the zone of established flow (Fig. 7). For each of the zones, Albertson et al. presented the following relationships (1):

(a) Distribution of centerline velocity for flow from orifice,

$$V_{max}/V_o \text{ versus } X/D$$

where

V_{max} = maximum longitudinal velocity at a normal section,
V_o = mean velocity at the outlet section,
X = distance downstream from the outlet, and
D = diameter of the outlet pipe.

(b) Distribution of longitudinal velocity in zone of establishment of flow from orifices,

$$(r - D/2)/X \text{ versus } V_x/V_o$$

where

r = radial distance normal to the longitudinal centerline of the basin, and
V_x = longitudinal velocity at point (X, r).

(c) Distribution of longitudinal velocity in zone of established flow from orifices,

$$r/X \text{ versus } (V_x/V_o)\ (X/D)$$

Other significant plots were presented, but only those that relate to the problem at hand are mentioned here. The reader is referred to another report (4) for additional plots and analysis.

Figure 8 shows a comparison of the data collected downstream of the culvert outlets (6 runs) and those plotted in the other reports (1, 2).

Because the velocity distribution at the culvert outlet is nonuniform in contrast to the uniform distribution for the orifice, it seemed more reasonable to compare the arithmetic mean of the velocities measured along a centerline vertical at station X, $V_{x\,ave}$, with an arithmetic mean of the velocities measured along a centerline vertical at the outlet, $V_{o\,ave}$. The maximum velocity for an orifice is equal to the mean velocity, which is not the case for usual pipe flow. The data collected during this study are superimposed over the prediction curve shown in Figure 8. In the range X/D < 8.0, the prediction curve is conservative with the exception of the data for the low tailwater runs. For the range X/D > 8, the culvert data follow the prediction curve.

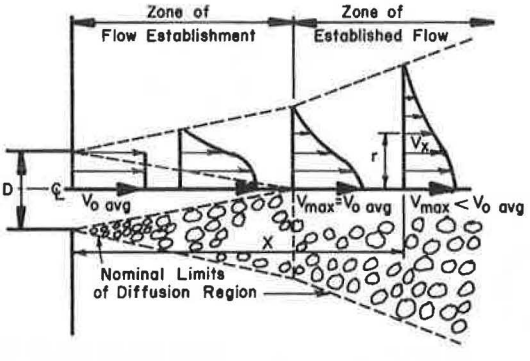

Figure 7. Zone of flow establishment and zone of established flow.

DESIGN CONSIDERATIONS

The curves recommended for design purposes are those shown in Figure 8 used in conjunction with those shown in Figures 9 and 10. The $V_{o\,ave}$ to be used with data shown in Figure 8 for basin design can be obtained by using the formula

$$V_{o\,ave} = KQ/A \qquad (1)$$

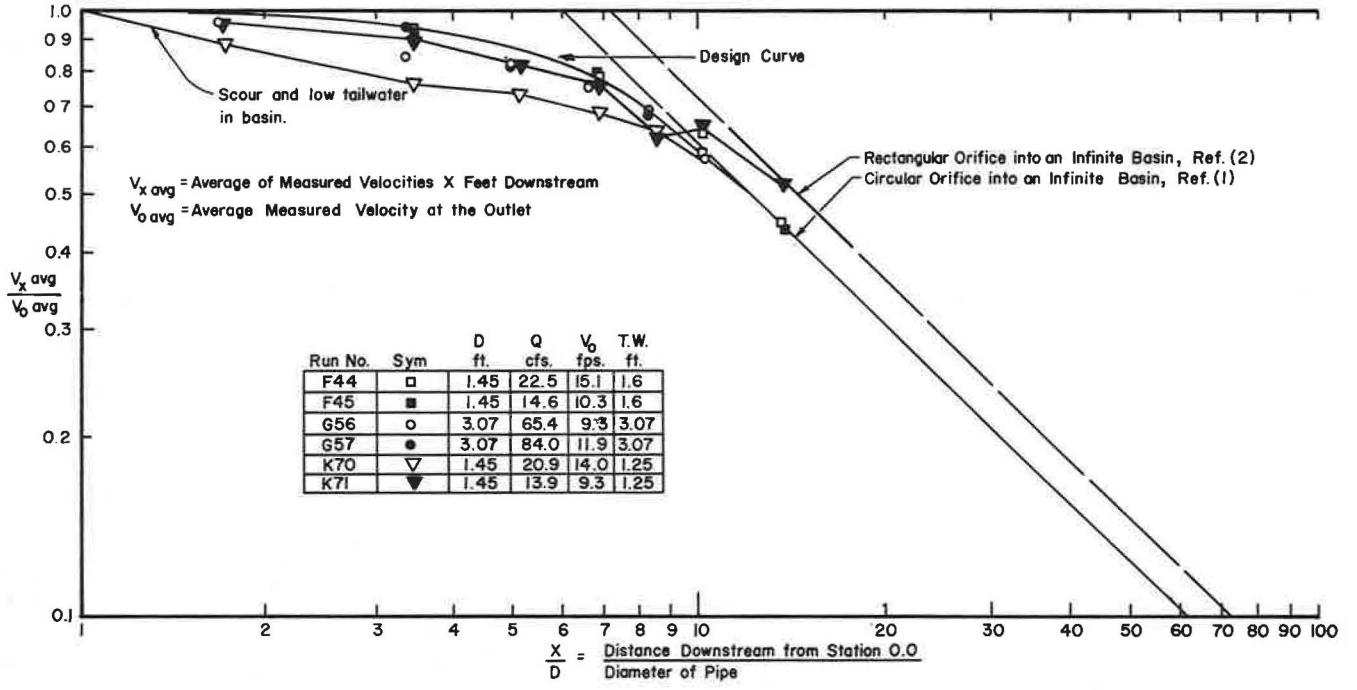

Run No.	Sym	D ft.	Q cfs.	V_o fps.	T.W. ft.
F44	□	1.45	22.5	15.1	1.6
F45	■	1.45	14.6	10.3	1.6
G56	○	3.07	65.4	9.3	3.07
G57	●	3.07	84.0	11.9	3.07
K70	▽	1.45	20.9	14.0	1.25
K71	▼	1.45	13.9	9.3	1.25

Figure 8. Distribution of centerline velocity from submerged outlets.

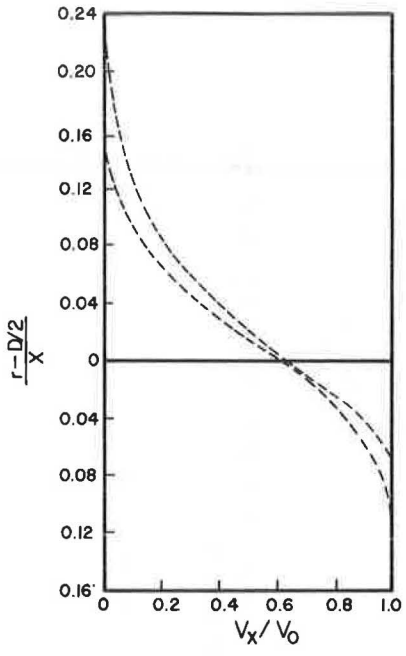

Figure 9. Distribution of transverse velocity for X/D < 6.

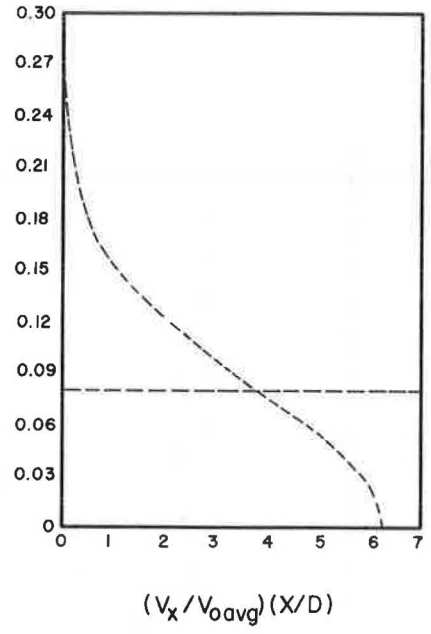

Figure 10. Distribution of transverse velocity for X/D > 6.

where Q is the design discharge, A is the gross cross-sectional area of the culvert, and K is a constant relating Q/A to the arithmetic mean of the vertical velocity profile. Values of K, obtained from 34 runs with smooth pipe having 18-in. and 36-in. diameters, ranged from 0.96 to 1.16 with an arithmetic mean of 1.07. It was not possible to correlate these values with Froude number or other dimensionless parameters; therefore, the value K = 1.1 is suggested for design purposes for smooth pipe.

Only 2 sets of data were available for corrugated pipe. The values of K were 1.14 and 1.21 with the former value associated with a typical maximum design discharge and the latter value with a Q well over the usual design discharge. It is suggested that K = 1.15 be used for corrugated pipe.

Whether the core of the jet is diverted to one side of the basin seems to depend on the ratio of the basin width, W_b, to the pipe diameter. With a large ratio, there is little danger of such an occurrence, but when $W_b/D \leq 4$ jet attachment to a bank or wall is a possibility. Data from this study do not adequately define the ratio where jet attachment will first occur.

High Tailwater Basins

There are 2 solutions to the scour problem for the high tailwater cases. One is to riprap the banks for a sufficient distance downstream, and the other is to increase the cross-sectional area of the culvert so that the exit velocity is tolerable and little scour occurs downstream of the outlet. If culvert flare is sufficiently gradual, the entire section will be occupied by the flow, and this will result in a low exit velocity; with large flare angles, the flow will separate from one wall and a large eddy in the basin will hold the flow against the other wall. The following example illustrates design techniques.

For a high tailwater basin, discharge, Q = 330 ft^3/sec; tailwater, d_t = 7 ft; and smooth pipe diameter, D = 6 ft. The task is to compute (a) the rock size required to prevent scour and (b) the maximum velocity in the channel 60 ft downstream of the outlet.

The design parameters are as follows: $Q/D^{2.5} = 330/6^{2.5} = 330/88.3 = 3.74$ ft$^{1/2}$/sec; $d_t/D = 7/6 = 1.16$; and $y_o/D = 6/6 = 1.00$.

The rock size, d_m, required to prevent scour below culverts is given elsewhere (6, 7). In this case $d_s/D \simeq 0$, where d_s is the depth of scour, for $d_m/D = 0.1$ (smallest recommended size). Therefore, $d_m = 0.1 \times 6 = 0.6$ ft is used. With a smooth pipe, K = 1.1 and $V_{o\,ave} = K(Q/A) = 1.10 \times (Q/D^{2.5}) \times [D^{2.5}/(\pi/4)D^2]$ or $V_{o\,ave} = 1.4(Q/D^{2.5}) \times \sqrt{D} = 1.4 \times 3.74 \times 2.45 = 12.8$ ft^3/sec. $X/D = 60/6 = 10$. Figure 8 shows that $V_{x\,ave}/V_{o\,ave} = 0.6$ when $X/D = 10$. Therefore, at a distance 60 ft downstream, mean velocity on the centerline vertical is given by $V_{x\,ave} = 0.6 \times 12.8 = 7.7$ ft^3/sec. At a distance $D/2 = 3$ ft above the bed, the velocity distribution can be estimated by using data shown in Figure 10. $V_{o\,ave}D/X = (12.8 \times 6)/60 = 1.28$.

Values of $(V_x/V_{o\,ave})(X/D)$, such at 6, 5, and 4, are used to obtain values of r/X from data shown in Figure 10, and then r and V_x are computed. The following results are obtained.

$(V_x/V_{o\,ave})(X/D)$	r/X	$r = X(r/X)$	$V_x = (V_x/V_{o\,ave})(X/D)(V_{o\,ave}D/X)$
6	0.03	1.8	7.7
5	0.06	3.6	6.4
4	0.075	4.5	5.1
3	0.100	6.0	3.8
2	0.13	7.8	2.5
1	0.17	10.3	1.8
0	0.24	14.4	0

The velocity profile at X = 60 ft and at a distance $D/2 = 3$ ft above the bed is shown in Figure 11. In general when $V_{x\,ave}$ (mean velocity at centerline vertical) has been decreased to a value 1.5 times the velocity that is compatible with the downstream channel, the basin can be terminated. In the example, the basin could be terminated at 60 ft if the downstream channel could withstand a velocity of $7.7/1.5 = 5.1$ ft^3/sec.

A 6- by 6-ft box culvert carrying 420 ft^3/sec would have the same velocity at the submerged outlet and the same $V_{x\,ave}$ 60 ft downstream if it is assumed that $X/W_o \simeq X/D = 60/6 = 10$. To predict the size of rock needed to prevent scour below box culverts, one can use the data published in another report (7).

Nonscouring, Low Tailwater Basins

The problem of describing expanding jets on rigid rock floors is similar in many respects to that of jets discharging into an infinite basin of fluid. However, with the rough floor there is a large decrease in fluid momentum in the downstream direction caused by the dynamic force of the fluid on the rock. With low tailwater, the force should be even more pronounced.

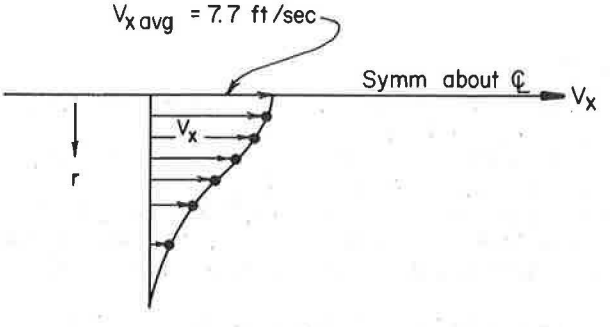

Figure 11. Transverse velocity profile.

The Colorado State University study does not adequately describe the downstream decay of velocity within nonscouring rock basins when the tailwater is below the pipe invert. However, some observations are given in order to supply a design criterion until more detailed studies are undertaken.

When the tailwater level is below the crown of the culvert outlet, the flow plunges onto the bed and spreads laterally very rapidly. The lateral expansion can be described by the angle θ (Fig. 58, 6). Watts (4) shows that θ is approximately 3 deg when $d_t/D \geq 1$ and the bed slope is

zero. The data were crude and scattered around the curve that is shown. Moreover, the expansion of such a jet is too complex to be accurately described by only 3 variables: θ, slope, and d_t/D.

However, continuing with this model, at any point downstream of the outlet, the width of the jet is $W_j = 2X \tan \theta + D$, and the average velocity of the jet is

$$V_{ave} = Q/[2X \tan \theta + D)y]$$

where y is the difference between the elevation of the bed and the elevation of the tailwater at point X. When the bed is horizontal, $y = d_t$ for all X.

When V_{ave} is reduced to a level compatible with the downstream channel, the rock riprap can be terminated. V_{ave} will be about $\frac{2}{3}$ of the maximum velocity on the centerline at any section X.

The following example is given.

For a low tailwater, nonscouring basin, discharge, $Q = 50$ ft^3/sec; barrel diameter, $D = 3$ ft; tailwater depth, $d_t = 1$ ft; brink depth, $d_b = 2.0$ ft; barrel slope, $S = 1$ percent; and available rock size, $d_m = 1.3$ ft.

The task is to design a nonscouring basin for a plain outlet. The design parameters are as follows: $Q/D^{2.5} = 50/3^{2.5} = 50/15.6 = 3.2$ ft$^{1/2}$/sec; $d_t/D = \frac{1}{3} = 0.33$; $d_b/D = \frac{2}{3} = 0.66$; $d_m/D = 1.3/3 = 0.43$; and $d_t/d_b = \frac{1}{2} = 0.50$.

According to Simons et al. (Figs. 51 and 52, 6), no scour will occur when this riprap is used. $\tan \theta = 0.18$ for $S = 1$ percent and $d_t/d_b = 0.50$ (Fig. 58, 6).

The depth of flow at any section X downstream is $Y = d_t + SX/100 = 1 + X/100$ and so $V_{ave} = Q/\{(2X \tan \theta + D)[1 + (X/100)]\} = 50/\{(0.36\ X + 3)[1 + (X/100)]\}$. If V_{ave} is to be reduced to 2 ft^3/sec, X = 41 ft. The width of the jet for X = 41 ft is $W_j = (0.36 \times 41 + 3) = 18$ ft. Thus, the minimum basin dimensions are L = 41 ft and $W_b = 18$ ft.

The same procedure may be employed with the metal end section except that D would be replaced by the width of the end section, 2D, in the equation. That is, $V_{ave} = Q/[(2X \tan \theta + 2D)y] = Q/[2(X \tan \theta + D)y]$.

The new expression for V_{ave} is valid provided $d_t/D \leq 0.4$; otherwise, with higher tailwater, the jet will not expand in the end section, and the computations would be carried out as for a plain outlet.

CONCLUSIONS

A method for the analysis and design of energy basins at culvert outfalls where the high tailwater prevails is presented. Velocity-predicting equations used in conjunction with experimentally derived design aids (5, 6, 7) can be used to proportion a satisfactory basin.

ACKNOWLEDGMENTS

We are indebted to the Wyoming State Highway Department, the Federal Highway Administration, and the Engineering Experiment Station at Colorado State University, joint sponsors of this project.

REFERENCES

1. Albertson, M. L., Dai, Y. B., Jensen, R. A., and Rouse, H. Diffusion of Submerged Jets. ASCE Trans., Vol. 115, 1950, pp. 639-697.
2. Yevjevich, V. M. Diffusion of Slot Jets With Finite Orifice Length-Width Ratios. Colorado State Univ., Fort Collins, Hydraulics Paper 2, 1956.
3. Murota, A., and Muraoka, K. Turbulent Diffusion of the Vertically Upward Jet. Proc., Twelth Congress of IAHR, Colorado State Univ., Fort Collins, Vol. 4, Part 1, 1967.
4. Watts, F. J. Hydraulics of Rigid Boundary Basins. Colorado State Univ., Fort Collins, PhD dissertation, 1968.
5. Stevens, M. A. Scour in Riprap at Culvert Outlets. Colorado State Univ., Fort Collins, PhD dissertation, 1969.

6. Simons, D. B., Stevens, M. A., and Watts, F. J. Flood Proctection at Culvert Outlets. Colorado State Univ., Fort Collins, Publ. CER 69-70 DBS-MAS-FJW4, 1970.
7. Stevens, M. A., Simons, D. B., and Watts, F. J. Riprapped Basins for Culvert Outlets. Paper presented at the 50th Annual Meeting and published in this RECORD.

RIPRAPPED BASINS FOR CULVERT OUTFALLS

Michael A. Stevens and Daryl B. Simons, Colorado State University; and
Frederick J. Watts, Department of Civil Engineering, University of Idaho

The sizing of riprap for culvert outlet basins is a difficult problem because the flow field at the outlets of many culverts is rapidly varied and 3-dimensional. Most available riprap design methods are primarily applicable to 2-dimensional uniform flow problems. For the purpose of developing more information on the behavior of riprap at culvert outlets, 288 model tests on basins for circular and rectangular culverts were conducted at Colorado State University. The models ranged in size from a 6- by 12-in. rectangular culvert with ¼-in. riprap to a 36-in. diameter pipe with 7-in. diameter rock. A method for the design of rock-riprapped basins for culvert outfalls was developed from a study of the model data. The method and design aids are presented in this paper. The method and aids are applicable for culvert flows with H2 or M2 water surface profiles near the brink, that is, mild sloping or horizontal culverts with drawdown at the outlet. The riprapped basin can be designed as a rigid-rock basin or, alternatively, as a scoured-rock basin if available rock is too small to prevent scour.

•AT MANY culvert outlets, it is necessary to reduce the kinetic energy of the flow and to match the flow velocity from the outlet basin with that of the downstream conveyance channel. There are available a number of good energy-dissipator designs, such as the St. Anthony Falls basin (1) and the Bureau of Reclamation stilling basin (2). The cost of these concrete structures can be relatively large in terms of the total cost of the culvert. Rock-lined outlet basins will be a feasible alternative for many culvert outlet structures. The question facing the designer is, "What size of rock and what basin dimensions are required for a rock-riprapped culvert outlet basin?"

The Wyoming State Highway Department, in conjunction with the Federal Highway Administration, sponsored a research program at Colorado State University to study riprapped basins at culvert outlets. The research program developed into an extensive model study program covering most of the range of culvert outlet flow conditions. A large portion of the tests were conducted with 6-in. diameter and 6- by 12-in. model culverts. For these small models, riprapped basins with ¼-, ½-, 1-, 1⅓-, and 2-in. median sieve diameter rock were tested. Model-to-prototype scaling parameters were checked by tests on 12-, 18-, and 36-in. diameter culverts. The largest model involved 7-in. diameter rock that was tested with a flow of 100 ft^3/sec in the 36-in. diameter culvert. A study of the model test results developed into a methodology for the design of rock outlet basins.

The content of this paper is limited to the design of riprapped basins for circular and rectangular culverts without flared end sections in which the water surface profile is either an M2 or H2 profile. M2 and H2 water surface profiles are obtained in mild sloping and horizontal culvert barrels when the tailwater depth is less than the brink depth at the outlet. For culverts with M1 water surface profiles, the method persented by Watts et al. (3) should be used to size nonscouring rock basins. The design of rock basins for culverts on steep slopes has been presented elsewhere by Simons et al. (4).

Sponsored by Committee on Surface Drainage of Highways.

DATA FOR DESIGN

The important variables that affect scour in rock at outfalls of culverts on horizontal or mild slopes are as follows:

1. The flow variables, where
   - Q = culvert discharge,
   - y_o = flow depth at the plane of the culvert outlet, and
   - d_t = tailwater depth at the plane of the culvert outlet;
2. The geometry of the culvert, where
   - D = pipe diameter,
   - H_o = height of the rectangular culvert, and
   - W_o = width of the rectangular culvert;
3. The geometry of the scour hole or basin or both shown in Figure 1, where
   - d_s = depth of scour,
   - L_s = length of the scour hole,
   - W_s = width of the scour hole,
   - L = length of the basin,
   - W_b = width of the basin, and
   - h = height of mound; and
4. The properties of the rock, where
   - d_m = effective grain size of the rock mixture.

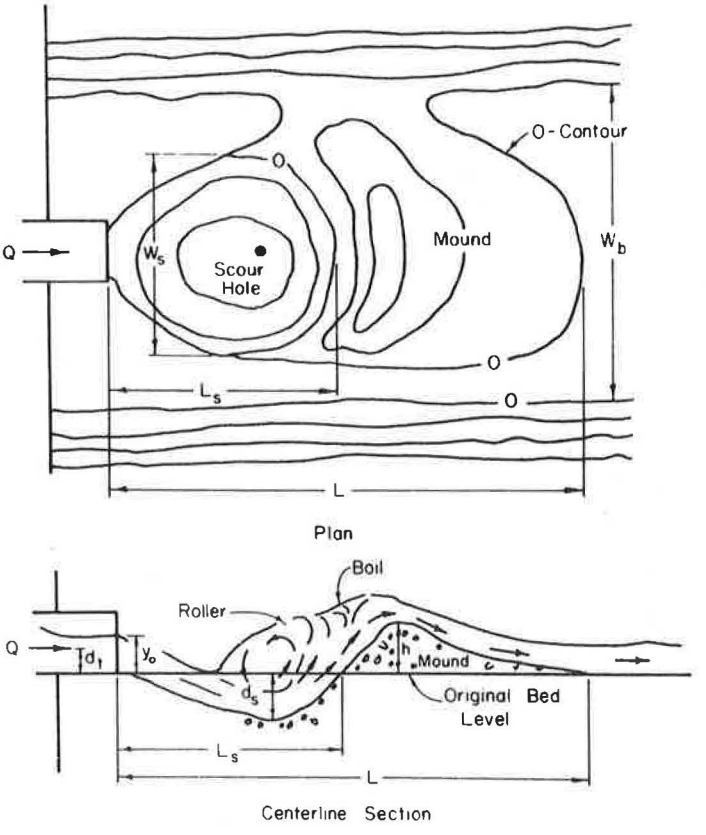

Figure 1. Riprapped basin.

The effective grain size diameter is computed from the equation

$$d_m = \left[\sum_{1}^{10} d_i^3/10\right]^{1/3}$$

where

$d_i\,(i = 1) = (d_0 + d_{10})/2$,
$d_i\,(i = 2) = (d_{10} + d_{20})/2$,
. . ., and
$d_i\,(i = 10) = (d_{90} + d_{100})/2$.

The d_0, d_{10}, . . ., and d_{100} terms are the rock-size values taken from a plot of "percentage finer by weight" versus "sieve diameter" curve for the rock mixture.

The experimental programs, conducted at Colorado State University, have been reported by Stevens (5) and Chen (6). From the analyses of the experimental data, the following aids for the design of riprapped basins were prepared.

Brink Depth at the Outlet

For horizontal and mild-sloping culverts discharging onto basins built to the level of the barrel invert, the relationship between discharge, brink depth, and tailwater depth are shown in Figure 2. The dashed curves are estimates of the relationship for

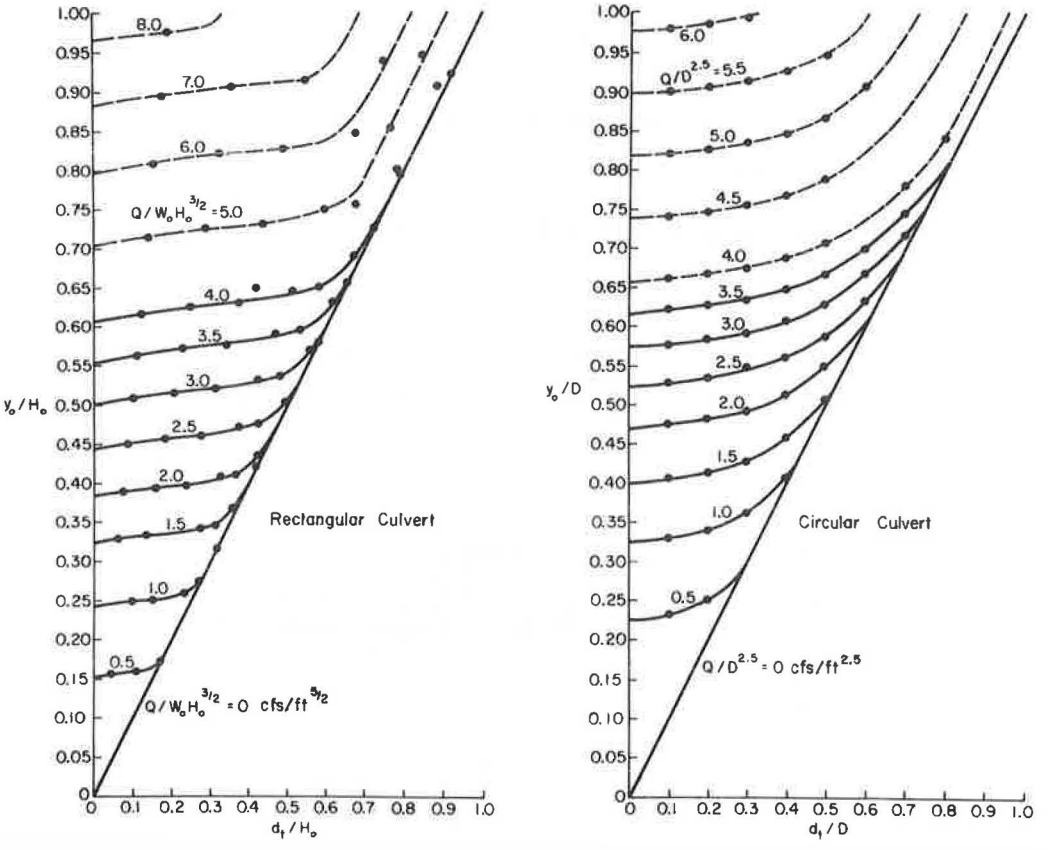

Figure 2. Effect of tailwater on brink depth in horizontal and mild-sloping culverts.

field-sized culverts. In 6-in. diameter models the curves are displaced because the zone of negative pressure at the crown near the outlet is much more pronounced than in large barrels. For 6-ft diameter barrels the influence of negative crown pressure is very small. This scale effect has been discussed by Simons et al. (4).

For rock-riprapped basins with widths greater than 2 culvert diameters, the tailwater level will be at the normal stream water surface elevation at the culvert outlet. This condition is not valid for the concrete basins studied by Watts (7).

Depth of Scour

The relations between the scour depth, d_s, rock size, d_m, tailwater depth, d_t, and the discharge, Q, are shown in Figure 3. The data were obtained from horizontal culvert models but are applicable to culverts on mild slopes.

It was found that, if the flow velocity at the outlet, V_o, tailwater depth, d_t, and the brink depth, y_o, were the same in a rectangular and circular culvert, then the scour depth, d_s, was approximately the same for a given rock size, d_m. The discharge ratios, $(Q/W_oH_o^{3/5})/(Q/D^{5/2})$, have been computed from the data shown in Figure 2 for the conditions that $y_o/H_o = y_o/D$ and $d_t/H_o = d_t/D$. The average values of the discharge ratios have been plotted as the curve shown in Figure 4. This curve can be used to convert rectangular culvert scour data to scour in equivalent circular culvert basins or vice versa. This conversion is illustrated in the accompanying design example.

Figure 3c shows the effect of the brink depth distortion on small models by the $Q/D^{2.5} = 4.04$ and 5.00 $ft^3/sec/ft^{5/2}$ curves. For these discharges in 6-in. models, the pipe flows nearly full at the outlet, but the upper streamlines are directed toward the bed of the basin in an abnormal manner. The effect of directing the upper streamlines toward the bed is an increased scour depth. Thus, the curves shown in Figure 3c for $Q/D^{2.5} = 4.04$ and 5.00 $ft^3/sec/ft^{5/2}$ indicate more scour than would be anticipated in interpolating between the $Q/D^{2.5} = 3.02$ and $Q/D^{2.5} = 6.28$ $ft^3/sec/ft^{5/2}$ curves, which are not affected by negative pressure at the crown near the outlet. The $Q/W_oH_o^{3/2} = 4.26$ $ft^3/sec/ft^{5/2}$ curve shown in Figure 3a is another example of the same effect. The brink depth distortion decreases as the pipe diameter is increased.

In a number of model tests, a phenomenon that has been labeled mound-controlled scour occurred. This type of scour is very evident in the results shown in Figure 3c. At very low tailwater depths, scour was less than at higher tailwater. For these tests, a relatively high mound of rock was formed that reduced the flow of water along the center of the basin and totally obstructed additional rock migration. The flow had the capacity to scour rock from the bed, but the rock could not be lifted over the top of the mound.

At greater tailwater depths, the relative height of the mound was less, and there was no movement of the bed material at the equilibrium depth of scour. However, when the mound was removed, the same flow scoured the basin to a greater depth.

Length of Scour Hole

The lengths of the scour holes for all tests on circular and rectangular culvert outlets are shown in Figure 5 for $d_s/d_m \leq 18$ and in Figure 6 for $d_s/d_m > 8$.

Length of Basin

The distance from the barrel outlet to the downstream end of the mound, L, is related to the length of the scour hole, L_s, and to the relative tailwater depth, d_t/y_o, as shown in Figure 7.

Width of Scour Hole

For circular and box ($W_o = H_o$) culverts, the width of the scour hole is primarily a function of the scour depth. The data shown in Figure 8 are for cases where W_b/W_o or

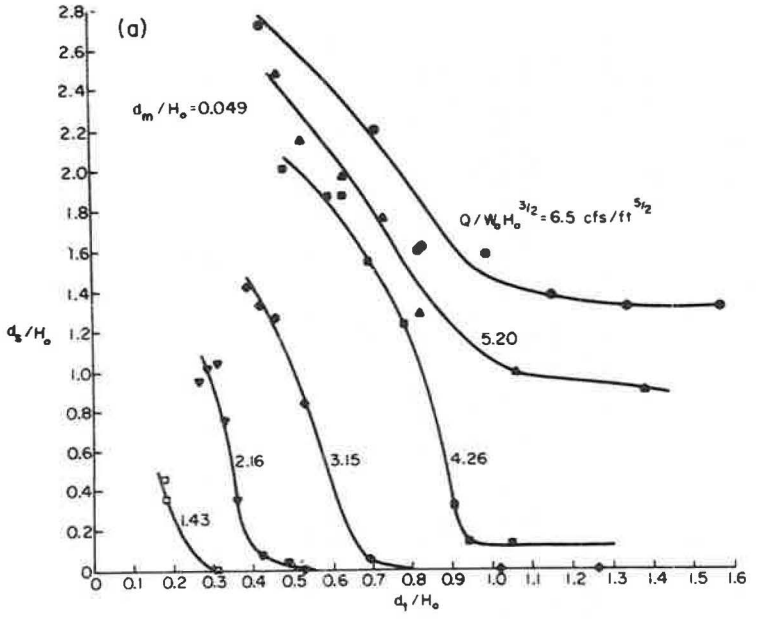

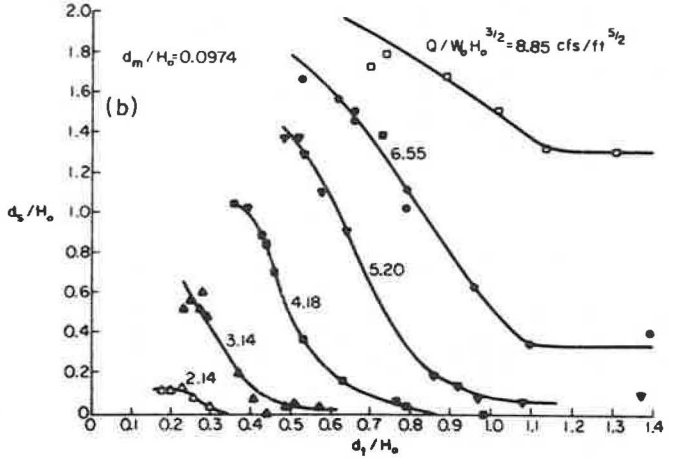

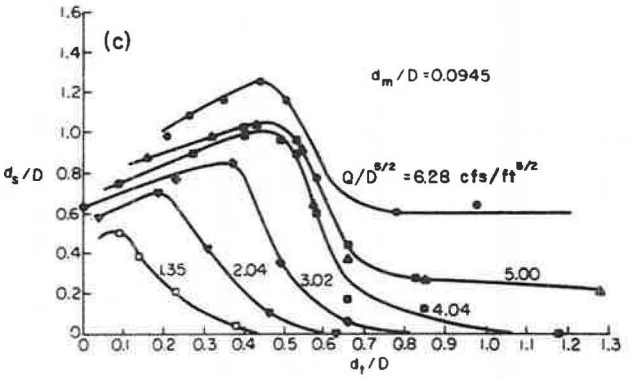

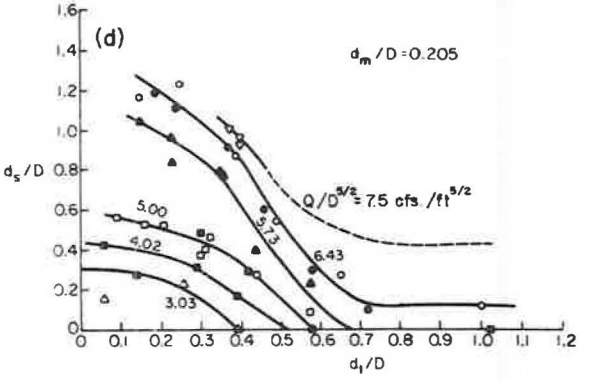

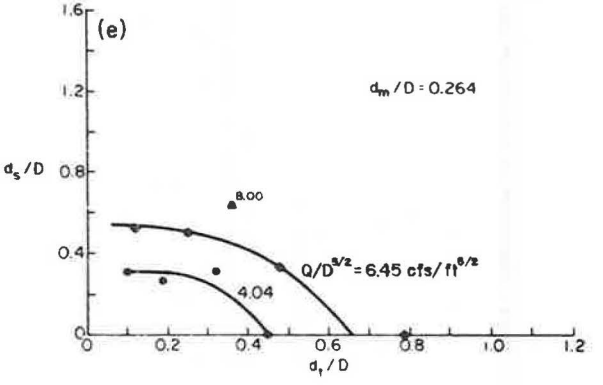

Figure 3. Depth of scour for plain outlets.

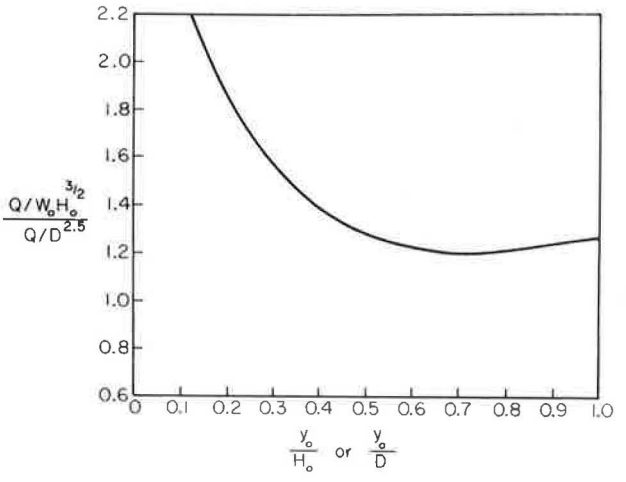

Figure 4. Discharge ratios for equal scour depths.

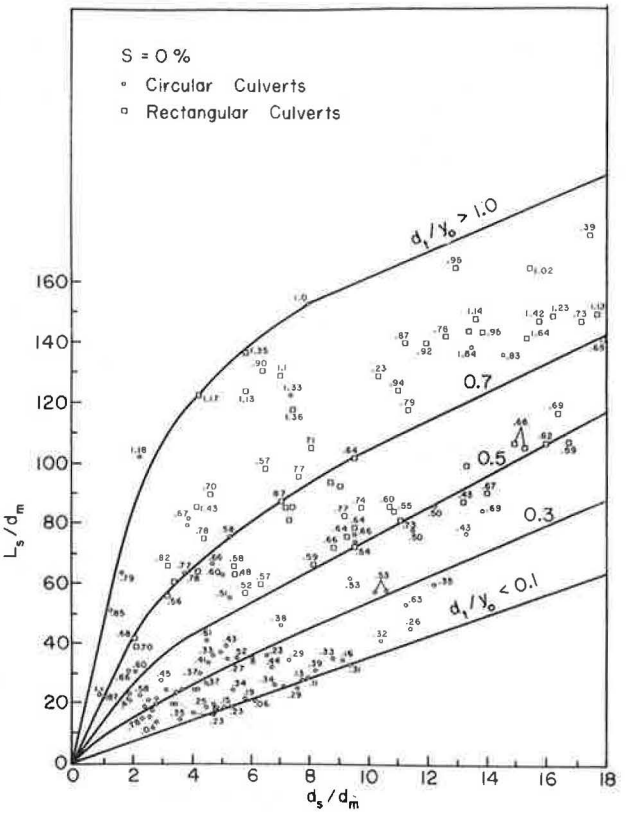

Figure 5. Length of scour hole.

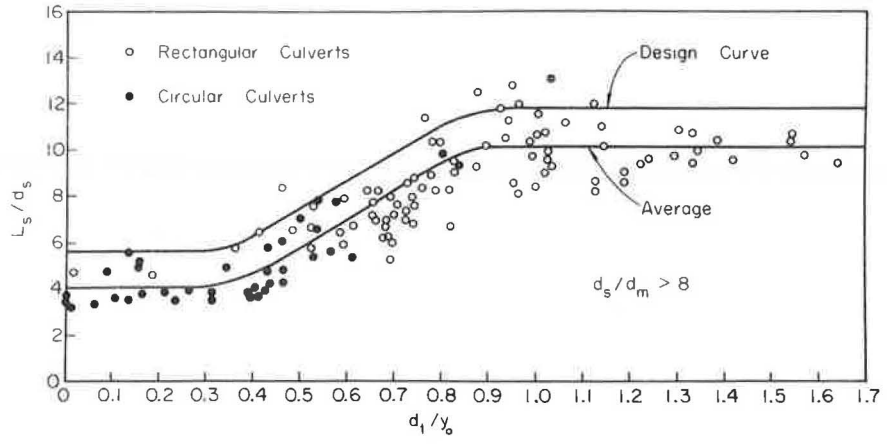

Figure 6. Length of scour hole, $d_s/d_m > 8$.

W_b/D was 4 or greater. With smaller relative basin widths, the scour hole was slightly wider.

For those rock basins that did not scour, model tests indicated that the jet would expand in the basin according to the relationships shown in Figure 9.

RECOMMENDED FIELD STRUCTURES

As the result of the model test program, 3 recommended rock-riprapped basins for culvert outfalls were developed. They are the nonscouring, the hybrid, and the scoured basins shown in Figure 10. The principal components of the 3 recommended basins are the apron, end slope, side slopes, underslope, and embankment slopes. For a given set of outlet conditions, the dimensions of these components are dependent on the rock size, d_m.

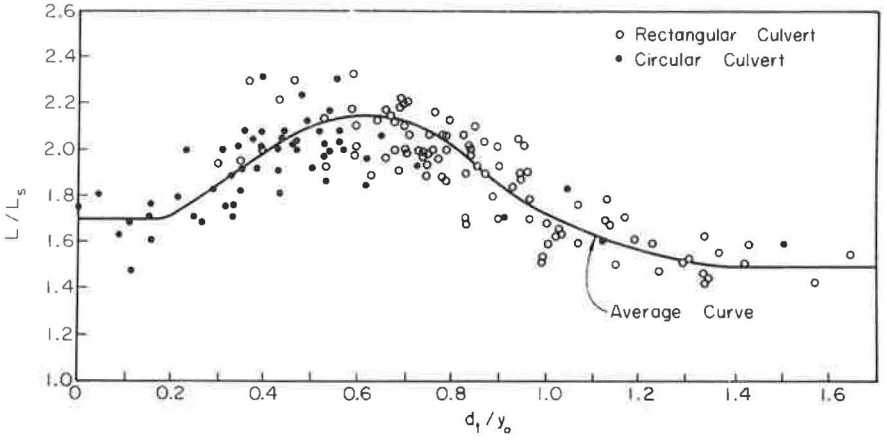

Figure 7. Distance to end of mound.

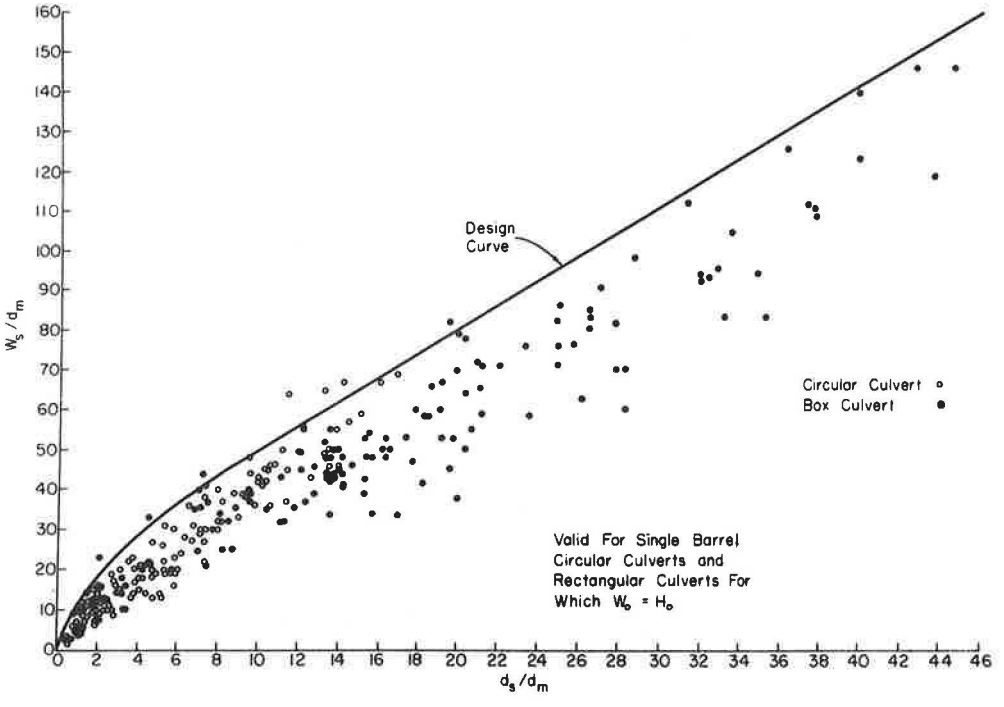

Figure 8. Width of scour hole.

Nonscouring Basin

After the rations $Q/W_oH_o^{3/2}$ and d_t/H_o have been computed, y_o/H_o can be obtained from data shown in Figure 2. The depth of scour, d_s/H_o, can then be determined from data shown in Figure 3. If the available rock is of size d_m so that $d_s/H_o = 0$, the dimensions of the components of the nonscouring basin are found in the following manner.

The lateral expansion rate, tan θ, is determined from data shown in Figure 9. The function of the rock basin is to reduce the outlet velocity, V_o, to the allowable downstream channel velocity, V_{ch}. The continuity equation at the basin outlet requires that $V_{ch} = Q/W_b(d_t + LS/100)$, where S is the percentage of basin slope. If the basin width is approximately the same as the natural channel width, the term LS/100 should be dropped. Also $W_b = 2L\tan\theta + W_o$. The solution of these equations will yield the length of the apron, L, and the width of the basin, W_b, at the downstream end of the basin.

The apron should be placed at the elevation of the culvert invert at the outlet and on the same slope as the culvert barrel. The minimum recommended thickness of the apron, T, is either $2d_m$ or d_{100}, whichever is greater.

The end slope terminates the apron (Fig. 10) and provides protection against local scour at the end of the basin. If degradation is anticipated in the downstream channel, the end slope can be carried to a depth E to give some protection to the structure. The recommended end slope is 2:1 with a thickness, B, equal to the greater of d_{100} or $2d_m$ and a minimum drop, E, equal to T.

Riprap is required along the road embankment in the immediate vicinity of the outfall to protect against any splash or spray and to control the action of rollers that may form in the corners of the structure. The rock should be extended on the embankment slope to a height 1.5F above the invert. The value of F is the greater of y_o or d_t. The thickness of the embankment slope, B, should be the greater of $2d_m$ or d_{100}.

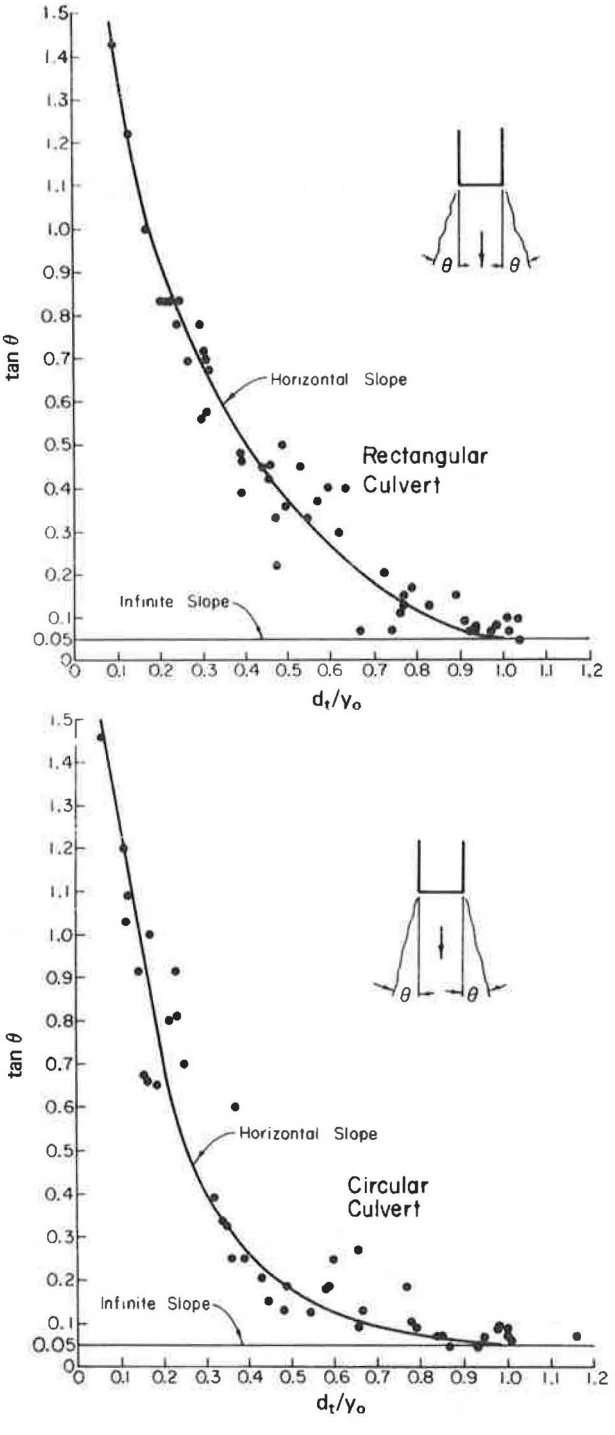

Figure 9. Estimate of angle of lateral expansion for horizontal and mild-sloping culverts.

The underslope prevents movement of materials from under the culvert. A cutoff wall extending downward a distance 2T below the apron may be used in lieu of the underslope.

The side slopes extend from the culvert outlet to the termination point of the end slope. If the channel is not confined, the volume of riprap for the side slopes should be placed on the natural side slopes of the downstream channel or on the horizontal surface adjacent to the apron riprap.

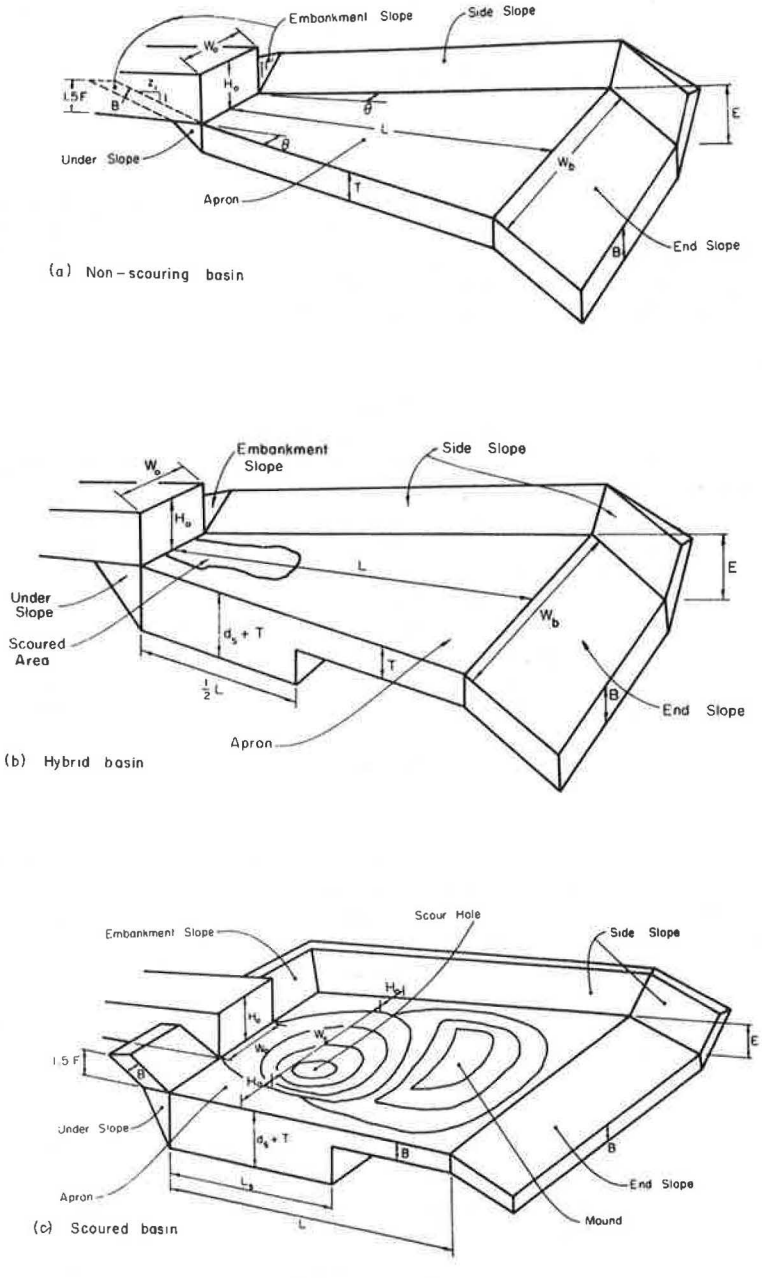

Figure 10. Recommended riprapped basins.

The dimensions of a standard nonscouring basin for a circular pipe culvert are the same as those described earlier except that W_o and H_o are replaced by D, the pipe diameter.

If $d_t/y_o \geq 1.0$, the average velocity at the culvert outlet is similar to that below the stilling basins studied by the Bureau of Reclamation (2). That is, there is no acceleration at the outlet when $d_t/y_o \geq 1.0$. The Bureau's recommended rock size to prevent scour is given by the expression $V_o^2/gd_m = 2.5$ for rock with a specific weight of approximately 2.65. At Colorado State University in model tests on culverts with $d_t/y_o \geq 1.0$, the d_m required to prevent scour was less than that given by the Bureau. One possible explanation is that the turbulence level is much higher downstream of hydraulic jump stilling basins than it is below culvert outfalls in which there is no well-defined jump.

For the case in which $d_t/y_o \geq 1.0$, the nonscouring basin can be sized by the method outlined earlier, but a better method has been given by Watts et al. (3). The 2 methods give approximately the same apron dimensions.

Hybrid Basin

The hybrid basin covers conditions where a basin scours slightly but not enough to give the efficient type of energy dissipation that results from basins with large scour holes. Then, if $0 < d_s/d_m < 2.0$, an additional volume of rock is added to the apron and underslope of the nonscouring basin (Fig. 10b) so that the jet will not penetrate the apron.

The determination of the dimensions W_b and L are in the design example. All other dimensions are the same as those for the nonscouring basin.

Scoured Basin

It is permissible to allow a riprapped basin to scour if the basin is sized correctly. Rather than preforming the scour hole, one will usually find it more convenient to construct the apron level with the culvert invert on the same slope as the barrel and to rely on the plunging jet to form the scour hole and mound (Fig. 10c).

The design of the embankment slope, side slopes, end slope, and underslope is the same as that for the previous 2 basins. The apron is now rectangular in plan and contains the major portion of the rock used in the structure.

For the scoured basin, the length of the basin is governed not by the allowable channel velocity downstream but by the need to provide a landing area for that rock moved from the scour hole. The mound is an integral part of the structure and, if it is somehow removed, the scour hole would deepen and penetrate the apron resulting in partial failure or failure of the basin. The design of a scoured basin is illustrated in the next section.

For circular barrels, the variables W_o and H_o are replaced by the pipe diameter D.

Filter Requirements

All side slopes about the outlet basin that are riprapped should be provided with suitable filters to prevent the movement of embankment materials through the riprap. That portion of the basin on the upstream side of the scour hole behind the embankment and underslope should always be provided with a filter. A filter is not recommended for the remainder of the basin when the riprap is well graded and the natural material is cohesive.

Authoritative discussions of riprap gradation and filter design are given by Sherard et al. (8) and by the Bureau of Reclamation (9).

DESIGN EXAMPLE

Consider a circular culvert on a mild slope (M2 profile), where slope S = 1.7 percent; discharge Q = 680 ft^3/sec; pipe (1,108-in. SPP) D = 9 ft; tailwater d_t = 3.6 ft; brink depth y_o = 5.3 ft; and allowable downstream velocity V_{ch} = 8.8 ft^3/sec.

The flow parameters at the outlet are as follows: $Q/D^{2.5} = 680/9^{2.5} = 680/243 = 2.80$ $ft^3/sec/ft^{5/2}$; $d_t/D = 3.6/9 = 0.40$; $d_t/y_o = 3.6/5.3 = 0.68$; and $y_o/D = 5.3/9 = 0.59$.

Depth of Scour

From the curves shown in Figure 3, the depth of scour d_s is found for various mean rock diameters d_m, as follows:

d_m/D	d_m(ft)	d_s/D	d_s(ft)	Reference
0.049	0.44	1.80	16.2	See following
0.0945	0.85	0.61	5.5	Figure 3c
0.205	1.85	0.0	0	Figure 3d

From data shown in Figure 3a, the depth of scour for $d_s/D = 0.049$ can be found by converting the flow parameter $Q/D^{2/5}$ into its equivalent parameter for a box culvert, $Q/W_oH_o^{3/2}$. $(Q/W_oH_o^{3/2})/(Q/D^{2.5}) = 1.26$ for $y_o/D = 0.59$ (Fig. 4). Therefore, the equivalent box culvert flow is $Q/W_oH_o^{3/2} = 1.26 \times 2.80 = 3.53$ ft^3/sec/ft$^{5/2}$. $d_s/H_o = d_s/D = 1.80$ for $d_t/H_o = d_t/D = 0.40$ (Fig. 3). Hence, $d_s = 1.8 \times 9 = 16.2$ ft. A plot of d_s versus d_m is shown in Figure 11a.

Length of Scour Hole

The length of the scour hole is determined from data shown in Figures 5 and 6. Recall that $d_t/y_o = 0.68$.

d_s(ft)	d_m(ft)	d_s/d_m	L_s/d_m	L_s/d_s	L_s(ft)	Reference
16.2	0.44	37	—	9.5	154	Figure 6
5.5	0.85	6.5	80	—	68	Figure 5
2.4	1.20	2.0	44	—	53	Figure 5
0.0	1.70	0	00	—	0	—

The values of L_s and d_m are shown in Figure 11b, and a smooth curve is drawn through the computed points.

Required Length of Basin

When no long-term degradation is anticipated, the length of the basin, L, is shown in Figure 7 (for $d_s/d_m \geq 2.0$). The value of L_s is taken from the smoothed curve shown in Figure 11b.

d_m(ft)	L_s(ft)	L/L_s	L(ft)	Reference
0.44	133	2.1	280	Figure 7
0.85	90	2.1	190	Figure 7
1.20	53	2.1	110	Figure 7
1.70	—	—	62.5	See following

For the rock size that does not scour ($d_m = 1.7$ ft), the length of the basin will depend on the maximum allowable average velocity in the downstream channel, V_{ch}. From data shown in Figure 9b, $\tan\theta = 0.10$ for $d_t/y_o = 0.68$. The depth at the distance L downstream of the outlet is $y = d_t$ if it is assumed that d_t is the normal depth for the design discharge. Then, $L = [1/(2\tan\theta)][(Q/d_tV_{ch}) - D] = 62.5$ ft. The L versus d_m relationship is shown in Figure 11c.

Width of Scour Hole and Basin

The scour hole width is obtained from data shown in Figure 8, and the apron width, W_b, is given by the equation $W_b = W_s + 2D$.

d_s(ft)	d_m(ft)	d_s/d_m	W_s/d_m	W_s(ft)	W_b(ft)	Reference
16.2	0.44	37	134	58	76	Figure 8
5.5	0.85	6.5	38	32	50	Figure 8
2.4	1.20	2.0	18	22	40	Figure 8
0.0	1.70	0	—	—	22	See following

For $d_m \geq 1.70$ ft, there is no scour, and the width of the basin, W_b, at a distance L downstream of the pipe outlet is $W_b = 2L\tan\theta + D = 21.5$ ft. The W_b versus d_m curve is shown in Figure 11d.

Volume of Riprap Required

If the ratio d_m/d_{100} is known, the volume of rock required for the different basins can be computed. A typical volume versus d_m curve is shown in Figure 11e. Generally, the smallest rock size that will not scour yields the minimum rock-volume basin.

Final Selection of the Basin

The volume versus d_m curve can be converted to a capital cost versus d_m curve if the costs of each size of rock, delivered to the site, are known. From this information the most economical basin can be selected. Each basin will perform well at the given design discharge; however, scouring basins are more susceptible to failure than hybrid or nonscouring basins if the design discharge is exceeded. Simons et al. (4) have defined a safety factor against failure, and additional rock can be added to the apron so that all designs have the same safety factor. This additional rock would modify the volume versus d_m and capital cost versus d_m curves. The final decision could be made on the modified capital cost versus d_m curve.

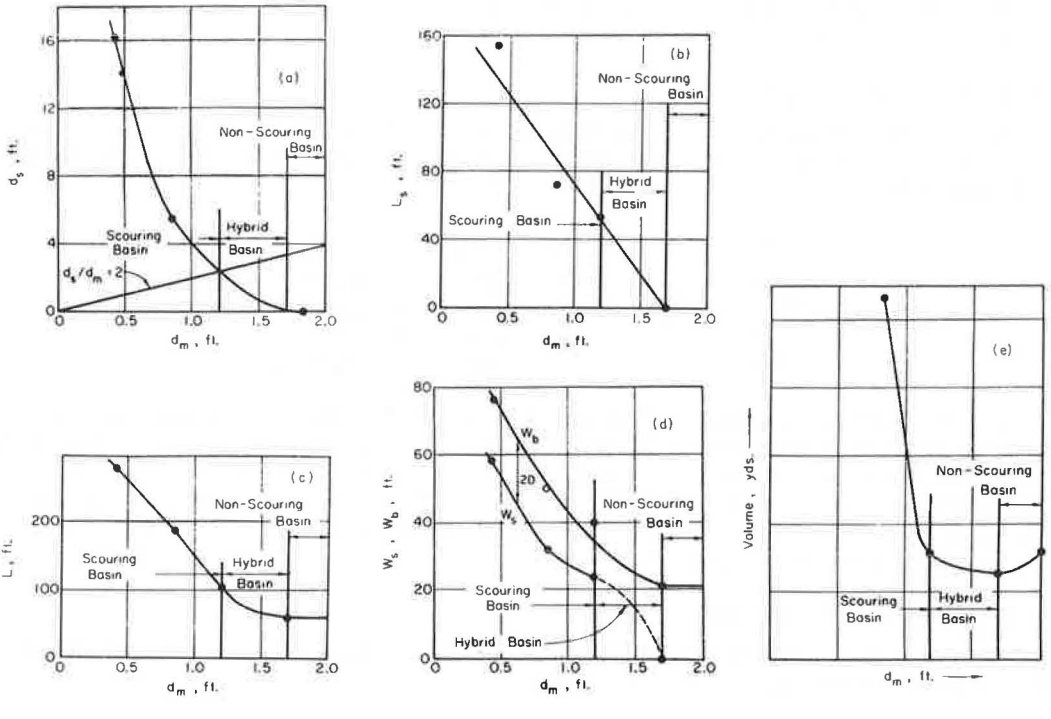

Figure 11. Dimensions for design example basin.

Multibarrel Culverts

The design of rock basins for multibarrel culverts is essentially the same as that for single-barrel culverts provided that all barrels are the same size. If there are equal discharges in all barrels, the depth of scour and the length of scour hole and basin are computed by using the same procedure that is outlined in the previous example; that is, the scour depth and the length of scour hole and basin for an n-barrel culvert carrying Q_t are the same as those for a single barrel discharging Q_t/n. The width of the scour hole is given by the equation

$$W_{sn} = W_s + (n - 1)(W_o + S)$$

or

$$W_{sn} = W_s + (n - 1)(D + S)$$

where

W_{sn} = width of the scour hole for n barrels,
W_s = width of the scour hole for a single barrel,
n = number of barrels, and
S = spacing between the barrels, assumed to be the same between all the barrels.

There is a greater chance of failure in the riprapped basin for multibarrel culverts than there is for single-barrel culverts. If one barrel of a multibarrel culvert is blocked with debris, the remaining barrels carry more water, and this increase in flow may be great enough to cause the rock basin to fail. The designer might consider riprapping multibarrel outlet basins with larger rock than the design procedure indicates.

CONCLUSIONS

A method for the design of rock-lined basins for culvert outfalls has been developed from model test data. The recommended rock-lined basins are suitable for single-barrel or multibarrel installations for both circular and rectangular outlets. The method provides for alternative rock basin designs depending on the size of the available rock. If the available rock will not prevent scour at the outlet, then a scoured basin design may be feasible. The cost of the most economical rock basin design should be compared with the cost of concrete and fabricated metal outlet structures before the outlet basin design is selected.

The design aids for riprapped culvert outlet basins were developed from model tests because the flow at the outfall is usually rapidly varied and 3-dimensional. Stable riprap sizes for such flow fields are different from those for uniform 2-dimensional flow. The information for scoured basin designs is presented because, in many cases, the rock size required to prevent scour is greater than the available rock sizes.

ACKNOWLEDGMENTS

We are indebted to the Wyoming State Highway Department and the Engineering Experiment Station at Colorado State University, joint sponsors of this project.

REFERENCES

1. Blaisdell, F. W. Development and Hydraulic Design, St. Anthony Falls Stilling Basin. ASCE Trans., Vol. 113, 1948, pp. 483-520.
2. Hydraulic Design of Stilling Basins and Bucket Energy Dissipators. Technical Information Branch, U.S. Bureau of Reclamation, Denver, Eng. Monograph 25, 1958.
3. Watts, F. J., Simons, D. B., and Stevens, M. A. Analysis of Rigid Outfall Basins With High Tailwater. Paper presented at the 50th Annual Meeting and published in this Record.

4. Simons, D. B., Stevens, M. A., and Watts, F. J. Flood Protection at Culvert Outlets. Colorado State Univ., Fort Collins, Publ. CER 69-70 DBS-MAS-FJW4, 1970.
5. Stevens, M. A. Scour in Riprap at Culvert Outlets. Colorado State Univ., Fort Collins, PhD dissertation, 1969.
6. Chen, Y. H. Scour at Outlets of Box Culverts. Colorado State Univ., Fort Collins, MSc thesis, 1970.
7. Watts, F. J. Hydraulics of Rigid Boundary Basins. Colorado State Univ., Fort Collins, PhD dissertation, 1968.
8. Sherard, F. J., Woodward, R. J., Gizienski, S. F., and Clevenger, W. A. Earth and Earth-Rock Dams. John Wiley and Sons, New York, 1963.
9. U.S. Bureau of Reclamation. Design of Small Dams. Govt. Printing Office, Washington, D.C., 1965.

DESIGN CRITERIA FOR CONTROLLED SCOUR AND ENERGY DISSIPATION AT CULVERT OUTLETS USING ROCK AND A SILL

Donald A. Thorson, Department of Civil Engineering,
South Dakota School of Mines and Technology;
Arunprakash M. Shirole, City of Minneapolis; and
Mansour Karim, South Dakota Department of Highways

This study establishes the criteria for the effective design of rock-basin energy dissipators for flow from culverts without or with a transverse sill. Design tables have been prepared on the basis of laboratory studies with 175-, 3-, and 6-in. diameter culvert models on a zero slope with a low tailwater. Models of standard end flares were used to simulate the culvert outlet conditions. Stable rock sizes and basin geometry can be determined by using the design tables developed in the study. The design tables provide data for flows up to a discharge factor, $Q/D^{2.5}$, of 13.5 and are applicable for angular rock as well as rounded rock. The tables are used in examples for design of rock basins for no-scour situations and controlled depths of scour. The study concludes that the rock basin should have a width of at least 3 pipe diameters and divergence angles of 1:3 when no sill is used and 1:1.75 when a sill is used. The length of the basin is dependent on the culvert discharge, culvert diameter, size of rock, extent of permissible scour, and use of a sill. The sill of this study was placed at the flared end and was 1 diameter long and 0.3 diameter high. The tables, by means of dimensionless parameters, make it possible to select the proper sized rock to realize a selected velocity reduction and a degree of scour control.

•THE CONTROL of erosion at the outlet of culverts under highways is a demanding prot lem. The complex interplay between the many involved parameters puts limitations on a complete solution. Economy of construction, designer's time, aesthetics, and safety factors were considerations prompting the use of rock and a simple sill for this study.

The objectives of this study are to determine the following by means of model simulation of flow from circular culverts onto basins of rock riprap:

1. Proper size of rock for stability to movement and ability to dissipate the flow energy,
2. Effect of the shape of the rock (rounded or angular),
3. Proper geometry of the rock basin with regard to width and length and the expansion angle from the culvert outlet, and
4. Effect and proper dimensions of sills at the end of the flared end.

Pertinent to this study is the state of the flow just as it leaves the circular section of the culvert and enters the end transition. In other words, the designer by his analysis has brought the flow through the culvert and now wonders what to do with it at the brink of the circular outlet. Variables necessary to describe the flow at the brink are as follows:

Sponsored by Committee on Surface Drainage of Highways and presented at the 50th Annual Meeting.

Q = volumetric rate of discharge,
D = inside diameter of culvert,
d_b = depth of flow at the brink,
ρ = mass density of the water,
μ = dynamic viscosity of water,
g = gravitational acceleration, and
V_b = average velocity of flow at the brink.

After leaving the circular culvert, the flow enters a flared end. The flared end has dimensions proportioned to the diameter of the culvert according to a standard concrete flared end used by the South Dakota Department of Highways (Fig. 1). After leaving the flared end, the flow discharges onto a rock basin that has the following characteristics:

d = size of riprap (an average diameter determined by passing and retention on specified square-opening screens),
ρ_s = mass density of rock riprap,
d_1 = depth of flow over the rock basin at the outlet end of the flared end,
d_2 = depth of flow at the downstream end of the rock basin,
ℓ_1/ℓ_2 = divergence ratio of the sides of the basin (Fig. 2),
W_b = width of the basin at the flared-end outlet,
d_s = depth of scour hole,
L_s = length of scour measured from flared-end outlet,
L_d = length to downstream edge of dune measured from flared-end outlet,
W_s = width of scour hole,
L = length of basin to which velocity is reduced to v, measured from flared-end outlet, and
v = average velocity of flow at a specified distance L downstream from the flared-end outlet.

Preliminary laboratory observations demonstrated that the best location for a simple, rectangular sill would be downstream from the flared-end outlet a distance of about 1 to 2 pipe diameters. However, because such a location would present a safety hazard on the right-of-way and would present a costly construction problem, it was decided to

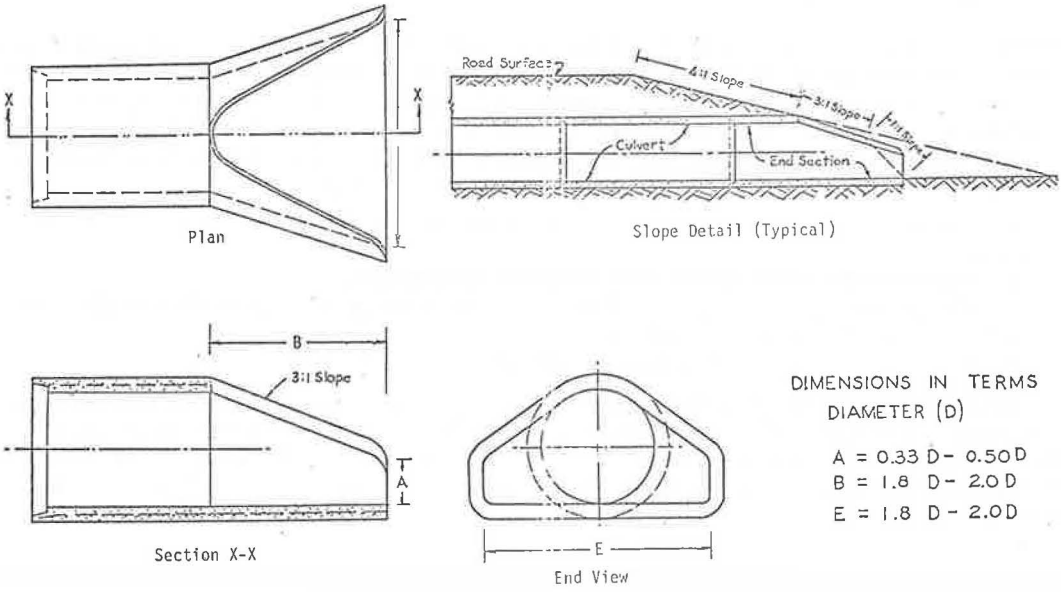

Figure 1. Dimensions of the standard concrete flared end.

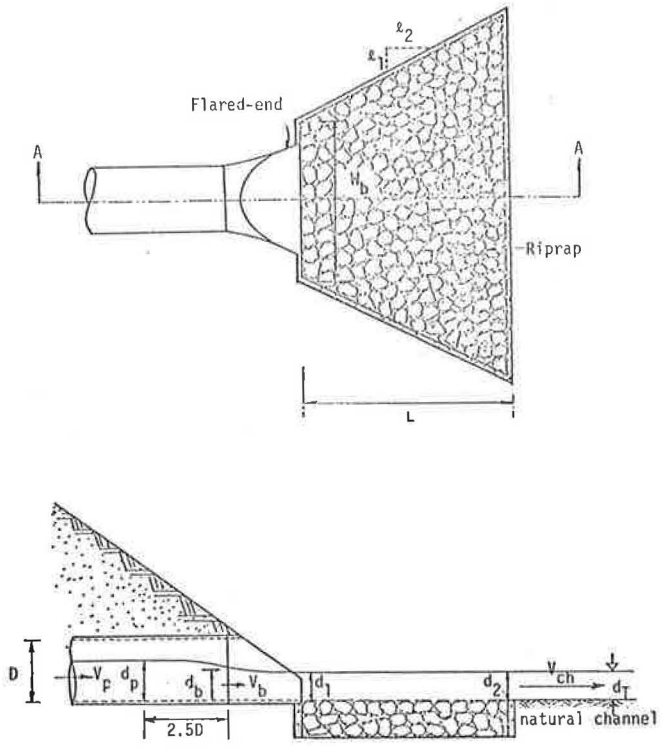

Figure 2. Definition of parameters.

confine this study to a sill location immediately downstream from the flared-end outlet. This location has a definite advantage in that the sill can be incorporated in an end-wall construction. The sill dimensions to be considered are as follows (Fig. 3):

W = length,
P = height, and
t = thickness of the sill.

Many forces, such as pressure, gravitation, viscosity, traction, lift, and drag, influence the energy dissipation efficiency of a bed of rock riprap. In addition, the many variables of the kinematics and geometry involved preclude a rigorous theoretical analysis. This necessitates recourse to model studies to obtain quantitative relationships necessary for design.

Parameters combining the many variables can best be established by having in mind conventional force ratios, useful scaling ratios, and meaningful comparison relations.

The dimensionless parameter $\rho Q/\mu D$ indicates the influence of fluid viscosity and can be shown to be related to the Reynolds number. On the basis of previous research (5, 6) this parameter can be considered to have no significant influence on the energy dissipation by a bed of rock riprap. Subsequent experiments of this study confirm this assumption.

Study of a dimensionless form Froude number, $\rho Q^2/[g(\rho_s - \rho)D^5]$, would disclose that, all other factors being constant in comparisons, a relatively large variation in ρ_s would be required to bring about a significant change in the Froude number. Small variations in specific gravities of rock will not be important.

A meaningful form of the Froude number is complicated by 2 possible regimes of flow at the brink of the culvert: full-pipe flow and partly full flow. For full-pipe flow, $Q/D^{2.5}$ is a commonly accepted term; and, because it can be related to partly full flow through

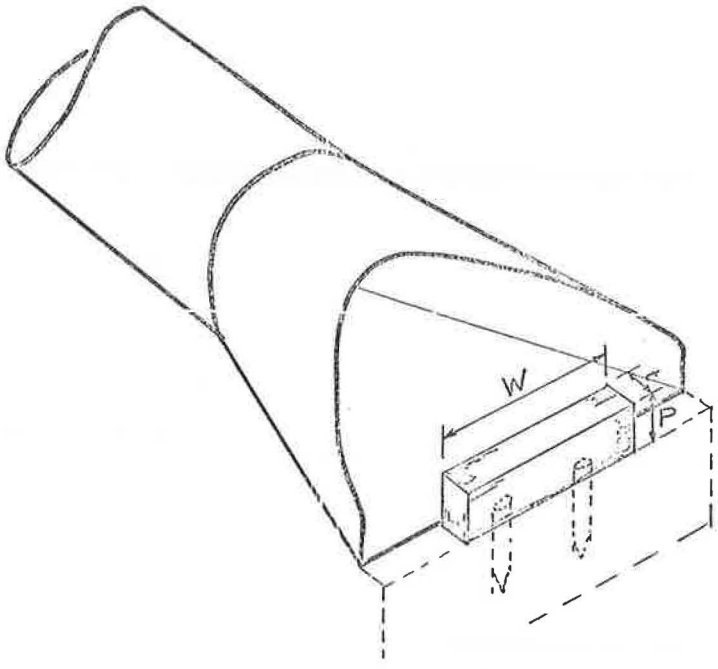

Figure 3. Dimensions and location of sill.

dimensionless ratios, it will be used for this study. This term has dimensions of $ft^{1/2}/sec$ because $\sqrt{g}$ has been dropped from the denominator.

This study is limited to a culvert with a zero slope. This should present no difficulty in making comparisons with sloped culverts by using $Q/D^{2.5}$ (sometimes called the discharge factor) as long as the pipe is flowing full. However, for partly full and a given discharge, a pipe with a steep slope would have a jet of a higher $V/d_b^{0.5}$ value than that which would occur for the jet of this same rate of flow in a pipe with a zero slope. Just what effect the higher momentum jet in the steep pipe would have will not be determined. As long as the culvert slope is "mild" the difference would probably be slight.

The study is confined to the use of rock with a Corey shape factor of approximately one (i.e., the length, breadth, and thickness of a rock are quite comparable). Nonscour or controlled scour of the riprap bed is required as a precondition for design. This sets the parameter, d_s, equal to 0 or 1 or 2 times d. For this study, the slope of the riprap bed is to be considered to be horizontal.

From the review of literature (1, 3, 4, 8) and field and laboratory observations, a limitation can be made regarding tail-water without putting too significant a restriction on the usefulness of the data gathered from this study. For the large majority of situations in the field the natural channel, downstream from the rock-basin energy dissipator, is wider than the basin itself. This results in a channel depth of flow less than that in the rock basin. As long as the rock in the basin is fully innundated (i.e., rock is then being lifted by full buoyant force), the most critical case of scour within the rock basin is being realized. This is so because an increase in depth of backwater on the rocks immediately begins to reduce the jet velocity and provides a cushion for energy dissipation.

However, because the jet, when so submerged, $d_T > D$, does not diffuse so readily as when free, the subsequent velocities in the downstream section of the basin and consequently in the following channel can be greater than when there is no tailwater. This would be a less frequently occurring situation. Therefore, the only tailwater condition considered in this study was less than the depth of flow on the rock basin. A barrier

was placed at the end of the rock basin to ensure that the rock was fully submerged during a test.

EXPERIMENTAL STUDIES

Laboratory Model

Model studies were conducted in a 12-ft long, 6-ft wide and 2-ft high wooden flume. The culvert models were of smooth plastic pipe with 1.75-, 3-, and 6-in. inside diameters. Fiberglass models of the standard concrete end flare used by the South Dakota Department of Highways were used to simulate the culvert end conditions (Fig. 1).

Rock of the following sizes (ASTM standard sieve sizes) was used as riprap:

Size (in.)	Passing Sieve (in.)	Retained on Sieve (in.)
0.500	0.500	0.375
0.525	0.525	0.44
0.750	0.750	0.625
0.875	0.875	0.75
1.000	1.000	0.875
1.500	1.500	1.25
2.000	2.000	1.75
3.000	3.000	2.50

Separate tests were made by using quarried rock (crushed, angular limestone with an average apparent specific gravity of 2.69) and field rock (rounded conglomerate shales, quartz, and occasionally sandstone, with average apparent specific gravity of about 2.63). The rock riprap of a selected size was dumped in a basin to form a horizontal riprap bed level with the pipe invert. Placing of some of the rock by hand was required to attain a level bed.

Flows

The rock bed was subjected to different flow conditions. Average velocities were determined at required transverse sections by dividing the total flow by measured cross-sectional areas. Where possible, the velocity of flow was checked with an Ott current meter. Water elevations and bed elevations were determined with a point gage. The flows at which movement of rocks was imminent (i.e., incipient motion) along with those for 1-d and 2-d scour to occur were noted. (Scour depths equal to the size of the riprap were referred to as 1-d scour, and scour depths equal to twice the size of the riprap were referrred to as 2-d scour.)

Observing the flow patterns made it possible to determine the limits of the boundaries of the basin required for no erosion outside of the basin. The effectiveness of these selected boundaries was checked by placing fine sand (passing ASTM sieve no. 30) along the outside of these boundaries and by directing the flow over the basin again. The erosion pattern on this sand confirmed the proper basin boundaries.

Sills

Because of the long testing procedure adopted with any one size of rock, it was decided to select just one size of sill and compare its performance with the various angular and rounded rocks. The selection was based on observations using the 6-in. pipe and sills of lengths W equal to 2-D, 1½-D, 1-D, and ¾-D. The 2-D length stretched completely across the end of the flared-end outlet.

Each length was observed with 5 different heights, P, equal to 0.1-D, 0.2-D, 0.25-D, 0.3-D, and 0.4-D. It was discovered that the thickness of the sill was of no concern from a hydraulic standpoint because, even at the lowest flows, the water sprung clear from the sides and top of the sill at the upstream edges. The sills used had a thickness of 0.1-D.

ANALYSIS OF DATA

Model Similitude

Whether reliable similitude could actually be attained with rocks was of great concern. However, comparisons of data taken clearly indicated the similarity of performance of the 1.75-, 3- and 6-in. models. When the reliability of this similitude was established, subsequent tests were conducted by using the 6-in. model.

Geometry of the Basin

Observations during the numerous tests made it clear that the width of the basin at the flared-end outlet must be at least equal to 3-D. This was necessary to prevent scouring by the eddies on either side of the jet rotating in opposite directions. A divergence ratio of 1:3 was needed to contain any permitted scour from the culvert jet at high as well as at low flows. This shape of basin also prevented the scouring of any fine sand placed outside the basin. The desirable depth of the rock basin is equal to two times the maximum rock size of the armor plus the depth of the filter blanket required below. Filter blanket design procedures are well defined elsewhere (7, 9).

Dimensionless Scour and Energy-Dissipating Relations

Some of the main considerations of this study can be reduced to an equation relating dimensionless parameters and a conventional expression of Froude number.

$$L/D = f[(Q/D^{2.5}),\ (D/d),\ (v/V_p),\ (d_s/D)]$$

When the data are reduced to this dimensionless form and plotted in the manner shown in Figure 4 and points of incipient motion, 1-d scour, and 2-d scour are noted, a great deal is revealed about the relationship of these variables.

Plots of this type were made for angular rock, with and without sills, and for rounded rock, with and without sills. These types of plots could be used for design purposes. However, because they present so much information in such detailed form they are not considered the most convenient manner of data presentation for design criteria. Ultimately, tabulated information was extracted from these plots and is given later in this report.

Length of the Basin

The proper length of a rock basin, as considered in this study, would (a) reduce the velocity of pipe flow to a tolerable or noneroding velocity on the downstream channel and (b) be long enough to contain the scour hole and dune material if any scouring is to be permitted.

The dimensionless plots shown in Figure 4 were made for reductions of velocity of flow to $0.5V_p$, $0.4V_p$, and $0.3V_p$ when no sill was used and to $0.3V_p$ and $0.2V_p$ when the sill was used. V_p is the average velocity in the pipe calculated from measured discharge Q, and the depth of flow, d_p, measured 2.5-D upstream from the brink of the circular pipe.

Further reductions in velocities were limited because the jet had diverged and contacted the sides of the flume. Use of a wider flume or a smaller culvert model would have permitted further velocity reduction studies. However, because the velocity reductions are based on the average velocity in the pipe 2.5-D upstream from the brink and because this velocity is less than the brink velocity or critical velocity, the percentage of velocity reduction is greater for partly full pipes than one might think if accustomed to working with brink or critical velocities.

The use of the design tables for partly full pipe flow when the brink of critical velocity is prescribed (which probably is the more usual situation) is facilitated by curves relating depth of flow in pipe, brink depth, and critical depth dimensionlessly to the discharge factor (Fig. 5). Figure 5 used with the following data for partly filled and standard pipes should enable the designer to enter the design tables based on V_p. Area ratios of partly filled pipes for depth-diameter ratios are as follows:

d_s/D	a/A
0.0	0.000
0.1	0.052
0.2	0.143
0.3	0.252
0.4	0.373
0.5	0.500
0.6	0.626
0.7	0.748
0.8	0.858
0.9	0.950
1.0	1.000

Areas and $D^{2.5}$ for standard pipe sizes are as follows:

Diameter (in.)	$D^{2.5}$ ($ft^{2.5}$)	A (ft^2)
12	1.00	0.785
18	2.76	1.77
24	5.65	3.14
30	9.88	4.91
36	15.6	7.06
42	22.9	9.62
48	32.0	12.6
54	43.0	15.9
60	55.9	19.6
66	70.9	23.7
72	88.2	28.3

Examples of various applications of these criteria to design will be presented later.

If no scouring is to be permitted within the basin, then the length required to attain a desired velocity reduction governs the length of the basin. If a scour hole is to be allowed, however, the velocity just downstream from the dune may be sufficiently small that no additional length of basin is needed. In this case the length that is needed to contain the scour hole and dune governs the required length of the rock basin. These lengths to contain holes of controlled depth of scour can be generalized as follows:

1. For 1-d scour, a length of 4-D is needed to contain the scour hole and dune (an L_s of about 2-D and an L_d of about 4-D); and
2. For 2-d scour, a length of 6-D is needed to contain the scour hole and dune (an L_s of about 3-D and an L_d of about 6-D).

These criteria are reflected in the data given in the design tables. The dimensionless lengths, L/D, for no-scour are given below the single underlined values and above the double underlined values. If a 2-d scour is to be allowed for a given velocity reduction, the proper L/D values for a given discharge factor are given below double underlined values and above triple underlined values. These dimensionless lengths are given for various rock sizes expressed in a dimensionless form, D/d, equal to from 2 to 8.

Depth of Flow on Basin

The depth of the backwater was, for all practical purposes, identical with the depth of flow of the jet itself. This depth of flow was greatest at the culvert outlet, d_1, and diminished slightly toward the end of the basin, d_2. Because this change in downstream depth was so small, only the maximum upstream depth d_1 is given in the tables for design considerations. These depths varied from about 0.2-D for low flows without sills to 0.5-D for high flows with sills.

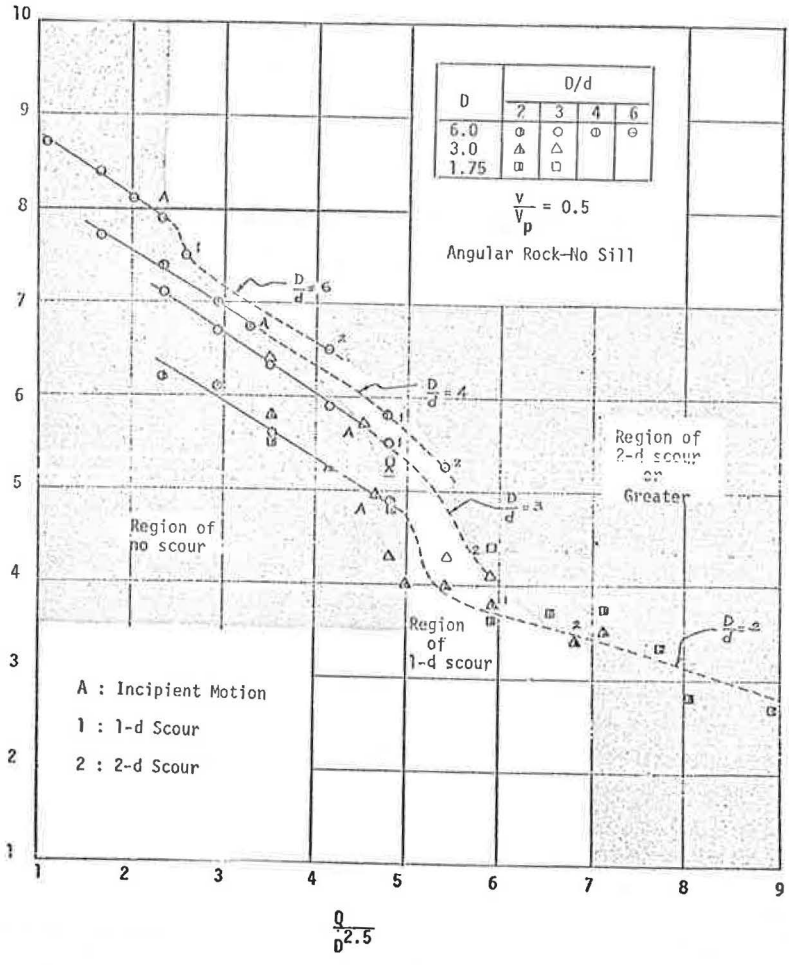

Figure 4. Dimensionless scour and energy-dissipating relations.

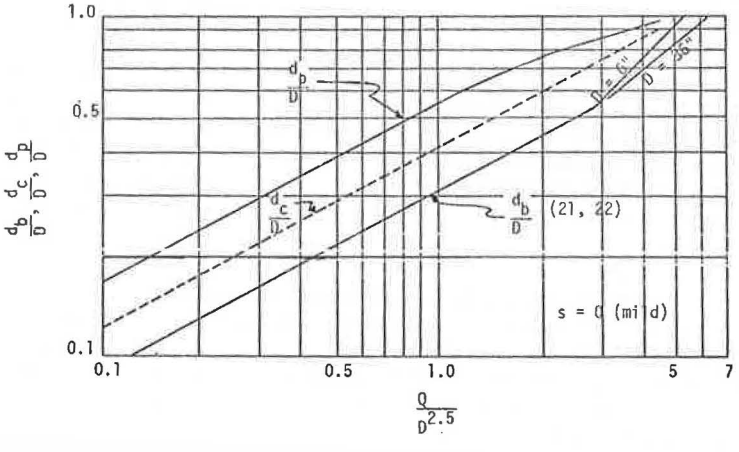

Figure 5. Dimensionless depths of flow versus discharge factor.

TABLE 1

LENGTH RATIO OF BASIN FOR VELOCITY REDUCTION RATIO OF 0.5, NO SILL

$Q/D^{2.5}$	d_1/D_{max}	L/D for v/V_p = 0.5				
		8 D/d	6 D/d	4 D/d	3 D/d	2 D/d
1.00	0.25	9.10	8.65	8.00	7.75	6.90
1.25	0.25	8.95	8.50	7.85	7.60	6.75
1.50	0.25	8.80	8.35	7.70	7.45	6.65
1.75	0.25	8.70	8.25	7.60	7.30	6.50
2.00	0.25	8.50	8.15	7.50	7.20	6.40
2.25	0.25	7.70	8.00	7.30	7.00	6.25
2.50	0.25	7.45	7.85	7.15	6.90	6.10
2.75	0.25		7.60	7.05	6.75	5.95
3.00	0.25		7.30	6.90	6.60	5.85
3.25	0.25		7.05	6.00	6.45	5.70
3.50	0.25		6.90	6.65	6.30	5.60
3.75	0.25		6.70	6.45	6.20	5.45
4.00	0.25		6.55	6.25	6.05	5.35
4.25	0.25		6.40	6.10	5.95	5.20
4.50	0.25			6.00	5.70	5.05
4.75	0.25			6.00	6.00	4.95
5.00	0.25			6.00	6.00	4.80
5.25	0.25			6.00	6.00	4.20
5.50	0.25			6.00	6.00	4.00
5.75	0.25			6.00	6.00	4.00
6.00	0.25				6.00	4.00
6.25	0.25				6.00	4.00
6.50	0.25					4.00
7.00	0.25					4.00
7.50	0.25					6.00
8.00	0.25					6.00

Note: W_b = 3D and ℓ_1/ℓ_2 = 1:3.

TABLE 2

LENGTH RATIO OF BASIN FOR VELOCITY REDUCTION RATIO OF 0.4, NO SILL

$Q/D^{2.5}$	d_1/D_{max}	L/D for v/V_p = 0.4				
		8 D/d	6 D/d	4 D/d	3 D/d	2 D/d
1.00	0.25	10.95	10.35	9.60	9.40	9.05
1.25	0.25	10.85	10.15	9.45	9.20	8.90
1.50	0.25	10.70	10.00	9.35	9.10	8.75
1.75	0.25	10.55	9.85	9.20	9.00	8.55
2.00	0.25	10.30	9.75	9.10	8.85	8.40
2.25	0.25	9.75	9.55	9.00	8.70	8.25
2.50	0.25	9.60	9.40	8.85	8.60	8.05
2.75	0.25		9.30	8.75	8.45	7.95
3.00	0.25		9.20	8.60	8.35	7.75
3.25	0.25		9.15	8.50	8.15	7.55
3.50	0.25		9.05	8.40	8.05	7.40
3.75	0.25		9.05	7.85	7.90	7.20
4.00	0.25		8.95	7.50	7.75	7.05
4.25	0.25		8.85	7.25	7.65	6.90
4.50	0.25			7.35	7.00	6.75
4.75	0.25			6.80	7.05	6.55
5.00				6.65	6.80	6.40
5.25	0.25			6.45	6.30	6.10
5.50	0.25			6.35	6.10	5.85
5.75	0.25			6.30	6.00	5.70
6.00	0.25				6.00	5.45
6.25	0.25				6.00	5.30
6.50	0.25					5.15
7.00						4.80
7.50	0.25					6.00
8.00	0.25					6.00

Note: W_b = 3D and ℓ_1/ℓ_2 = 1:3.

TABLE 3

LENGTH RATIO OF BASIN FOR VELOCITY REDUCTION RATIO OF 0.3, NO SILL

$Q/D^{2.5}$	d_1/D_{max}	L/D for v/V_p = 0.3				
		8 D/d	6 D/d	4 D/d	3 D/d	2 D/d
1.00	0.25	12.80	11.90	11.20	10.85	10.65
1.25	0.25	12.65	11.75	11.05	10.90	10.45
1.50	0.25	12.50	11.55	10.95	10.75	10.30
1.75	0.25	12.35	11.45	10.85	10.65	10.10
2.00	0.25	12.10	11.25	10.70	10.50	10.00
2.25	0.25	11.85	11.05	10.60	10.35	9.80
2.50	0.25	11.80	10.95	10.45	10.25	9.65
2.75	0.25	11.75	10.80	10.30	10.10	9.50
3.00	0.25		10.70	10.20	9.95	9.30
3.25	0.25		10.65	10.10	9.80	9.10
3.50	0.25		10.60	10.00	9.65	9.00
3.75	0.25		10.60	9.40	9.50	8.80
4.00	0.25		10.50	9.10	9.45	8.65
4.25	0.25		10.40	8.85	9.30	8.50
4.50	0.25			8.60	9.00	8.30
4.75	0.25			8.40	8.80	8.15
5.00	0.25			8.20	8.35	7.95
5.25	0.25			8.05	7.90	7.65
5.50	0.25			7.95	7.75	7.40
5.75	0.25			7.90	7.60	7.20
6.00	0.25				7.50	7.05
6.25	0.25				7.40	6.90
6.50	0.25					6.75
7.00	0.25					6.40
7.50	0.25					6.00
8.00	0.25					6.00

Note: W_b = 3D and ℓ_1/ℓ_2 = 1:3.

TABLE 4

LENGTH RATIO OF BASIN FOR VELOCITY REDUCTION RATIO OF 0.3, WITH SILL

$Q/D^{2.5}$	d_1/D_{max}	L/D for v/V_p = 0.3				
		8 D/d	6 D/d	4 D/d	3 D/d	2 D/d
1.00	0.4	9.20	8.75	7.80	7.65	7.20
1.25	0.4	9.00	8.50	7.65	7.50	7.00
1.50	0.4	8.75	8.25	7.50	7.35	6.80
1.75	0.4	8.50	8.00	7.30	7.10	6.60
2.00	0.4	8.30	7.80	7.25	7.05	6.50
2.25	0.4	6.00	7.50	7.00	6.85	6.30
2.50	0.4	6.00	6.70	6.80	6.65	6.15
2.75	0.4		5.75	6.75	6.50	5.85
3.00	0.4		4.75	6.60	6.35	5.80
3.25	0.4		4.05	5.20	6.20	5.60
3.50	0.4		4.00	5.05	6.00	5.40
3.75	0.4		4.00	5.00	5.70	5.05
4.00	0.4		6.00	6.00	5.70	5.05
4.25	0.4		6.00	6.00	5.50	4.90
4.50	0.4		6.00	6.00	4.90	4.70
4.75	0.4			6.00	4.70	4.50
5.00	0.4			6.00	4.60	4.35
5.25	0.4			6.00	4.55	4.25
5.50	0.4			6.00	4.50	4.10
5.75	0.4				6.00	4.05
6.00	0.4				6.00	4.00
6.25	0.4				6.00	4.00
6.50	0.4				6.00	4.00
7.00	0.4				6.00	4.00
7.50	0.4				6.00	4.00
8.00	0.4				6.00	4.00
10.00	0.5				6.00	4.00
11.00	0.5					4.00
13.50	0.5					6.00

Note: W_b = 3D and ℓ_1/ℓ_2 = 1:1.75.

Comparison of Rounded and Angular Rock

In this study the "hydraulic" performance of one type of rock compared to another is based on its stability to movement and ability to dissipate the flow energy.

The angular rock, as would be expected, is slightly more effective in dissipating energy, but the difference is so slight as to be insignificant. At any rate, when the tables were prepared for design purposes, the length specified for a proper velocity reduction is sufficient that rounded rock will accomplish this task.

Considering the superior ability of angular rock to interlock, one would expect the rounded rock to move before equivalent-sized angular rock. However, this was not noticeable in this study. The complicated interplay of lift, drag, gravity, and other body forces gives the rounded rock as good an advantage as the angular. This was partly explained when the specific gravity of the rock was determined. Even though the angular rock had a greater specific gravity, it weighed less per rock than the rounded. It follows that, if rock is selected to perform according to size, as in this study, rounded field rock will be as stable as angular quarried rock.

When the begin-scour or incipient motion of a rock-bed material as a function of $Q/D^{2.5}$ was considered as a criterion, the values of this study compare favorably with those given by Laushey (3). When compared on a velocity basis, the point of incipient motion agrees with the Isbash formula (2).

TABLE 5

LENGTH RATIO OF BASIN FOR VELOCITY REDUCTION RATIO OF 0.2

$Q/D^{2.5}$	d_1/D_{max}	L/D for v/V_p = 0.2				
		8 D/d	6 D/d	4 D/d	3 D/d	2 D/d
1.00	0.4	12.95	12.00	11.40	10.40	9.25
1.25	0.4	12.90	11.90	11.20	10.20	9.15
1.50	0.4	12.85	11.80	11.00	10.05	9.00
1.75	0.4	12.80	11.75	10.85	9.90	8.90
2.00	0.4	12.75	11.65	10.65	9.75	8.80
2.25	0.4	10.90	11.60	10.50	9.60	8.65
2.50	0.4	8.70	11.40	10.30	9.45	8.55
2.75	0.4		11.15	10.10	9.30	8.40
3.00	0.4		10.50	9.90	9.15	8.30
3.25	0.4		8.90	9.75	9.00	8.15
3.50	0.4		6.75	9.55	8.85	8.00
3.75	0.4		6.45	9.45	8.65	7.85
4.00	0.4		6.15	9.30	8.50	7.75
4.25	0.4		6.00	9.20	8.25	7.60
4.50	0.4		6.00	9.10	7.80	7.45
4.75	0.4			8.75	7.50	7.35
5.00	0.4			7.50	7.35	7.20
5.25	0.4			6.75	7.20	7.00
5.50	0.4			6.25	7.05	6.60
5.75	0.4				6.75	6.25
6.00	0.4				6.45	6.00
6.25	0.4				6.10	5.75
6.50	0.4				6.00	5.55
7.00	0.4				6.00	5.30
7.50	0.4				6.00	5.20
8.00	0.4				6.00	5.00
10.00	0.5				6.00	5.00
11.00	0.5					5.00
13.50	0.5					6.00

Note: W_b = 3D and ℓ_1/ℓ_2 = 1:1.75.

Figure 4 shows that the larger rock size appears to dissipate the energy of the flow better than the smaller rock size. The spreading of the flow is more efficient with the larger rock size. A particular rock size cannot be expected to be stable beyond a certain value of $Q/D^{2.5}$. Beyond this value, some structure (such as a sill) is necessary for satisfactory stability and energy dissipation. This is significant for the use of graded rock. The design must be based on the smaller rock size when graded rock is used.

Sill Performance

When flow patterns were compared for various combinations of lengths and heights of sills, the final choice to be studied was a 6-in. sill length (W = 1-D) with a height of 1.8 in. (P = 0.3-D).

The experimenters were reluctant not to pursue further the study of some of the other sills. For example, a 9-in. sill with a height of 1.8 in. developed the most efficient energy-dissipating action in the form of a jump within the flared-end transition. However, with this type of action went some scouring effects on the highway side-slope area.

The 12-in. sill (W = 2-D), although also effective in producing a confined jump, was not studied in detail because there was no way silt and debris could be swept away around the sides at low flows.

The sill causes the jet to diverge more rapidly. The divergence angle that will encompass the jet streams and any resulting scour pattern with the sill is ℓ_1/ℓ_2 = 1:1.75. W_B = 3-D is still sufficient.

Although the sill was not effective in advancing the discharge factor at which incipient motion occurred, it did retard scouring with respect to a given flow without a sill. For a given flow the sill reduced the length of the distance to the end of scour and to the end of the dune. The sill was effective in reducing the length required to decrease the culvert velocity to a specified percentage when compared with riprap action and no-sill condition.

The 1-d scour hole requires a length of 4-D to contain it. The 2-d scour hole requires a length of 6-D. These are the same general lengths as were specified for scour with no sill. However, these holes with the sill are wider than without. The sill spread the energy out over a larger area. Even though the length of the scour holes had not changed considerably, slightly more volume of rock had been removed. The energy involved in producing a wider hole along with energy lost in the sill-defected jet results in an overall shorter basin for a given velocity reduction.

Comparisons of the amount of required riprap show that more than one-third less riprap is needed with a sill as compared with the same protection offered by riprap without a sill. The other advantage of the sill, of course, is that, for a given size of rock with sill, a greater flow can be allowed through a culvert for a given allowable scour.

DESIGN OF ROCK BASINS

Within the limits of the experimental results of this report, a basin formed of rock or rock and a sill can be designed to control scour and dissipate the flow to a specified average velocity tolerable by the downstream channel. Using the design tables and Figure 5 and knowing the culvert discharge and diameter and the desired downstream channel velocity, the designer can determine the proper length of the basin, divergence angle, size of rock, approximate basin depth of flow, whether a sill will be required, and whether a no-scour basin or a basin of controlled depth of 1-d or 2-d can be attained.

The depth of flow, as measured in the model culvert, and the subsequent velocity ratios v/V_p are referenced to a position 2.5-D upstream from the brink of the culvert (d_p, v_p). Studies were also limited to the model culvert in a horizontal (s = 0) position. Figure 5 has been prepared to enable the designer to enter the design tables for partly full pipe flow. Figure 5 also allows the designer to compare the brink depth of flow for the horizontal laboratory model pipe with the actual depth of flow at the brink of the culvert of the field case under study.

The following examples will best illustrate how the tables and Figure 5 are used to arrive at basic dimensions of a rock basin.

Example 1

Assume that, for a culvert, D = 3 ft, Q = 60 ft ^{3}/sec, v_{ch} = 3 fps, and $Q/D^{2.5}$ = 60/15.6 = 3.85.

Figure 5 shows that the pipe flows partly full. $d_p/D \sim 0.9$, $a/A = 0.95$, $A = 7.06$ ft^2, $A_p = (0.95)(7.06) \sim 6.7$ ft^2, $V_p = Q/A_p = (60/6.7) \sim 9$ fps, and $v_{ch}/V_p = 3/9 = 0.33$. For $Q/D^{2.5} = 4.00$, L/D = 9.45 for D/d = 3 (Table 3).

Therefore, with 12-in. rock the basin could have a length of about 30 ft, W_b = 9 ft, ℓ_1/ℓ_2 = 1:3, depth of flow on the basin is 9 in. (0.25-D), and no scour is expected. If a 9-in. rock is used (D/d = 4), 1-d scour would occur, but the basin would not have to be quite so long (L/D = 9.1). The action within the scour hole and over the dune would dissipate some energy. With 6-in. rock (D/d = 6), 2-d scour would occur, and the basin should be a little longer (L/D = 10.5). If 18-in. rock were available (D/d = 2), the basin could be shorter (L/D = 8.65), and no scour would occur.

A study of Figure 4 and the tables (around the regions between incipient motion and 1-d scour) shows that until a scour hole has developed the contribution of the hole and dune to dissipate energy is not available. Within these regions of flow, a lower discharge can actually require a longer basin than the design tables show for a higher discharge. This could be true until the higher discharge had formed the hole and dune.

Example 2

If the 60 ft ^{3}/sec in example 1 is for a1- or 2-year occurrence and if a recurrence factor of 2 is assumed, then Q = 120 ft 3/sec, D = 3 ft, v_{oh} = 3 fps, and $Q/D^{2.5}$ = 120/15.6 = 7.7.

Figure 5 shows the pipe flows full. A_p = 7.06 ft^2, V_p = 120/7.06 = 17 fps, and v_{oh}/V_p = 3/17 ~ 0.18, say 0.2. The design tables show that, without a sill, 18-in. rock (D/d = 2) or larger would be needed to control the flow within the limits of 2-d scour or less. For $Q/D^{2.5}$ = 8.00, L/D = 6.00 for D/d = 3 (Table 5).

With a sill and 12-in. rock, the scour could be kept at 2-d. The sill with 18-in. rock could control the scour to 1-d depth, and the basin might be shortened to a length of 5.00-D. The maximum expected depth of flow on these basins would be 0.4-D. The divergence angle with the sill is 1:1.75. The sill has a length of 1-D (3 ft) and a height of 0.3-D (0.9 ft); W_b = 3D = 9 ft. If the rock in this example is larger than available or the scour greater than desired, then a larger culvert would be needed.

Example 3

Assume that, for a culvert, Q = 120 ft ^{3}/sec, D = 4 ft, v_{oh} = 3 fps, and $Q/D^{2.5}$ = 120/32 = 3.75.

Figure 5 shows that the pipe flows partly full. d_p/D = 0.9, a/A = 0.95, A = 12.6 ft^2, A_p = (0.95) (12.6) = 11.95, V_p = 120/11.95 ~10 fps, and v_{oh}/V_p = 0.3.

For $Q/D^{2.5}$ = 3.75 and with a sill for 1-d scour and 8-in. rock (D/d = 6), L/D = 4.00; for no scour and 16-in. rock (D/d = 3), L/D = 5.70 (Table 4). d_1 = 0.4D, W_b = 3D, ℓ_1/ℓ_2 = 1:1.75, and W = 4 ft.

For $Q/D^{2.5}$ = 3.75 and with a sill for 1-d scour and 8-in. rock (D/d = 6), L/D = 4.00; for no scour and 16-in. rock (D/d = 3), L/D = 5.70 (Table 4) · d_1 = 0.4D, W_b = 3D, ℓ_1/ℓ_2 = 1:1.75, and W = 4 ft.

For $Q/D^{2.5}$ = 3.75 and without a sill for 2-d scour and 8-in. rock, L/D = 10.60; for 1-d scour and 12-in. rock, L/D = 9.40; for no scour and 16-in. rock L/D = 9.50 (Table 3). d_1 = 0.25D, W_b = 3D, and ℓ_1/ℓ_2 = 1:3,

Comparing the various rock sizes used in the basin of this flow, with and without a sill, shows the effectiveness of the sill in dispersing the jet and reducing the required length of basin.

SUMMARY AND CONCLUSIONS

Relevant to this study is the attempt to simplify the design procedure as much as possible and still keep within the realm of significance of the governing experimentally determined data. The following conclusions are made on the basis of the laboratory investigations with quarried angular rock and rounded field rock, in basins without a sill and in basins with a sill, acting at the outlet of 1.75-, 3- and 6-in. diameter circular culverts on a zero slope with a standard flared end.

1. The upstream width of the rock basin should be at least 3-D;
2. The divergence angle of the rock basin downstream from the standard flared end should be 1:3 when no sill is used and 1:1.75 when a sill is used;
3. The proper length of the basin is governed by criteria given in Tables 1 through 5 [this length is dependent on the culvert discharge, culvert diameter, size of rock, extent of permissible scour (no scour, 1-d scour, or 2-d scour), and whether a sill or no sill is to be used in conjunction with the basin at the end of the culvert flared end];
4. If rock is selected according to size by reference to square openings, and if the rock length is about equal to its width and thickness, then there is no significant difference between rounded field rock and angular quarried rock when scour stability and energy-dissipation ability are compared;
5. For given high flows, a sill of a length equal to D and a height of 0.3-D proves more effective in reducing scour and culvert velocities in a length of basin shorter than when no sill is used; and
6. Similitude of performance of rock basins can be attained with small culver models (1.75, 3, and 6 in. and rock sizes from ½ to 3 in (this similitude is apparently independent of Reynolds number).

REFERENCES

1. Argue, J. R. New Structure for Roadway Pipe Culverts. Jour. Institution of Engineers, Vol. 132, No. 6, June 1960.
2. Isbash, S. V. Construction of Dams by Depositing Rock in Running Water. Trans. Second Congress on Large Dams, Vol. 5, 1936, pp. 123-136.
3. Laushey, L. M. Design Criteria for Erosion Protection at the Outlet of Culverts., Univ. of Cincinnati, Sept. 1966.
4. McPherson, M. B., and Meredith, D. D. Factors in the Design of Culvert Energy Dissipators. Univ. of Illinois, 1963.
5. Mehrotra, S. C. Scale Effects in Model Tests of Rock Protected Structures. Univ. of Iowa, MS thesis, June 1967.
6. Parkin, A. K., Trollope, D. H., and Lawson, J. D. Rockfill Structures Subject to Water Flow. Jour. Soil Mech. and Found. Div., Proc. ASCE, Vol. 94, No. SM4, July 1968, p. 1036.
7. Sherard, J. L., Woodward, R. J., Gizienski, S. F., and Clevenger, W. A. Earth and Earth-Rock Dams. John Wiley and Sons, New York, 1963.
8. Stevens, M. A. Scour in Riprap at Culvert Outlets, Colorado State Univ., Fort Collins, PhD dissertation, 1969.
9. Design of Roadside Drainage Channels. U. S. Bureau of Public Roads, Hydraulic Engineering Circular 6, April 1962.

EVALUATION OF THREE ENERGY DISSIPATORS FOR STORM DRAIN OUTLETS

John L. Grace, Jr., and Glenn A. Pickering,
U. S. Army Engineer Waterways Experiment Station

Results of model tests of 3 commonly used energy dissipators for storm drain outlets are reported. The limiting discharges for various sized models of stilling wells, U. S. Bureau of Reclamation Type VI basins, and St. Anthony Falls stilling basins were determined. Charts were prepared for each type of energy dissipator and show the maximum recommended discharge that will result in good performance for given outlet diameters and structure widths in terms of the outlet diameter. With these charts and other known parameters, the designer can select the type of dissipator best suited to protect the outlet.

•RESEARCH previously conducted at the U. S. Army Engineer Waterways Experiment Station (WES) and reported by Bohan (1) gives generalized results for determining the extent of localized scour to be anticipated in cohesionless soils downstream from storm drain outlets. Also presented in this report are results for determining the size and extent of stone required to provide a stable horizontal blanket of riprap with top elevation the same as the outlet invert as a means of preventing localized scour. With these results the designer can estimate the expected scour and then decide on the degree of protective works that will be required. A scour hole with an appropriate cutoff wall might be permissible; riprap placed on a stable horizontal blanket may be adequate; a compromise of depth of scour and riprap may be desirable; or an energy dissipator may be required.

A field performance study that permitted observation of drainage and erosion control facilities at several Army and Air Force installations throughout the United States has been conducted by WES during the past few years. One of the results of this study was the indication that there is an urgent need for practical guidance in the selection and design of energy dissipators for drainage facilities.

Several energy dissipators have been developed for use at storm drain outlets. The research reported here was initiated as an effort to evaluate the applicability and limitations of three of the most commonly used energy dissipators: a stilling well, the U. S. Bureau of Reclamation (USBR) Type VI basin, and the St. Anthony Falls (SAF) stilling basin.

MODELS AND TEST PROCEDURES

A 1:5-scale model of a 48-in. diameter pipe outlet was used to study the various energy dissipators in a 16-ft wide, 5.5-ft deep, and 40-ft long test flume (Fig. 1). The trapezoidal channel downstream from the energy dissipators was molded in sand with side slopes of 1 on 3, and the area immediately downstream from the basin outlet was protected with riprap. A filter cloth was placed between the sand and riprap to prevent slumping of the riprap blanket. Models of the 3 energy dissipators are shown in Figure 2.

Sponsored by Committee on Surface Drainage of Highways and presented at the 50th Annual Meeting.

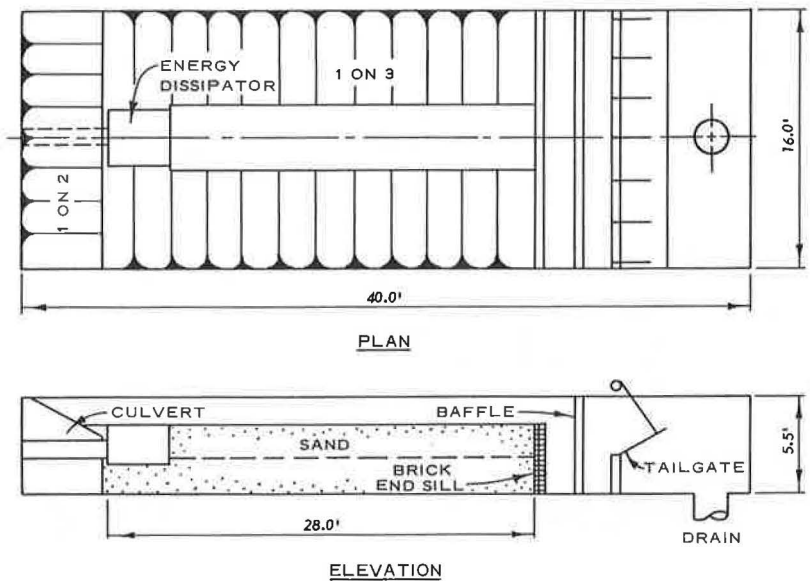

Figure 1. Experimental facilities.

Water used in the operation of the models was supplied by pumps, and discharges were measured by means of calibrated venturi meters. Steel rails set to grade along the sides of the flume provided a reference plane for measuring devices. Water surface elevations were measured by means of point gages, and velocities were measured with a pitot tube. Tailwater elevations were regulated by a gate at the downstream end of the flume.

Before each series of tests was begun, the channel downstream of the energy dissipator was molded to the trapezoidal shape and flooded slowly in order to prevent erosion of the stream bed. The procedure used to determine the maximum or limiting discharge with a particular energy dissipator was to set a low discharge, observe the flow conditions with various tailwater depths, and then increase the discharge and repeat until the flow conditions were considered unacceptable. The highest discharge that was considered satisfactory was reset and allowed to run for a given period of time to determine whether the riprap downstream from the dissipator was sufficiently large to prevent failure. Also, in some tests, velocity and wave height measurements were made and sand scour patterns were recorded. If wave heights, velocities, or scour or all of these downstream from the riprap were excessive with this flow, the discharge was reduced and the procedure repeated until the flow was considered acceptable. Photographs of flow conditions, both satisfactory and unsatisfactory, were made with each design.

The general design practice that has developed in recent years relative to highway culverts results in the conclusion that most of these structures convey discharges 4 or 5 times the diameter of the culvert raised to the $\frac{5}{2}$ power. The magnitude of this quasi-dimensionless parameter will vary depending on the particular site or structure, but it is a useful descriptive parameter for classifying the relative design capacity of such structures. It is also related to the Froude number of flow commonly used in open-channel hydraulics. For example, the Froude number of full-pipe flow at the outlet of a circular pipe is unity for a $Q/D_o^{5/2}$ ratio of 4.5. Thus, the main objective of this study was to determine the limiting $Q/D_o^{5/2}$ ratio for various sizes of each of the stilling devices investigated.

STILLING WELL

The stilling well consists of a vertical section of circular pipe affixed to the outlet end of a storm drain outfall. Components of a typical stilling well are shown in Figure 3. In order to be effective, the top of the well must be located at the elevation of the invert of a stable natural drainage basin or artificial channel. The area adjacent to the top of the well, including the side slopes and outfall ditch, is usually protected by riprap or paving.

Energy dissipation is accomplished by the expansion of flow that occurs in the well, the impact of the fluid on the base and wall of the stilling well opposite the pipe outlet, and the change in momentum resulting from redirection of the flow. Important advantages of an energy dissipator of this type are that energy loss is accomplished without the necessity for maintaining a specified tailwater depth in the vicinity of the outlet and that construction is simpler and less expensive because the concrete formwork necessary for a conventional basin is eliminated.

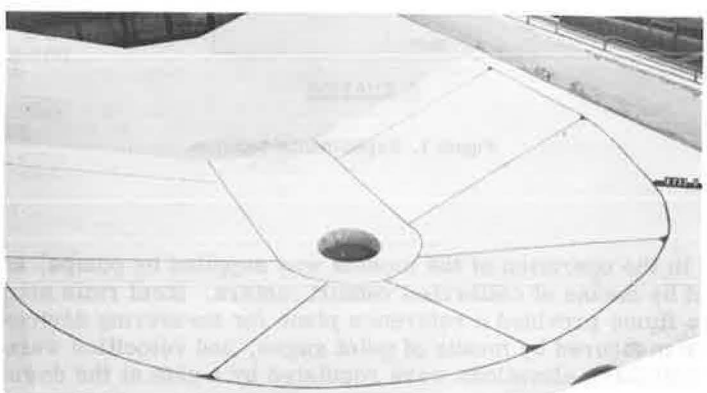

stilling well

USBR Type VI basin

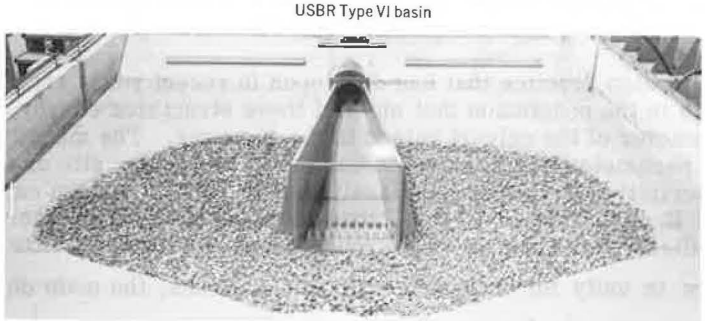

SAF stilling basin

Figure 2. Models of stilling well, USBR Type VI, and SAF stilling basin.

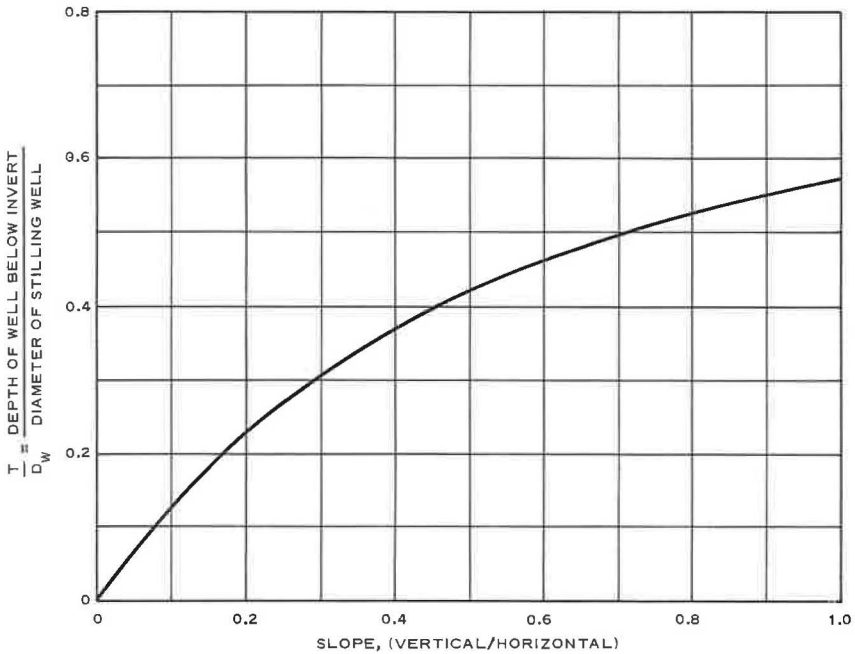

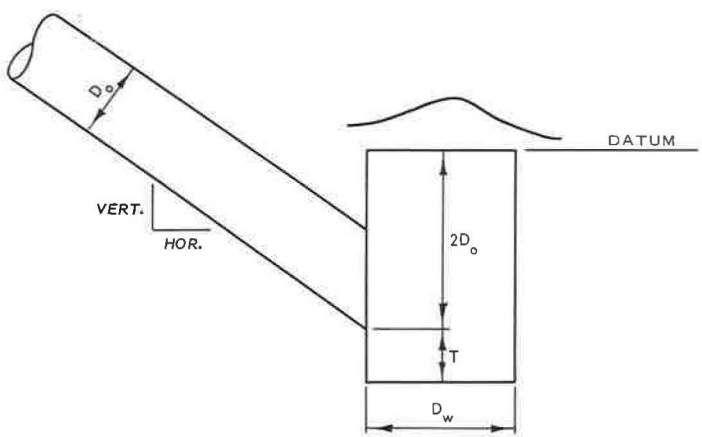

Figure 3. Stilling well.

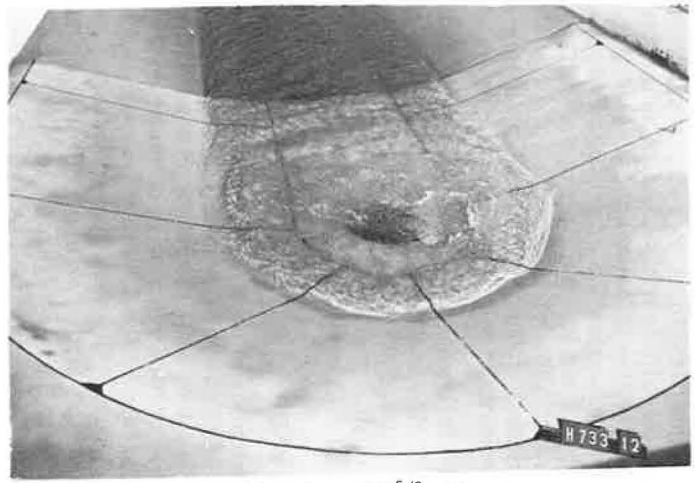

(a) satisfactory, $Q/D_o^{5/2} = 3.5$

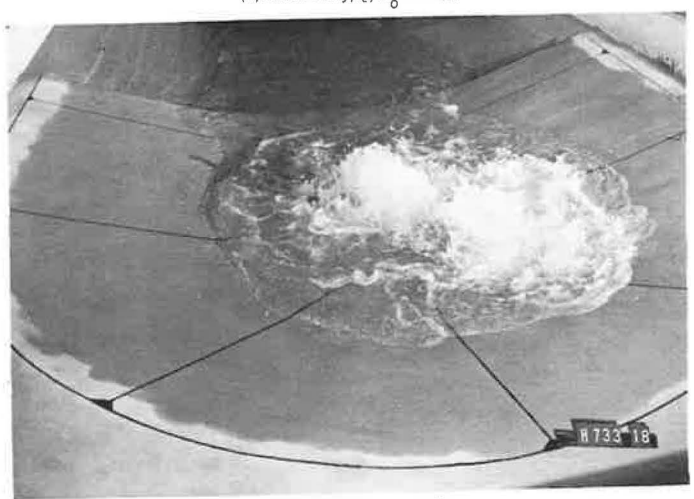

(b) unsatisfactory, $Q/D_o^{5/2} = 10$

Figure 4. Flow conditions with stilling well.

The stilling wells tested in this study were designed according to recommendations reported by Grace (2) from tests conducted on 9 model stilling wells. The recommended height of stilling well above the invert of the incoming pipe is 2 times the diameter of the incoming pipe, D_o. The recommended depth of well below the invert of the incoming pipe is dependent on the slope of the incoming pipe and the diameter of the stilling well, D_w, and can be determined from the plot shown in Figure 3.

Flow conditions, both satisfactory and unsatisfactory, that resulted with a stilling well diameter twice that of the incoming pipe are shown in Figure 4. The subject model investigations indicated that satisfactory performance could be maintained for $Q/D_o^{5/2}$ ratios as large as 2.0, 3.5, 5.0, and 10.0 respectively and stilling wells with diameters 1, 2, 3, and 5 times that of the incoming storm drain. These ratios were used to calculate the relations among actual storm drain diameter, well diameter, and maximum discharge recommended for selection and design of stilling wells (Fig. 5).

USBR TYPE VI BASIN

The Bureau of Reclamation impact-energy dissipator is an effective stilling device even with deficient tailwater. Dissipation is accomplished by the impact of the incoming jet on the vertical hanging baffle and by eddies that are formed by changing the direction of the jet after it strikes the baffle. Best hydraulic action is obtained when the tailwater elevation approaches, but does not exceed, a level halfway up the height of the baffle. Excessive tailwater, on the other hand, will cause some flow to pass over the top of the baffle. This should be avoided if possible. With velocities less than 2 fps, the incoming jet could possibly ride underneath the hanging baffle. Thus, this basin is not recommended with velocities less than 2 fps. It is believed that the possibility of cavitation or impact damage to the baffle can be prevented if an entrance velocity of 50 fps is not exceeded with this device. The general arrangement of the Type VI basin and the dimensional requirements based on the width of the structure are shown in Figure 6.

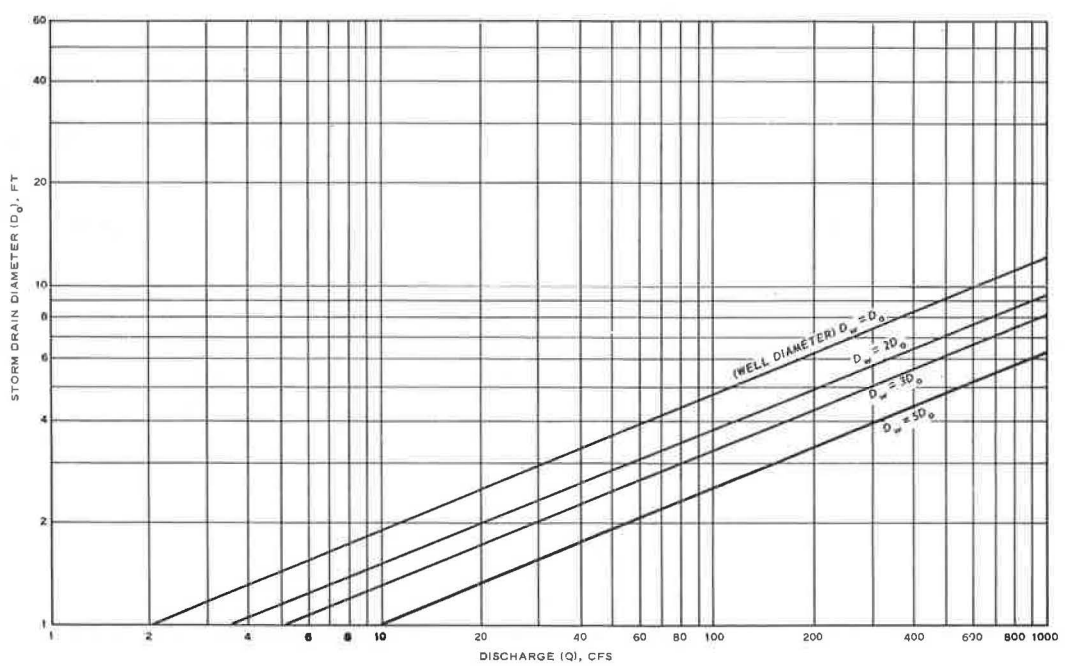

Figure 5. Storm drain diameter versus discharge for stilling well.

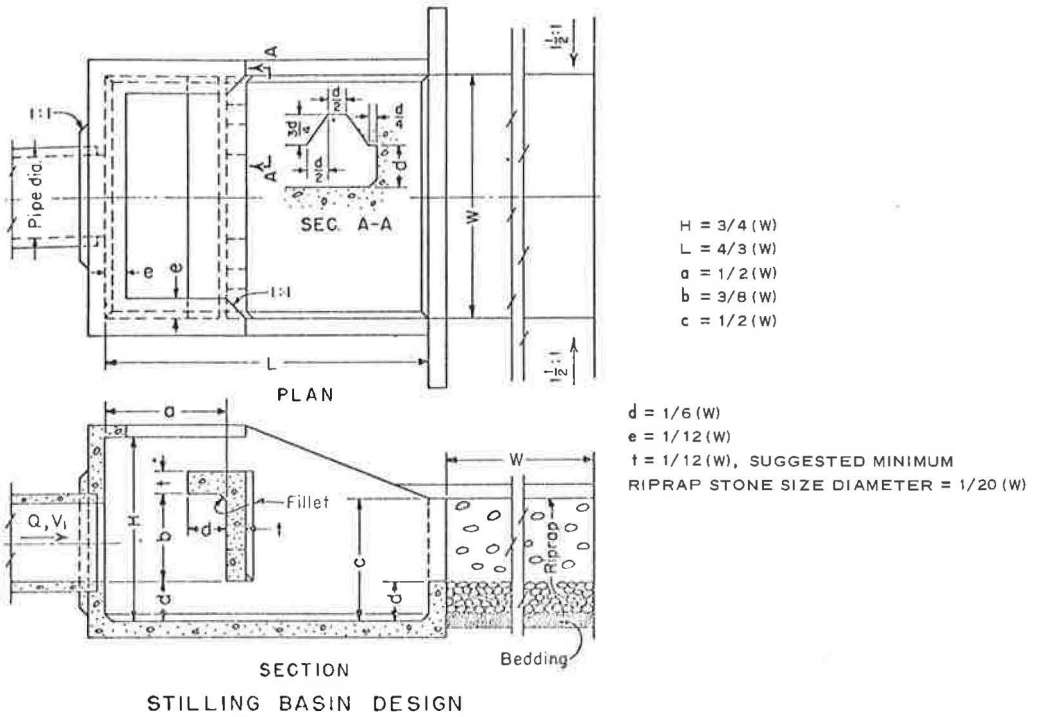

Figure 6. USBR Type VI basin.

Only one model was used to test the limitations of the Type VI basin. The model was 3.3 ft wide and was designed according to recommendations reported by Beichley (3). Results of tests with the subject model basin, which had a width 4 times the diameter of the incoming pipe, indicated that the limiting $Q/D_o^{5/2}$ ratio was approximately 7.6. This value was slightly less than that recommended by Beichley (3) in terms of the Froude number at the storm drain outlet. However, the results from his study were used, with slight adjustment, to obtain conservative design criteria for other basin widths. The results of this analysis are given in Table 1.

Photographs of flow conditions with the model basin are shown in Figure 7. The recommended relations among discharge, outlet diameters, and basin widths are shown in Figure 8. If the discharge and the size of the incoming pipe are known, the required width of the basin can be determined from the design curves, and other dimensions of the basin can be computed from the equations shown in Figure 6.

TABLE 1

RESULTS OF TESTS WITH ENERGY DISSIPATORS

Type of Energy Dissipator	Relative Diameter, D_o	Maximum $Q/D_o^{5/2}$
Stilling well	1	2.0
	2	3.5
	3	5.0
	5	10.0
USBR Type VI basin	1	0.6
	2	2.2
	3	4.5
	4	7.6
	5	11.5
	7	21.0
SAF stilling basin	1	3.5
	2	7.0
	3	9.5

SAF BASIN

The St. Anthony Falls stilling basin is a hydraulic jump basin. All the dimensions of this basin are related in some way to the hydraulic jump. A reduction in the basin length from that of a natural hydraulic jump is achieved through the use of appurtenances con-

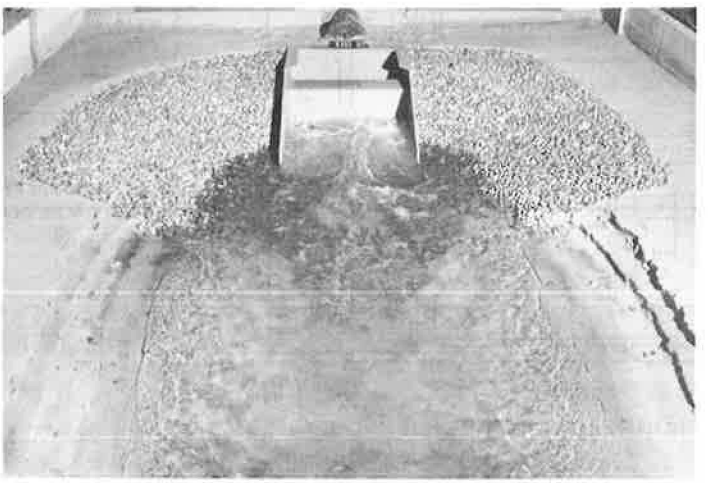

(a) satisfactory, $Q/D_o^{5/2} = 6.9$

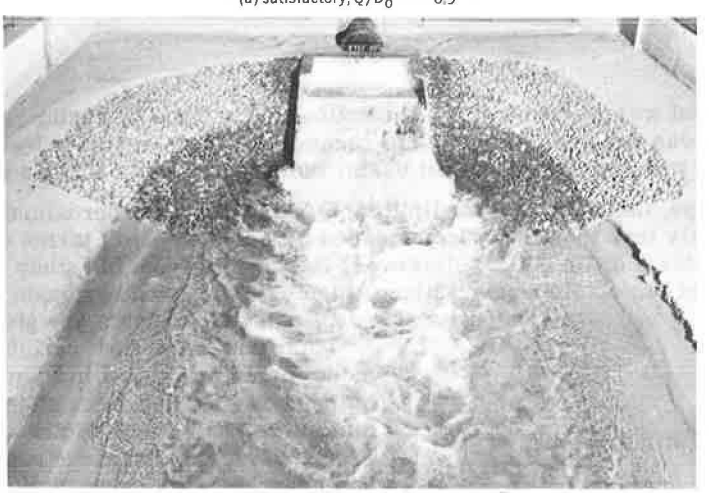

(b) unsatisfactory, $Q/D_o^{5/2} = 13.5$

Figure 7. Flow conditions with USBR Type VI basin.

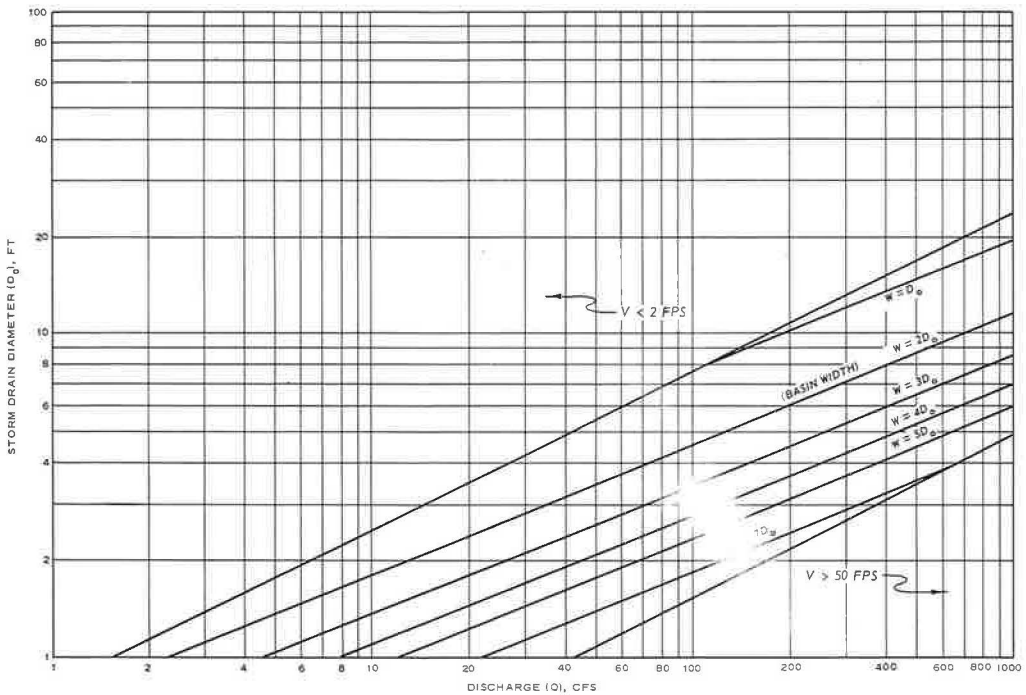

Figure 8. Storm drain diameter versus discharge for USBR Type VI basin.

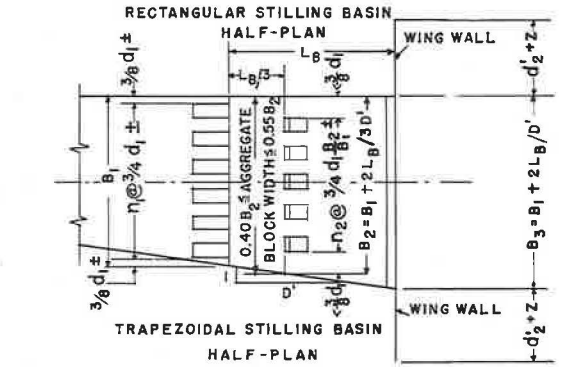

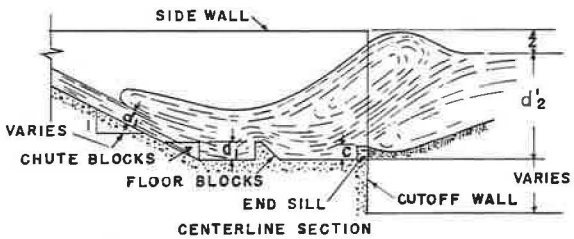

DESIGN EQUATIONS

(1) $F = \frac{V_1^2}{gd_1}$ (2) $d_2 = \frac{d_1}{2}(-1 + \sqrt{8F + 1})$

(3a) F = 3 TO 30 $d_2^1 = (1.10 - F/120)\, d_2$

(3b) F = 30 TO 120 $d_2^1 = 0.85\, d_2$

(3c) F = 120 TO 300 $d_2^1 = (1.00 - F/800)\, d_2$

(4) $L_B = \frac{4.5 d_2}{F^{0.38}}$ (5) $Z = \frac{d_2}{3}$ (6) $c = 0.07 d_2$

Figure 9. SAF stilling basin.

sisting of chute blocks, floor blocks or baffle piers, and an end sill. General details of the SAF basin are shown in Figure 9. Dimensions of the chute blocks and floor blocks may be modified slightly to provide reasonable construction dimensions without materially affecting the efficiency of the structure.

Models of 6 different SAF basins were tested. These basins were constructed according to recommendations made by Blaisdell (4) from model tests at the St. Anthony Falls Hydraulic Laboratory. Stilling basins that were 1, 2, and 3 times as wide as the outlet were tested with drops from the invert of the outlet to basin floor of $\frac{1}{2}$ and 2 times the outlet diameter. The basins with widths of 2 and 3 times the outlet diameter were flared 1 on 8 with respect to the centerline of the structure. Maximum discharges in the range that the basins could be expected to operate were chosen for design. The size of the basin elements and the basin length were adjusted for the 2 apron elevations tested. The velocity of flow entering the basin was assumed to be the same as the velocity at the outlet of the storm drain for the basins with a drop from the invert of the outlet to the basin floor of one-half the outlet diameter. A slight increase of the velocity at the outlet was assumed for the velocity entering the basin ($V_b = 1.15\ V_o$) with a drop from the invert of the outlet to the basin floor of 2 times the outlet diameter. With the discharge, velocity entering the basin, and the basin width known, the depth of flow entering the basin was then computed. These values were used to design the basin according to the design equations shown in Figure 9. Comparisons of flow conditions for the various basins were made with tailwater depths that were just sufficient to produce a hydraulic jump in the basin (approximately 0.85 the theoretical depth required for a hydraulic jump).

Results of tests indicated that within the limits investigated the drop from the invert of the outlet to the basin apron had little effect on the limiting $Q/D_o^{5/2}$ ratios. Maximum values of 3.5, 7.0, and 9.5 respectively were indicated for 1 D_o, 2 D_o, and 3 D_o wide SAF stilling basins. These values compared favorably with those used for the design

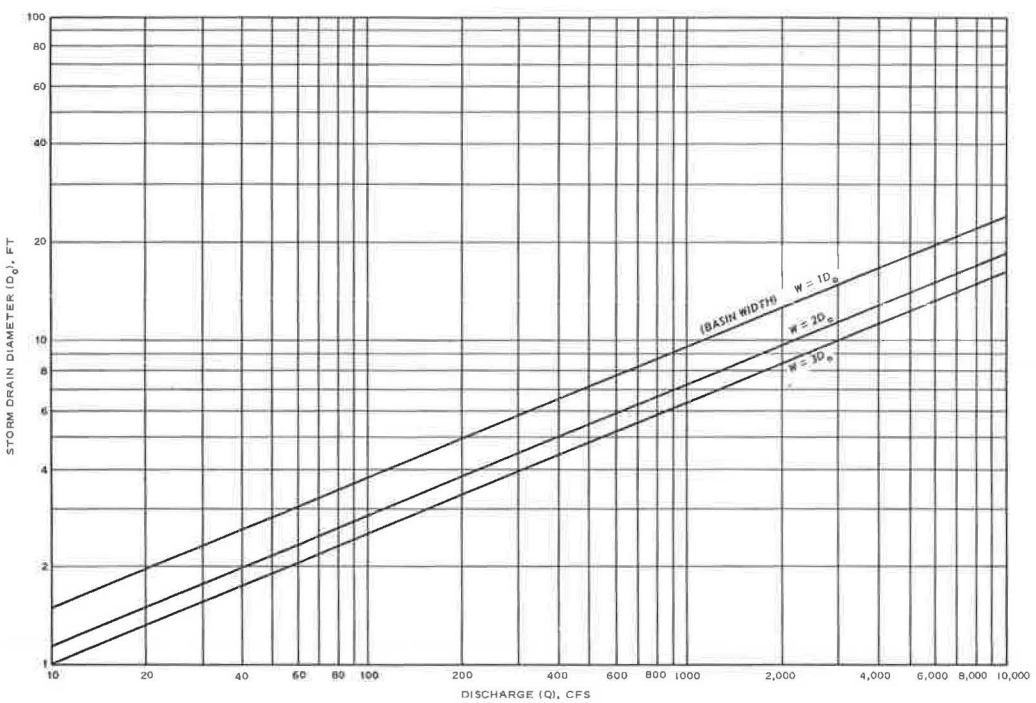

Figure 10. Storm drain diameter versus discharge for SAF stilling basin.

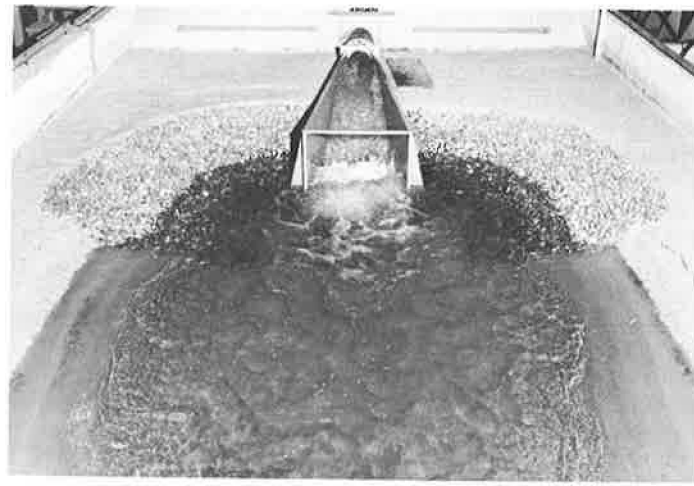

(a) satisfactory, $Q/D_0^{5/2} = 6.9$

(b) unsatisfactory, $Q/D_0^{5/2} = 12.0$

Figure 11. Flow conditions with SAF stilling basin.

of the basins. These results were used to determine the relations recommended for design and are shown in Figure 10. Photographs of flow conditions with the SAF stilling basin are shown in Figure 11.

DISCUSSION OF TESTS

The practice of siting outlets, equipped with or without energy dissipators, high relative to a stable downstream grade in order to reduce quantities of pipe and excavation is the primary cause of gully scour. Erosion of this type may be of considerable extent depending on the location of the stable section relative to that of the outlet in both the vertical and downstream directions. Storm drain outlets and energy dissipators should be located at sites where the slope of the downstream channel or drainage basin is naturally mild enough to remain stable under the anticipated conditions or else it should be controlled by ditch checks, drop structures, or all of these other means, to a point where a naturally stable slope and cross section exist.

A scour hole or localized erosion is to be expected downstream of an outlet even if the downstream channel is stable. The severity of scour depends on the conditions

existing or created at the outlet. Guidance relative to the extent of scour to be anticipated downstream of a culvert or storm drain outlet is presented in another report (1) as well as size and extent requirements of horizontal blankets of riprap for protection of outlets. These generalized results offer considerable guidance because one can estimate the extent of localized scour to be anticipated in stable channels of cohesionless soils downstream of an outlet and then decide what degree of protection is required. For example, is the anticipated scour hole that is a good energy dissipator permissible with an appropriate cutoff wall that protects the outlet? Are the size and extent of riprap required for a stable horizontal blanket practicable? Is it practicable to compromise depth of scour and size of riprap by providing a preformed and riprap-lined scour hole? Is an energy dissipator required?

The tests and data analyses reported here are given in Table 1 to indicate the range of applicability or maximum discharge capacity for various widths of 3 commonly used energy dissipators relative to the diameter of the incoming culvert or storm drain outlet, D_o. Based on these values of the relative maximum discharge capacity for comparable relative widths of the 3 energy dissipators, the stilling well is particularly suited to the lower range of discharges, the USBR Type VI basin to the intermediate range of discharges, and the SAF stilling basin to the higher range of discharges. However, all 3 energy dissipators are applicable for general drainage and erosion control practice. Comparative cost analyses will indicate which of the devices is the most economical energy dissipator for a given installation.

With information such as that developed for each of the 3 energy dissipators, the designers can, knowing the outlet diameter and design discharge, determine the applicability and necessary dimensions of each type of energy dissipator. In some cases, more than one type of dissipator may be applicable and in such cases local terrain, tailwater conditions, and cost analyses will determine the most practical energy dissipator for protecting the outlet. For example, with a 60-in. diameter culvert and a design discharge of 390 ft^3/sec, either a 10-ft wide ($2\,D_o$) SAF stilling basin or a 20-ft wide ($4\,D_o$) USBR Type VI basin or a 20-ft diameter ($4\,D_o$) stilling well could be used. With a 48-in. diameter culvert and a design discharge of 110 ft^3/sec, either a 4-ft wide ($1\,D_o$) SAF stilling basin or an 8-ft diameter ($2\,D_o$) stilling well or a 10-ft wide ($2.5\,D_o$) USBR Type VI basin could be used.

Some form of protection consisting of expansions either paved or riprap-lined or both is required to prevent excessive scour downstream of energy dissipators. It is considered that either horizontal or vertical expansion or both to permit dissipation of excess kinetic energy in turbulence rather than direct attack of the channel boundaries is most practical. Guidance is needed in this area as well as for selection of the size and extent of riprap required downstream of energy dissipators. In general, the unpublished results of WES investigations of riprap protection downstream of hydraulic structures indicate that the minimum average size of stone required for protection of an exit channel downstream of an energy dissipator can be described by the following empirical relation:

$$d_s = D\left(V/\sqrt{gD}\right)^3$$

where

d_s = minimum average size of stone, ft, usually termed d_{50} indicating that 50 percent by weight of a graded mixture is finer than the respective diameter,
D = depth of flow in channel downstream of structure, ft,
V = average velocity of flow in channel, fps, and
g = gravitational acceleration, ft/sec.

The protection should be extended downstream for a minimum distance equivalent to the width of the energy dissipator.

Additional options are desired that are more economical than these commonly used energy dissipators, and WES is continuing research to develop several simple stilling devices that will be more appropriate for the range of low and intermediate discharges. Efforts will be concentrated to develop practical guidance relative to preformed, riprap-lined scour holes or plunge pools and paved aprons with and without end sills.

REFERENCES

1. Erosion and Riprap Requirements at Culvert and Storm-Drain Outlets. U.S. Army Engineer Waterways Experiment Station, Corps of Engineers, Vicksburg, Miss., Res. Rept. H-70-2, Jan. 1970.
2. Impact-Type Energy Dissipator for Storm-Drainage Outfalls Stilling Well Design. U.S. Army Engineer Waterways Experiment Station, Corps of Engineers, Vicksburg, Miss., Tech. Rept. 2-620, March 1963.
3. Beichley, G. L. Progress Report 13—Research Study on Stilling Basins, Energy Dissipators, and Associated Appurtenances: Section 14, Modification of Section 6 (Stilling Basin for Pipe or Open Channel Outlets, Basin VI). Bureau of Reclamation, U.S. Department of the Interior, Rept. HYD-572, June 1969.
4. Blaisdell, F. W. The SAF Stilling Basin. Agricultural Research Service and St. Anthony Falls Hydraulic Laboratory, Agricultural Handbook 156, April 1959.

ROUGHNESS ELEMENTS AS ENERGY DISSIPATORS OF FREE-SURFACE FLOW IN CIRCULAR PIPES

James M. Wiggert and Paul D. Erfle,
Virginia Polytechnic Institute and State University, Blacksburg; and
Henry M. Morris, Christian Heritage College of San Diego, California

•WATER flowing at high velocities can cause considerable erosion. This erosion, or scour, can occur at the outlet of drainage structures such as chutes and culverts on steep slopes and cause maintenance problems and occasional displacement of pipe. The erosive capability of flowing water is characterized by its velocity, which in turn gives the flow a high kinetic energy.

Reduction of the kinetic energy and velocity of flow to more acceptable levels with regard to scour nearly always requires the formation of a hydraulic jump. The hydraulic jump is a phenomenon that converts shallow, high-velocity flow to deeper, low-velocity flow while considerable kinetic energy is lost through the generation of extreme turbulence. Many outlet protection devices are stilling basins, designed so that the hydraulic jump is forced to form in the basin, and the soil materials of the drainage channel downstream is thus protected.

If the jump can be forced to form in the chute or the culvert itself, near the outlet, the stilling basin structure can be simplified or even eliminated. Studies have been under way for some time at Virginia Polytechnic Institute and State University on the use of large roughness bars, like sills, in steep, rectangular, open channels for conveyance of water to the downstream channel at safe velocities. These bars, called roughness elements, form a succession of small hydraulic jumps in the channel to cause the phenomenon known as "tumbling flow" (1). The results of these studies are summarized in other papers (2, 3). In general the use of properly designed roughness elements as energy-dissipation devices seems to be quite effective and economical under many conditions.

This report describes experiments on peripheral rings used in smooth, circular pipes, as roughness elements to reduce the velocity of flow. The studies pertain only to culverts flowing under inlet control on steep slopes, that is, pipes functioning as open channels with supercritical flow.

Model tests were made to investigate the feasibility of roughness elements as energy dissipators to reduce the kinetic energy of high-velocity, free-surface flows in pipes. Tests were made by using a 6-in. diameter Plexiglas pipe, 28 ft long, in the Hydraulics Laboratory. The model tests included 3 sizes of roughness elements and several different configurations of element spacing, location, and number. The model tests were performed at several discharges and slopes for each configuration.

In addition to the model tests, a short series of tests was performed on a 32-ft, 18-in. concrete pipe at the Industry Center. These tests, referred to as the prototype tests, were made to verify the model-prototype scaling ratios and to determine whether the pipe material significantly affected the results.

The purpose of the research, to dissipate the kinetic energy of high velocity flows, required steep slopes for all tests. Accordingly, the usual case was one of critical flow at the entrance of the pipe, with flow accelerating down the length of the pipe until the first roughness element was reached. At that point a forced hydraulic jump was formed, with extreme turbulence. The flow then typically encountered another rough-

Sponsored by Committee on Surface Drainage of Highways.

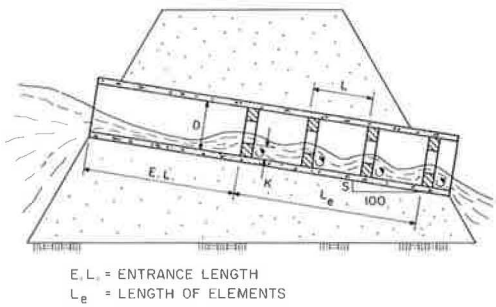

Figure 1. Tumbling flow in pipe culvert.

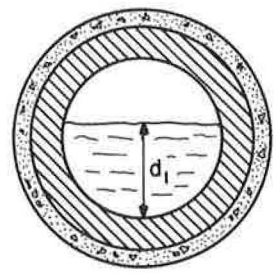

Figure 2. Roughness element in pipe.

ness element while still in the agitated condition from the first, and this pattern of action was repeated until a cyclic condition was reached, where the flow conditions around a roughness element were the same as those around another. This agitated flow—somewhat characterized by a greater depth over the element than before it, a fall into the "valley" between elements, and a form resembling a hydraulic jump before the element—is called "tumbling flow" by Morris (2). This then is the purpose of the roughness element: to cause an agitated condition that is the mechanism for a rapid decrease in the energy of the fluid flow, thus reducing the velocity of the flow at the exit of the pipe.

THEORETICAL CONSIDERATIONS

Consider a steeply sloping pipe culvert, containing bed roughness elements at regular intervals, as shown in Figure 1.

The pipe is laid on a slope of S percent and has an internal diameter of D ft. The roughness elements are spaced at a distance L and have square cross sections K on each side. The control depth d_1 is measured from the water surface to the upstream corner of the element crest at the pipe centerline (Fig. 2).

One repeating cycle of the tumbling flow is shown to a large scale in Figure 3. Distances are measured parallel to, and normal to, the pipe axis, which makes an angle θ with the horizontal. The percentage of slope is equal to 100 tan θ.

The momentum equation can be written for the body of water in 1 cycle, assuming that cyclically uniform flow has been established, as follows:

$$W \sin \theta - F_D - \tau_o LP = 0 \qquad (1)$$

in which W is the total weight of water in one repeating cycle, F_D is the drag force on the element, τ_o is the average bed shear stress over the spacing L, and P is the average wetted perimeter. W is equal to γAL, where A is the average cross-sectional area in length L, and R represents A/P, the average hydraulic radius in the length L; therefore, Eq. 1 becomes

$$F_D = PL(\gamma R \sin \theta - \tau_o) \qquad (2)$$

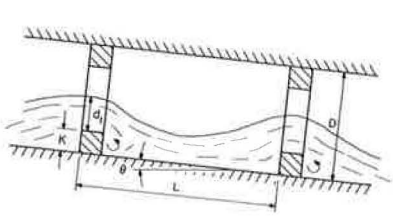

Figure 3. Tumbling flow cycle in pipe.

It is probable that in most cases τ_o will be small relative to $\gamma R \sin \theta$. If so, then approximately

$$F_D \cong \gamma AL \sin \theta = \gamma A(\Delta H) \qquad (3)$$

in which ΔH is the drop in channel-bed elevation in the length L.

The area A is impossible to determine without actual measurements of the flow profile, but it

would certainly be less than the cross section of the pipe itself. Therefore, the maximum possible drag force on an individual element could be calculated as

$$F_{D_{max}} = (1/4)(\pi D^2)(\gamma \Delta H) \tag{4}$$

The actual drag force would have to be determined experimentally and undoubtedly varies with the channel slope and discharge as well as with geometry of the roughness elements.

The energy equation can also be written for 1 cycle of the tumbling flow as follows:

$$H_j = L \sin \theta = \Delta H \tag{5}$$

In this equation, H_j represents the head lost in the hydraulic jump and associated phenomena in the 1 cycle. Because the flow is cyclically uniform, the entire gain in energy resulting from the drop in bed elevation must be exactly offset by the energy dissipated in the cycle.

Unless the elements are quite far apart, each element and its associated jump will interfere to some extent with the next jump and, thus, restrict the full development of the energy loss that could theoretically be induced by a single roughness element in a sloping channel. Consequently, H_j will be less than, or at most equal to, the head loss that could be caused by a single isolated element. It would seem, therefore, that both economy and smoothness of operation would require elements to be spaced as far apart as possible while the cyclically uniform tumbling flow is still maintained. This optimum spacing, however, must be determined experimentally because no data are now available with which to calculate it.

Finally, the process equation for cyclically uniform tumbling flow in a pipe culvert can be written as follows:

$$f(\rho,\ V_1,\ K,\ L,\ D,\ S,\ \gamma) = 0 \tag{6}$$

It is assumed here that K, the element height, is the single most important dimension of the flow geometry, to which the other dimensions L and D can be referenced. The reference velocity V_1 is the velocity at the control section on the element. Other velocities in the flow field can be referenced to this through the equation of continuity. The fluid density ρ is the basic physical property used in specifying the inertial forces and kinetic energies of the flow. The only other force of importance is that of gravity, represented by γ, the specific weight. The forces of viscosity, elasticity, and surface tension, though present and acting, are assumed to be relatively unimportant in comparison with inertial and gravitational forces, which determine the basic flow structure. The effect of potential energy in the flow is included by means of the slope term S.

By dimensional analysis, Eq. 6 can be modified to the following:

$$f(L/K,\ D/K,\ S,\ V_1^2/gK) = 0 \tag{7}$$

Each term in this function is now dimensionless. Such functions can often be determined explicitly by model testing. The last term can be extracted and set equal to a function of all the others. Thus,

$$V_1^2/gK = f(L/K,\ D/K,\ S) \tag{8}$$

Because Q is equal to $A_1 V_1$, this may be written as

$$Q^2 = gKA_1^2\, f(L/K,\ D/K,\ S) \tag{9}$$

A_1 is the area of flow at the control section and is, of course, primarily a function of the control depth d_1.

In a relation that is established between pipe size D and roughness element size K, the ratio of d_1 to K is some constant. This is so because d_1 depends on given hydraulic

parameters (discharge and slope) and geometry (pipe diameter and roughness element size). Thus, for a given value of discharge and slope

$$A_1 = m(b_1 d_1) = m(b_1)(nK) \tag{10}$$

where b_1 is the surface width at the control section and m and n are constants. The constants can all be incorporated in the functional expression, and Eq. 9 can then be modified to the following:

$$K = (Q/b_1\sqrt{g})^{2/3} f(L/K,\ D/K,\ S) \tag{11}$$

Equation 11 can be understood as the desired process equation for tumbling flow, specifying the required K for a given Q to ensure tumbling flow in the culvert. That is, if K is smaller than specified by Eq. 11, the flow would become supercritical and the distinct jumps would be eliminated. However, Eq. 11 requires an objective, experimental determination of the bounds of tumbling flow because the assumption underlying the development of the equation is the existence of the tumbling flow regime. Although tumbling flow can be observed, the point of beginning of tumbling flow relative to a parameter change is difficult to determine. Nevertheless, it is possible to make a positive statement about the occurrence of tumbling flow within constraints imposed by the experiments reported here. The experiments were generally in the tumbling flow regime, and the data show a narrow range of Froude numbers at the upstream position, that is, upstream of the first element before its effect is felt by the flow. Those numbers varied from more than 3 for the condition of 4 percent slope to nearly 6 for that of 10 percent slope. Thus, if there are sufficiently high upstream Froude numbers and the proper range of discharge and if the configuration of the roughness elements (L/K, K/D, number of elements at the downstream end) is within the range of the experiments, then tumbling flow will occur.

The tests performed indicated that a strong tumbling action occurred for a specific configuration of roughness elements. Specifically, 5 roughness elements in the downstream end of a pipe on steep slope with inlet control will produce tumbling flow when the ratio K/D is in the range 0.104 to 0.146 and the ratio L/K in the range 12.1 to 17.1. Accordingly, Eq. 9 can be rewritten

$$f[(Q^2/gA_1^2\ K),\ S] = 0 \tag{12}$$

This modification of Eq. 9 is possible because D/K and L/K are relatively constant and the behavior of the flow does not change much over the tested range of D/K and L/K. Furthermore, under conditions of tumbling flow over the roughness elements, the area and top width are functions of the pipe diameter D for fixed K/D ratio and for given discharge. Therefore, one can write Eq. 12 as

$$f[Q/(D^2\sqrt{gD},\ S] = 0 \tag{13}$$

a design equation under the constraints elaborated on earlier.

MODEL APPARATUS AND PROCEDURES

The model study portion of this project was performed in the Hydraulics Laboratory.

Water Supply

The water supplied to the experimental culvert was pumped from the sump in the laboratory to a constant head tank approximately 60 ft above the test flume. From the head tank the water was routed to a small, open forebay and then passed through the test culvert before it was returned to the sump. The flow was measured by a calibrated venturi meter and controlled at the flume by an 8-in. butterfly valve.

Test Flume

The model culvert pipe was placed in a 30-ft rectangular tilting flume capable of a slope range from horizontal to 25 percent (3 in./ft). The slope indicator on the flume was calibrated by using a cathometer prior to the experiments. The slopes tested were 4, 6, 8, and 10 percent respectively. The water, before entering the model pipe, entered a small open-head tank on the flume and was allowed to become quiescent before entering the model. A headwall was constructed in the flume with the pipe projecting through the headwall and into the flow. The headwall was sealed with a neoprene gasket to ensure that no leakage occurred.

Model Pipe

Concrete culvert pipe was modeled by using 6-in. diameter clear Plexiglas pipe sections joined by a bolted collar. Clear pipe was chosen for visual and photographic observations. A 6-in. section was chosen because the laboratory flow supply was inadequate for a complete range of flow conditions in a larger pipe. The length of the model pipe was originally 32 ft for the first test series (K = 0.375 in.), but later the pipe was shortened to 28 ft so that depth and velocity measurements could be made at the last element. The pipe extended 1 ft beyond the headwall forming a projected entrance condition. The outlet condition was a free overfall.

Holes were drilled on the bottom on 1-in. centers along half the length of the pipe. The roughness elements were held in place by a screw through the bottom of the pipe and into each element; plastic tape was placed over the holes so that no leakage would occur.

A $\frac{1}{4}$-in. slot was machined in the top of the pipe about midlength and over the last roughness element. Thus, measurements of depth and velocity could be made upstream of the elements and at the last roughness elements.

Roughness Elements

The roughness elements were peripheral rings, square in cross section, machined from sheet Plexiglas. Table 1 gives the dimensions and other geometric properties of all the rings tested. The rings were fastened to the pipe with a small screw. This method of fastening proved adequate, for the rings showed no tendency to move during or after the experiment. The last element had a portion of the top of the ring removed so that depth and velocity readings could be made directly over the ring.

The downstream element was, generally speaking, at the end of the pipe. In practice, the distance of the downstream face of the element from the plane of the outlet was about the relative distance K, the thickness of the element. This seemed to produce as much reduction in velocity as any other location.

TABLE 1

DIMENSIONS AND PROPERTIES OF ROUGHNESS ELEMENTS

Test	K (in.)	L (in.)	L/K	Number of Elements	K/D	L_e/D	E.L. (percent)
Model	0.375	2	5.33	96	0.0625	32	50
	0.625	9	14.4	4	0.104	6	90
	0.625	9	14.4	5	0.104	7.5	87.2
	0.875	6	6.88	30	0.146	30	46.8
	0.875	12	13.76	4	0.146	4	87.5
	0.875	12	13.76	5	0.146	10	83.6
	0.875	12	13.76	15	0.146	30	46.8
	0.875	15	17.1	5	0.146	12.5	80.1
	0.875	18	20.6	5	0.146	15.0	76.8
Prototype	1.875	27	14.4	5	0.104	7.5	65
	2.625	36	13.7	5	0.146	10	53

Measuring Apparatus

A minimum amount of instrumentation was needed to obtain the experimental data. The depth of flow over the element and in the pipe before the elements was measured by an electric point gage that could measure depths to 0.001 ft. The velocity of flow was measured by a pitot tube at mid-depth with 2 piezometer tubes. The piezometer tubes could be backflushed and vented to the atmosphere so that no air would be in the pitot tube or the piezometer tubes.

Experimental Procedure

After the rings were established in their desired positions and the pipe installed in the flume, the venturi's manometer was bled of all air, and water was allowed to enter the test flume. From the steepest slope, the flow was set so that at the last ring the pipe was flowing nearly or completely full. The depth and mid-depth velocity were recorded at the upstream position and at the last element. The flow was reduced and the depth and velocity were measured at the same upstream and downstream positions. This procedure was repeated for the subsequent slopes; however, the flow rates were the same as for the steepest slope.

Visual observations were also made. Included were position of the hydraulic jump at the lead element, strength of hydraulic jump between elements, and degree of turbulence indicated by the amount of air entrainment.

PROTOTYPE TESTS

Prototype tests were performed on an 18-in. concrete pipe at the Industry Center.

Apparatus

An 18-in. concrete pipe of four 8-ft sections was used for the prototype tests. The pipe lay in steel framework and was flush-mounted into a steel head box. The frame and head box acted as a unit supported at the midspan of the frame and by an elbow section of the main supply pipe bolted to the side of the head tank. With the use of a heavy-duty forklift truck, the entire frame and head box could be rotated about the pipe elbow to the desired slope. The slope range of the prototype tests was from the horizontal to 15 percent ($1\frac{3}{4}$ in./ft). The slope was measured with a steel scale and carpenter's level.

Water supplied to the tests was pumped from the Blackstone River by 2 vertical turbine pumps into the head box on the frame. The flow was measured by a calibrated orifice meter and controlled by a 24-in. butterfly valve.

Prototype Pipe

Four 8-ft sections of pipe of the tongue-and-groove type were used for the prototype tests. They were sealed together with neoprene O-rings, and no leakage occurred during the tests. The entrance was flush with the head box, and the exit was a free overfall. A hole was drilled in the pipe about midlength so that velocity and depth measurements could be made upstream of the roughness elements. Another hole was drilled in the pipe about 10 ft from the end of the pipe so that the flow over the elements in the pipe could be observed.

Roughness Elements

The roughness elements were made of laminated plywood, machined to the correct size, and coated with an epoxy paint. Two sizes of roughness elements were used and their geometric properties are also given in Table 1. They were positioned in the pipe by industrial banding or strapping material laid along the invert and top of the pipe. The banding was brought outside the pipe at the outlet and the second joint and finally fastened to the exterior of the pipe. This procedure was satisfactory, for the elements remained stationary and the banding did not interfere with the flow.

Measuring Apparatus

These tests were similar to the model tests in that a minimum amount of instrumentation was used to obtain the experimental data. The upstream depth was measured with the use of a rod lowered to the pipe invert and then raised to the water surface. A mark was inscribed on the rod indicating the pipe invert; the change in elevation of the inscribed mark above a datum on the exterior of the pipe to the water surface was measured with a steel scale to within $^1/_{16}$ in. The change in elevation was a measure of the depth of flow in the pipe. The outlet depth at the last element was measured in a similar fashion but by using the downstream pitot tube rather than a rod.

Velocity measurements were taken at mid-depth with pitot tubes. The downstream pitot tube was connected to a calibrated differential pressure transducer, and the pressure difference was registered on a Sanborn 150 recorder. The upstream pitot tube was connected to 2 piezometer tubes similar to those used for the model tests.

The experimental procedure used for the prototype tests was the same as that used for the model test.

ANALYSIS OF DATA

An attempt to reduce the experimental data to design formulas was made. Some of the plastic pipe data plots drawn for this purpose are shown. Figure 4 shows a graph of the computer friction factor f versus the Reynolds number N_R, both based on velocity and depth (through the hydraulic radius) over the last roughness element. The different symbols indicate the slope of the pipe. The legend gives the configuration of the roughness elements. No trend is discernible.

Figure 5 shows the friction factor plotted versus the Froude number N_F for the same data shown in Figure 4. Again, no trend is found. This is expected in the case of the Froude number because the flow over the elements in the fully developed tumbling condition should be similar to flow over a fall, and the Froude number should be close to one. Such is the case. Similarily, when the Chezy resistance formula, in the form $C/\sqrt{g}$, is plotted against the Reynolds and the Froude numbers, no trend is evident (Fig. 6).

An attempt was made to correlate an index of efficiency of element configurations versus the slopes tested. Because velocity reduction was the primary cri-

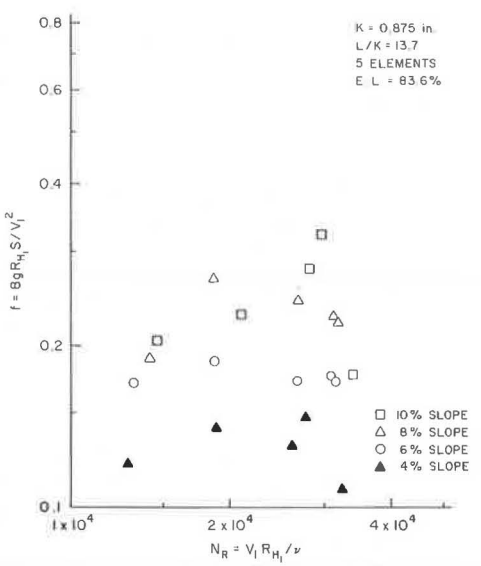

Figure 4. Friction factor versus outlet Reynolds number.

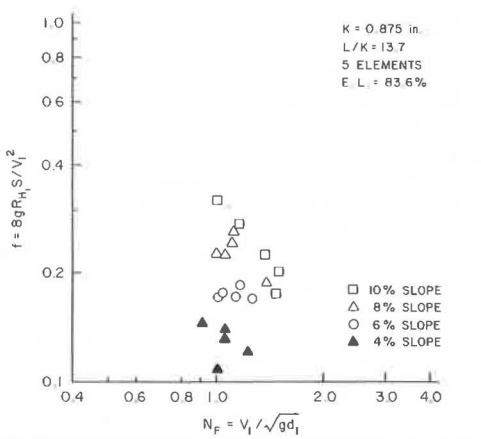

Figure 5. Friction factor versus outlet Froude number.

terion of the study, the percentage reduction of velocity was used as a measure of efficiency. Defining the velocity upstream of the first element as V_0 and the velocity at the last element as V_1, the percentage of velocity reduction is defined as $(V_0 - V_1)/V_1$. Figures 7 and 8 show that no functional relationship existed between percentage of velocity reduction versus slope for the elements tested.

The experimental data illustrate several points that should be noted. First the theory of hydraulic modeling and similitude indicates that the ratio of prototype discharge to model discharge should be equal to the length ratio to the $^5/_2$ power if the scaling relationship is governed by the Froude number. The data show that, for matched conditions of slope, roughness configuration, and Froude number at the upstream position, the discharge ratios for model and prototype are as predicted by the model ratio. Some of the upstream Froude numbers in the model tests were not taken in the same relative position as in the prototype because the relative entrance length for the plastic model pipe was so much longer. In these cases, a one-step, gradually varied flow calculation was made to find the Froude number in the model at an entrance length corresponding to that in the prototype. One group of tests was made by measuring the upstream Froude number at the location corresponding to the measuring point in the concrete pipe.

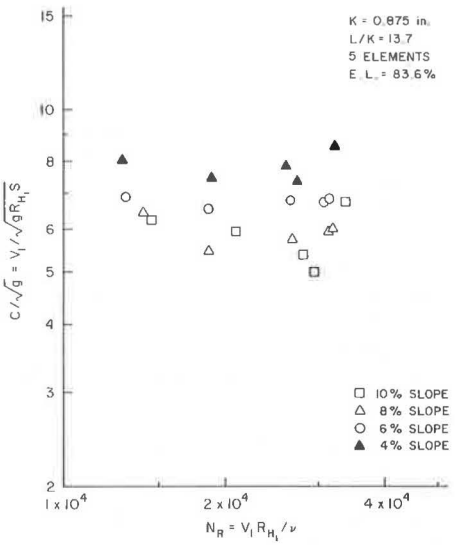

Figure 6. Chezy resistance coefficient versus outlet Reynolds number.

Another point in interpretation of the data is the reduction in velocity from the values of V_0 to those of V_1. (The values of percentage of reduction of velocity are significant because the high velocity at the outlet is the erosive mechanism.) Figures 7 and 8 show the range of velocity reduction.

A third set of items of data that should be noted are the Froude numbers at exit N_{F_1}. Those values are near unity, very nearly the optimum value.

Most of the data exhibited tumbling flow characteristics at the downstream elements as nearly as could be determined (necessarily a subjective judgment). Initially, tests

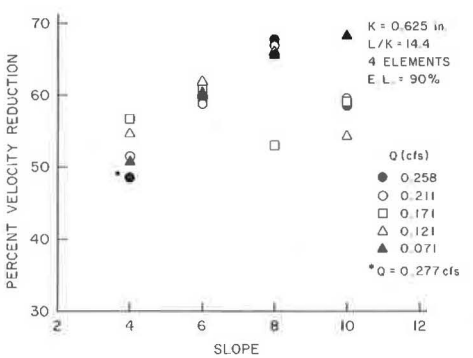

Figure 7. Percentage of velocity reduction versus slope for four 0.625-in. elements.

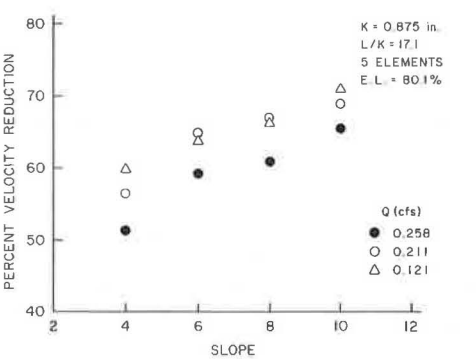

Figure 8. Percentage of velocity reduction versus slope for five 0.875-in. elements.

were run with entrance lengths in the plastic pipe only about half the length of the pipe. When later tests showed that nearly cyclic tumbling flow occurred with less elements (a total of four or five), most tests were made with the lesser numbers of elements. In order to justify a design containing only 5 elements, a further series of tests was made with 15 elements to determine the degree of velocity reduction and then to compare it to the velocity reduction attained with 5 elements. For a range of 4 values of slope and 5 values of discharge for each slope, the average increase in velocity reduction by 15 elements over the velocity reduction by 4 elements was approximately 5 percent. Therefore, there was only a marginal increase in velocity reduction for a much greater number of elements.

For most of the plastic-pipe tests the pipe was not flowing full at the exit. Although few of the data showed the full-flow condition, it was observed in some of the tests that sporadically the pipe went under pressure during conditions of high discharge. This pressurization occurred only in the lower end of the pipe, in the region of the roughness elements. The pressurization was more easily attained (that is, with lower discharges) for smaller slopes than for larger ones. The range of the tests was stopped at the point of sporadic pressurization. The next condition that would prevail with increasing discharge is complete pressurization with the pipe running full, and the hydraulic jump from rapid, free-surface flow to the full condition would move upstream to an equilibrium position.

The methods of measuring depths and velocities given in the description of the experiments were not sophisticated. However, the extreme turbulence of the flow, especially in the tumbling regime, and the resulting roughness of the water surface obviated the usefulness of refinement in the methods.

Although the experiments did not yield design equations by analysis of the figures shown, the subjective observation of tumbling flow did establish some bounds to the relations of discharge to Froude number and slope. This relation is discussed in the next section, but simply the relation of Eq. 13 was assumed to be independent of slope, and the data were examined for values of the parameter $Q/(D^2\sqrt{gD})$.

Because of concern regarding the ability of the flow to clean the pipe of material accumulating ahead of the roughness elements, a qualitative test was run. Several shovels full of gravel were placed in the pipe barrel of the prototype, and a flow of about 3 ft^3/sec was discharged through the pipe for 5 min. At the end of that time no gravel whatever remained in the pipe. It seems clear that gravel and silt deposits will not build up but rather will be washed out by the extreme turbulence of the flow.

Although the experiments indicate that gravel and similar deposits will wash out of the pocket formed by the roughness elements, it is possible that water would stand upstream of the elements, possibly causing problems in freezing and thawing situations or in insect control cases. The formation of a slot in the ring at the invert to permit complete drainage would not hamper the hydraulic performance of the design. An alternative would be a "flat" on the ring at the invert.

DESIGN METHOD

It is obvious that the introduction of roughness elements will increase the friction loses through the pipe barrel. The increased rate of energy loss through the region of the roughness elements will not change conditions upstream of the elements as long as the total loss in head from the jump at the first element to the pipe outlet is not greater than the head available at the point upstream of the first element. For increasing discharge, however, the rate of head loss will become greater, and the pipe will then flow full in the region of the roughness elements and upstream of them in an attempt to gain sufficient energy head to overcome the losses. Accordingly, it is readily apparent that for a given pipe diameter the upper limit of discharge is quite fixed if tumbling flow is to occur. This, of course, assumes that there is a proper range of K/D and L/K ratios as well as very steep slopes (greater than 4 percent). The data provided values of the parameter that would permit pipe size selection, values of $Q/(D^2\sqrt{gD})$. For the model-pipe tests the maximum values of this parameter ranged from 0.257 for 10 percent slopes to 0.210 for 4 percent slopes. For the prototype tests the value was 0.317 for

14.7 and 8.3 percent slopes. It is possible that the discharges for the prototype pipe were relatively larger because the determination of the transition from tumbling flow to full flow was more difficult to determine. Thus, higher relative discharges were permitted.

Even so, a simple design technique is available, the criterion being Eq. 13 rewritten as

$$D = (Q^2/0.0625g)^{1/5} \tag{14}$$

or

$$Q/(D^2\sqrt{gD}) = 0.25$$

which is valid for slopes greater than 4 percent, and with K/D ratios from 0.104 to 0.146 and L/D from 1.5 to 2.5 (corresponding to K/D = 0.104 and L/K = 14.4 and to K/D = 0.146 and L/K = 17.1 respectively).

CONCLUSIONS

The following conclusions can be made based on this research:

1. Peripheral roughness elements of proper relative size and spacing and of square cross section will cause considerable reduction of exit velocity in the case of pipes on steep slopes under inlet control and free exit, i. e., flowing partly full. The exit Froude number can be reduced to nearly unity.
2. The Froude law relationship is an accurate scaling parameter within the range of conditions studied in this report.
3. A satisfactory condition of tumbling flow will occur when 5 roughness elements of relative size K/D = 0.104 to 0.146 and L/D = 1.5 to 2.5 are used at the downstream end of the pipe and the pipe slope is greater than approximately 4 percent.
4. The size of pipe can be selected through the empirical criterion of Eq. 14.

ACKNOWLEDGMENTS

The research reported in this paper was performed under the auspices of a research and development grant from the American Concrete Pipe Association, and that support is gratefully acknowledged. Assistance during the experimental phase of the project was provided by Peter W. Delohery.

REFERENCES

1. Peterson, D. F., and Mohanty, P. K. Flume Studies of Flow in Steep Rough Channels. Jour. Hydraulics Div., Proc. ASCE, Nov. 1960, pp. 55-76.
2. Morris, H. M. Design of Roughness Elements for Energy Dissipation in Highway Drainage Chutes. Highway Research Record 261, 1969, pp. 25-37.
3. Morris, H. M. Hydraulics of Energy Dissipation in Steep, Rough Channels. Research Div., Virginia Polytechnic Institute, Bull. 19, Nov. 1968, 108 pp.

PERFORMANCE OF PLASTIC FILTER CLOTHS AS A REPLACEMENT FOR GRANULAR FILTER MATERIALS

Charles C. Calhoun, Jr., Joseph R. Compton, and William E. Strohm, Jr.,
U. S. Army Engineer Waterways Experiment Station, Vicksburg, Mississippi

This paper describes an investigation of the performance of plastic filter cloths used to replace granular filter materials. Laboratory or field performance data or both are given on 8 cloths. Laboratory tests were conducted on 7 cloths to determine their chemical and physical properties (e.g., opening size, percentage of open area, strength, absorption, resistance to weathering, and reaction to various chemicals) and their filtering abilities. Information on uses and performance of filter cloths at Corps of Engineers projects is given. Recommendations are made for filter criteria and physical characteristics of cloths for use in the design of drainage systems and the procurement of the filter cloth.

•GRANULAR filter material must meet 2 basic requirements: (a) The filter material must be fine enough to prevent infiltration of the material from which drainage is occurring (base material), and (b) the filter material must be much more permeable than the base material to permit free drainage. The Corps of Engineers (CE) and other investigators have performed comprehensive investigations to develop criteria for the design of granular filter systems that will satisfy these 2 basic requirements. Through this research and field experience, filter or design criteria have evolved to the stage that the engineer can, in most cases, confidently design a granular filter system that will function properly. In many cases, a graded (multilayered) filter is required in which each layer must meet the filter criteria with respect to adjacent materials. This involves placement of several different granular layers and is understandably costly and difficult to construct. Since 1962 the CE has used plastic filter cloths in some installations to replace certain granular layers of graded filters in drainage systems and, in some cases, to completely eliminate any filter or bedding material beneath riprap, rubble, or other stone protection. Prior to 1962 filter cloths have been used in the United States and other countries (although not by CE for drainage applications) and found to be very effective in some coastal structures (1).

Prior to 1967 only 2 filter cloths were known to be on the U. S. market, and their use was becoming widespread. Because the performance of these cloths had been satisfactory, CE specifications generally required one of these cloths by name or some other cloth of equal physical properties. Around 1967 other cloths were becoming available, and the CE had no standard acceptance criteria for use in specifications and no standard filter design criteria. In 1967 the Office of the Chief of Engineers and the U. S. Army Engineer Division, Lower Mississippi Valley (LMVD), authorized a study by the U. S. Army Engineer Waterways Experiment Station (WES) to develop acceptance specifications and design criteria for CE use of filter cloths. Eight different filter cloths were investigated, and some of the results of this study (2) are reported in this paper.

Sponsored by Committee on Surface Drainage of Highways and Committee on Subsurface Drainage and presented at the 50th Annual Meeting.

DESCRIPTION OF FILTER CLOTHS AND RESULTS OF LABORATORY TESTS

Table 1 gives some of the physical properties of 7 of the cloths investigated. The cloths will be referenced in this paper by the letter symbols given in Table 1. With the exception of cloth G, all of the cloths were manufactured in the United States. Cloths A, B, and C were made by the same manufacturer; the others were made by 4 different manufacturers. Six cloths were made of predominately polypropylene yarns, and one was made of polyvinylidene chloride yarns. The yarns used in the manufacture of the cloths varied considerably. Three cloths had round fibers and three had flat fibers. The round fibers varied in diameter from 0.003 to 0.015 in. The dimensions of the flat fibers were about the same for all cloths. Cloth F, the only unwoven cloth, was made by entangling fibers by needle punching and bonding by heat fusion. Cloth E was made of monofilament yarns in the fill direction and multifilament yarns in the warp direction.

Neither cloth E nor cloth F had distinct openings, and in fact cloth F had the appearance of felt. The other cloths that were woven of monofilament yarns had distinct rectangular openings. Because there were some variations in the opening sizes of the individual cloths and the openings were generally rectangular, the average opening size did not necessarily indicate what size of soil particle would pass the cloth. Because of this, a test procedure was developed to establish for each cloth an equivalent opening size (EOS) that is expressed in terms of a U. S. standard sieve number. The procedure is as follows: Approximately 150 gm of each of the following fractions of a rounded to subrounded sand was obtained:

U. S. Standard Sieve Number		U. S. Standard Sieve Number	
Passing	Retained On	Passing	Retained On
10	20	50	70
20	30	70	100
30	40	100	120
40	50		

Starting with the smallest size fraction of which more than 5 percent of the sand passed through the cloth, each successively coarser fraction was dry-sieved over the cloth for 20 min to determine that fraction of which 5 percent or less by weight passed the cloth. The EOS was taken as the finer or "retained on" size of this fraction. The equivalent opening sizes varied from the No. 30 to the No. 100 sieve. Open areas of the 5 cloths with distinct openings varied from 4.3 to 36 percent.

The tensile strengths of the cloths as determined by ASTM Method D 1682 varied considerably. The weakest cloth had a strength in the warp direction of only 31 lb, while the strongest cloth had a strength of 399 lb in the warp direction. Burst strengths of the cloths varied from 180 to 625 psi as determined by ASTM D 751-66T. Water absorption (CRD-C-575) was less than 1 percent for all cloths.

TABLE 1

PHYSICAL PROPERTIES OF FILTER CLOTHS

Cloth[a]	Color	Equivalent Opening Size[b]	Open Area (percent)	Avg Fiber Width (in.)		Avg Fiber Thickness (in.)		Tensile Strength (lb)		Elongation (percent)		Burst Strength (psi)	Absorption (percent)
				Warp	Fill	Warp	Fill	Warp	Fill	Warp	Fill		
A	Green	100	4.6	0.031	0.030	0.0085	0.0070	206	113	22.2	27.4	268	0.91
B	Black	70	5.2	0.031	0.029	0.0085	0.0070	388	257	22.4	26.8	542	0.13
C	Black	40	24.4	0.013[c]	0.014[c]	0.013[c]	0.014[c]	208	202	23.6	16.6	625	0.87
D	Black	100	4.3	0.030	0.028	0.0085	0.0070	399	244	17.0	24.6	528	0.38
E	White	—[d]	—[d]	0.003[c]	0.010[c]	0.003[c]	0.010[c]	127	231	10.6	26.3	316	0.08
F	Gray	—[d]	—[d]	0.003[c]	0.010[c]	0.003[c]	0.010[c]	31	104	11.3	40.3	180	0.31
G	Black	30	36	0.015[c]	0.013[c]	0.015[c]	0.013[c]	186	150	23.0	10.6	437	0.29

[a]Chemical composition of cloth A, polyvinylidene chloride, and of all others, polypropylene.
[b]U.S. standard sieve size.
[c]Round fiber.
[d]Could not test.

Tests were conducted to determine the effects of temperature (-60 to 180 F), acids and alkalies, oxidation, fuel spillage (JP-4), and sunlight (weatherometer). All the cloths were adversely affected by sunlight, particularly cloth F. Cloth F was also adversely affected by fuel spillage, and cloth A appeared to be affected by alkalies. All cloths withstood the other tests satisfactorily.

Filtration tests indicated that all 7 cloths evaluated would effectively retain sandy or silty soils in applications such as beneath riprap, although there was always some initial infiltration of fines. In these tests the filter cloth was secured in a permeameter and soil was loosely placed on top of the cloth. Water was then allowed to flow through the soil and filter cloth. The permeameter was instrumented such that hydraulic gradients through 1-in. increments of the soil and through the filter cloth could be measured. Special "clogging" tests were conducted where the soil above the cloth was composed of clean sands with various percentages of silt added for different tests. These tests indicated that cloths E and F tended to clog because of the migration of fines in a sandy soil. This tendency was measured by determining the ratio of (a) the hydraulic gradient through the cloth and the 1 in. of soil adjacent to the cloth to (b) the gradient through the entire sample. For sand samples containing 5 percent silt, this ratio was 1.67 for cloth. [(Gradient through 1 in. of soil and cloth)/(gradient through entire sample) = 1.67; e.g., head loss through the cloth and 1-in. thickness of soil above the cloth was greater than the average head loss per inch of soil for the entire sample.] Cloths A and E showed no measurable tendency to clog. For sand with 10 percent silt, ratios of 1.33 and 1.98 were measured for cloths E and F respectively. Visual inspections of these 2 cloths indicated a cake of fines had developed on the cloth. Although the ratio at 10 percent silt for cloth A was about 1.0, there was some caking of fines on the cloth, though not nearly to the extent observed on cloths E and F. Only cloths A, E, and F were subjected to clogging tests. Because there was no measurable clogging of cloth A, it was concluded that there would be no clogging of the remaining cloths that were similar to or had more open weaves than cloth A.

Filtration tests were also conducted to develop filter criteria for cloths used to wrap collector pipes where the backfill material will be a clean sand or gravel. These tests indicated that the sands would not pass the cloth if the 85 percent size of the sand was equal to or greater than the EOS of the cloth.

It is obvious from the variations in the cloths now available that an engineer would encounter difficulties in selecting a filter cloth to meet his specific need without guidance from a research program.

USES OF FILTER CLOTHS

An early phase of this study was to circulate questionnaires to CE offices to determine the filter cloths being used and their applications (3). Twenty-six of the 38 offices receiving questionnaires indicated that as of the latter part of 1969 they had used or would use filter cloths. Detailed information was received on uses of filter cloths at 46 projects. At 28 projects filter cloths had been used beneath riprap, rubble, articulated concrete mats, and other revetment materials. At 9 projects filter cloths had been used around pipes and well screens or for fabricating piezometer tips, and at 4 projects they had been used in drainage systems to prevent fines from soils being drained from entering granular filter layers. At 3 projects filter cloths had been used to stop grout, to protect slopes from erosion by surface runoff, or to bridge gaps in the concrete sheet pile wall. At the 46 projects, cloth A had been used 6 times; cloth B, 37 times; and cloths D and F, 1 time each. Cloths C and E had not been used at the time of the survey. Cloth G has not been used to date although a similar cloth, designated cloth Z, made by the same manufacturer was used at one site. (No laboratory tests were performed on cloth Z because its presence on the market was not known when tests were conducted on the other cloths. The EOS and the percentage of open area of the cloth appeared to be between those of cloth C and cloth G. Cloth Z is made of polyethylene yarns.)

Subdrain Systems

Both the Los Angeles and Ft. Worth Districts reported use of filter cloths to wrap subdrain pipes. In the Los Angeles District, filter cloth B was used to wrap individual joints of an open-joint subdrain pipe (1967), and in the Ft. Worth District perforated pipe was wrapped with cloth A (1966). In both instances the use of the cloth eliminated the necessity of a graded filter. A section of the subdrain in the Ft. Worth District (Sam Rayburn Dam) was removed during a visit by the principal author in February 1970, and the filter cloth showed no signs of deterioration or clogging, although the pipe perforations were partially clogged with an iron sludge. At the other installation, the subdrain system is functioning properly.

Figure 1. Installation of collector pipe and cloth A in subdrain system.

The Soil Conservation Service of the U. S. Department of Agriculture (4) installed subdrains near Orlando, Florida, to lower the water table in an agricultural test field. Although not a CE installation, this project is discussed because of the significant difference in the performance of 2 filter cloths subjected to conditions of high iron concentration. The 2 filter cloths used were cloth A and a cloth not included in the WES tests but similar in appearance to the nonwoven cloth F. Figure 1 shows the flexible, slotted, corrugated, plastic collector pipe and cloth A being installed in a trench. The trench was backfilled with the excavated soil, which was a fine sand (90 percent passing the No. 50 sieve). The flow and water table drawdown produced by the 2 systems were observed. The cloth similar to cloth F became clogged in a matter of weeks with an iron sludge. The sludge on the cloth was formed by "iron bacteria" that are common to the area and that oxidize and precipitate iron into the water. There was no sludge buildup on cloth A, although there was some buildup within the pipe as was the case at Sam Rayburn Dam. With periodic flushing, the system with cloth A has functioned properly since 1968.

At 4 CE projects cloth B was used to line trenches for subdrain systems that are now performing satisfactorily. The subgrade material varied from a silty gravel to a clayey silt. With the filter cloth between the subgrade material and the granular filter, the granular filter layer did not have to meet the filter criteria with respect to the subgrade material but had only to be coarse enough to prevent its entrance into the collector pipes.

Miscellaneous Uses

In 1964 filter cloth B was used in one instance in the Memphis District as a grout stop beneath grouted riprap. The cloth was placed on a gravel bedding, and riprap weighing up to 800 lb was placed on the cloth. The riprap was then grouted with a low-alkali Portland cement grout. The district was satisfied with the use of the cloth for this purpose.

In the Galveston District, cloth B was used in 1966 behind a retaining wall constructed from prestressed concrete sheet piles to prevent sand backfill from escaping from between the piles. The work was done in connection with a hurricane flood protection project, and the cloth has performed satisfactorily.

Cloth B was used in 7 projects in the fabrication of several hundred piezometer tips. At 3 projects, the tips were made by placing 1 wrap of filter cloth around the perforated end of a pipe; that perforated end was placed in sand contained in a bag made of the same cloth. At other projects, 2 layers of cloth were simply wrapped around the perforated ends of steel pipe. The piezometers were installed in MH, ML, and SM soils, and service records indicated good response and no clogging of the tips.

Beneath Riprap and Other Revetment Materials

Table 2 gives the use of filter cloths at 28 projects beneath riprap and rubble. The most common use was beneath riprap on the bottom or bank slopes of rivers, creeks, or other channels. Filter cloth was placed under articulated concrete mattresses and riprap along the Mississippi River (projects 3 and 4) and as protection for a highway fill paralleling the shore line of the Gulf of Mexico (project 5). Other uses of filter cloths have been in connection with breakwaters, protection at drop inlet structures, bridge pier protection, and groins. Cloth F was used only in a temporary diversion channel and was expected to be in service for only about 2 years (project 28).

At 19 of the 28 projects, filter cloths were placed directly on subgrade materials varying from fine sands to fat clays. In 3 cases (projects 4, 16, and 17), granular bedding was placed between the cloth and subgrade materials varying from medium to fine sands to silty clays. At 6 projects, granular bedding material was used above the filter cloth. Installation of the cloths was usually in accordance with the manufacturers' recommendations. When cloths were used on slopes, the slopes were shaped to grade, and the cloths were generally laid parallel to the centerline of the channel. The cloths were, in most cases, overlapped 8 to 12 in. and secured at 3-ft intervals with 15- to 18-in. long steel pins. Use of pins was unsatisfactory at 2 sites where the subgrade consisted of loose sands and stones or where other means were used to weight down the cloths prior to placing the revetment material. Problems were encountered when cloths had to be placed underwater, and various methods were used, such as putting the cloth on a frame and weighting the frame and cloth with stone or, in one instance, rolling the cloth on steel pipe and then letting the cloth unroll into the channel. At Island 40 (project 4) the cloth was bonded to the articulated concrete mats when they were cast, and the cloth and mat were successfully placed as a unit. At Big Bay Harbor, Michigan (project 19), the cloth was placed under 8 ft of water by divers. The cloth was overlapped 3 ft and secured with specially made $\frac{3}{8}$-in. diameter, 2-ft long steel pins. The procedure was reported to be inefficient.

The Memphis District reported that extreme care was necessary when placing 125-lb riprap on cloth A (project 2). Dropping stones from a height of 2 ft damaged cloth A, but dropping stones from 4 ft did not damage cloth B under almost identical conditions (project 1). The Pittsburgh District also reported tears in cloth A when 500-lb stones were dropped from a height of 2 ft. The manufacturer of cloth A does not recommend its use where high strength and abrasion resistance are required. The Tulsa District reported extreme care was also necessary when placing stones on cloth F.

No damage to the cloths from stone placement was reported at any of the projects where cloth B was used or at the one project where cloth D was used. Stones weighing 3,000 lb were placed on cloth B in the Kansas City District (project 12), and areas later uncovered showed no damage. It was reported that some tears occurred at the securing pins because of the stones creeping down 1-on-2 slopes. This did not occur on slopes 1 on 3 or flatter. The Pittsburgh District reported the same experience (project 23). At 8 projects, stones of various sizes were dropped directly on cloth B from heights of 2 to 5 ft, and no apparent damage occurred. Unsatisfactory factory-sewed seams were noted in 2 instances (projects 10 and 12) with cloths B and D. This situation has since been corrected, and factory-sewed seams for both cloths were considered satisfactory.

At only 2 of the 28 sites where filter cloths were used beneath riprap or other types of revetment was their performance as a filter material considered questionable. Performance of the cloths at all other sites was satisfactory, and their continued use was recommended by the various districts. In the 2 questionable cases (projects 3 and 5), the cloth used appeared not to have sufficient open area to allow for free drainage. At Holly Beach, Louisiana (project 5), a section of cloth B was lifted or "floated" out of position because of pumping action caused by high waves during a storm, but an immediately adjacent section of cloth G was practically undamaged. The cloths at these 2 sections were overlaid by revetment blocks. At Island 63 (project 3) there was apparently a buildup of hydrostatic pressures beneath cloth B in the sand slope, and bulges in the slope resulted. These 2 sites were full-scale test sections, and the performance of the filter cloths will be discussed in more detail in a later section.

TABLE 2

USES OF FILTER CLOTH BENEATH RIPRAP, RUBBLE AND ARTICULATED MAT

Division	District	Project No.	Project Description	Cloth	Material Used Beneath[a]	Installation Date	Max. Stone Weight (lb)	Max. Drop (ft)	Subgrade Material	Bedding Max. Size (in.)	Bedding Thickness (in.)
LMVD	Memphis	1	Clark's Corner Cutoff Bridge, Ark.	B	Riprap slope repair	Nov. 1964	125	4	SP fine		None
		2	Madison-Marriana Bridge 4, Ark.	A	Riprap slope repair	Nov. 1962	125	<1	SP fine		None
		3	Island 63	B	Revetment (ACM and riprap)	Sept. 1965	125	4	SP fine		None
		4	Island 40	B	ACM Revetment	Aug. 1968	N.A.	N.A.	SP m to f	1½[b]	4[b]
	New Orleans	5	Test sections, Holly Beach, La.	B and Z[c]	Shore protection	Jan. 1969	14	0	SP fine		None
		6	Calcasieu saltwater barrier	B	Riprap bedding	1966-67	1,400	5	SP	1½	6
	St. Louis	7	Wood River Drive and Levee, Ill.	B	Riprap on riverbank	Aug. 1968	300	3	SP-SM, SP		None
		8	Prairie du Pont Creek, Ill.	B	Riprap on creek bank	Nov. 1965	150	3	SP-SM, SP		None
	Vicksburg	9	Levee from Wasp Lake to Marksville, Miss.	B	Riprap bedding	Oct. 1965, 67	250	5	SP to CH	2½	6
		10	Columbia Lock and Dam, La.	D	Riprap bedding at outlet structure		2,000 riprap 6,000 derrick	0 0	SP to CH	4	9
MRD	Omaha	11	Channel stab., Gerring Valley, Nebr.	A and B	Riprap along channel slopes	1963-64, 66	900	3	ML		None
	Kansas City	12	Flood protection project, Topeka, Kansas	B	Riprap on channel slopes and bottom	Sept. 1968	3,000	<1	CL, ML SP fine		None
NCD	Buffalo	13	Presque Isle Pen., Pa.	B	Bedding of rubble groins	May-Nov. 1965	3,000	0	SP	2½	6
	Detroit	14	Kawkawlin River flood control project, Mich.	B	Riprap around bridge piers	June 1969	150	0	Clayey sand W/G		None
	St. Paul	15	Red Lake Cont. Dam, Clearwater, Minn.	B	Riprap slope protection	Oct. 1968	100	0	SM, SP		None
		16	Channel improvement, Polk and Clearwater Counties, Minn.	A	Riprap slope protection	Oct. 1963	250	3	ML, CL, SM	1½[b]	6[b]
		17	Channel improvement, Russ River, Cass County, N.D.	B	Riprap slope protection	Sept. 1967	150	3	SC	1½[b]	6[b]
		18	Remedial work, Sand Hill River, Polk County, Minn.	B	Fieldstone riprap in drop structure	Oct. 1967	250	2	CL, ML, SM		None
		19	Big Bay Harbor, Marquette County, Mich.	B	Rubble mound breakwater	1968	Core 1,000 Cover 6,000	0	SP		None
		20	Breakwater extension, Houghton County, Mich.	B	Rock berm	July 1968	500	<1	SP		None
NPD	Seattle	21	Libby Dam, Mont.	B	Riprap bedding	1967	10 in.	3	CL	-No. 4	24
ORD	Louisville	22	Temp. Lock and Dam 52, Ohio River, Ill.	B	Riprap slope protection	Dec. 1968	150	3	SP		None
	Pittsburgh	23	Hannibal Lock and Dam, Ohio River, Ill.	A	Riprap slope protection	1966-67	500	2	ML, CL, SM		None
SAD	Charleston	24	Morris Island Spoil Dike, Charleston Harbor, S.C.	B	Riprap bedding	March 1969	300	4	SM-OL w/shell	4	9
	Mobile	25	Lake Douglas, Bainbridge, Ga.	B	Riprap	July 1968	12 in.	0	SC		None
SPD	Sacramento	26	Plt River channel improvement, Modoc County, Calif.	B	Sack concrete	July 1969	1.25 ft^3	0	Unknown		None
SWD	Galveston	27	White Oak Bayou, Houston, Tex.	B	Riprap	1964	15 in.	2	SM, CL		None
	Tulsa	28	Kaw Dam, Ponca City, Okla.	F	Riprap slopes and bottom of diversion channel	1969	2,000	N.D.	SM, SP		None

[a]ACM = articulated concrete mat. [b]Bedding beneath the filter cloth. [c]Cloth Z made by the manufacturer of cloth G.

In one district, cloth A was used to temporarily protect excavated sand slopes from erosion. Surface water ran beneath the cloth and erosion occurred. In this case the cloth did not serve as a filter and is included here only as a matter of record and interest.

Figure 2. Conditions at bridge prior to repair work in 1962 by the Memphis District.

FULL-SCALE FIELD TESTS

Memphis District Tests

The Memphis District (5) has conducted full-scale field tests on cloths A and B in repair work (projects 1 and 2, Table 2) for 2 bridge abutments on the St. Francis River in Arkansas and as a replacement for gravel bedding beneath articulated concrete mattresses and riprap along the Mississippi River (project 3). During the first 3 years after the projects were completed, large scour pockets occurred immediately downstream of the bridges. These pockets extended some 50 ft landward and were 200 to 300 ft long. The scouring extended to the centerline of the approach roads, endangering the bridges. The condition at one bridge, shown in Figure 2, is typical of conditions at the other bridge. The areas had been protected by riprap on a gravel blanket. Repairs were made in 1962 and 1964 in the manner shown in Figure 3. The cloth in 6- and 12-ft widths was placed on the sand fill (medium to fine sand) and graded bank parallel to the water's edge, overlapped 8 in., and secured with 18-in. long pins at 3-ft intervals. As previously stated, 125-lb riprap dropped from 2 ft damaged cloth A, but drops of the

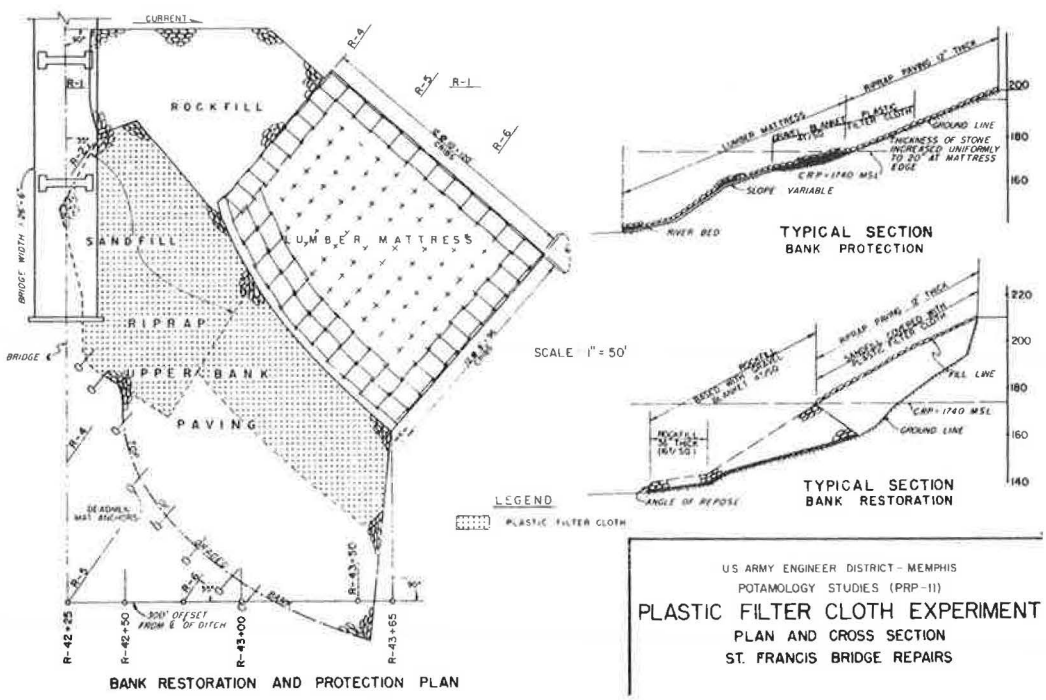

Figure 3. Bridge repair plan.

same weight material from 4 ft did not damage cloth B. The sites were inspected after each high water, and no change occurred in the repaired area. Figure 4 shows the condition of one of the repaired areas during an author's visit in 1969. The area was in excellent condition, as were the other repaired areas. The severity of the attack continuing in unprotected adjacent areas was evident from large scour holes noted in the banks immediately downstream of each repaired area.

Figure 4. Condition of repaired area in 1969.

During an author's visit, riprap was removed from sections of cloths A and B. Although the repaired area as a whole was in good condition, the condition of cloth A was poor. Tears, probably from riprap placement, and holes attributed to abrasion were noted in the cloth. Cloth B was in excellent condition. Samples of both cloths were obtained from the areas and tested at WES. Strength tests indicated there was no apparent deterioration of the fibers since the cloths were installed.

Figure 5 shows a layout of the test site at Island 63 in the Mississippi River near Greenville, Mississippi, where in 1965 filter cloth was placed under riprap and concrete mats in some areas and a 4-in. gravel blanket was used in other areas. The subgrade material was a fine sand. Figure 6 shows cloth B being placed. After the bank had been graded to a 1-on-3 slope, it was covered with two 18-ft wide sections (three 6-ft widths sewed together in the factory) and one 12-ft wide section (two 6-ft widths sewed together in the factory). The field seams perpendicular to the river edge were overlapped 8 in. and secured with 15-in. long pins at 3-ft intervals. The horizontal seams were sewed with nylon twine after it was found that the securing pins did not properly hold in the sand. The lower edge of the cloth was placed 4 ft underwater.

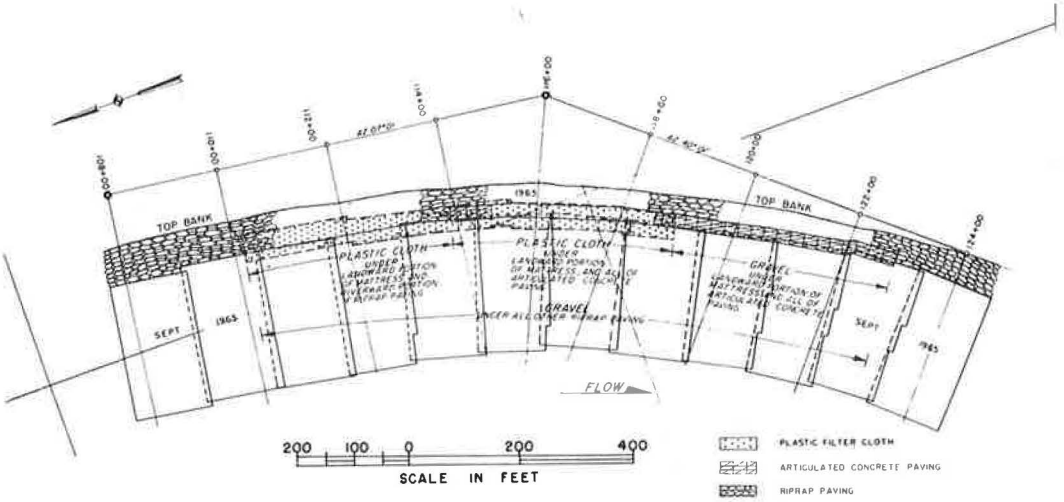

Figure 5. Island 63 test site.

Figure 6. Placement of cloth B at Island 63.

Figure 7. Island 63 revetted area underlaid with filter cloth (range 118+50).

This was accomplished by sewing ¾-in. reinforcement bars in a continuous line along the riverward edge of the cloth and by sewing additional bars (Fig. 6) perpendicular to the water's edge at 20-ft intervals. The cloth was then manually moved into the water. The weight of the rods was not sufficient to keep the cloth from billowing, and it had to be tamped into place. The revetment materials were placed directly on the cloth. The concrete mattresses extended past the filter cloth and granular bedding into the river.

Surveys and inspections were made by the Memphis District after each high-water season. During the first high-water period, scouring occurred in the lower part of the slope where no filter cloth had been placed. Inspections following each of the succeeding 2 high-water periods revealed that scour in the filter cloth area had apparently been stopped by the cloth. In the adjacent area where a gravel filter was used, the scour had progressed up the bank and into the riprap, requiring extensive repairs to the riprap sections. Figure 7 shows the condition of the concrete mattress revetment overlying the filter cloth, and Figure 8 shows the area where gravel filter material was used. It is obvious from a comparison of the 2 photographs that the filter cloth performed in a superior manner to the gravel filter. In the filter cloth area the only noticeable subsidence was at faulty field seams (center of Fig. 7).

Figure 9 shows a condition that existed in the riprap at its intersection with the mat (subsidence in the center of the photo resulted from a faulty field seam). The cloth had been bulging (first noticed in 1968) at the intersection and displacing the riprap. The bulges, 2 to 3 ft high all along the reach, may have resulted from excess pore water pressures being developed in the fine sand and causing the sand to "flow" beneath the cloth. Apparently, the continuous surcharge provided by the mats and their resistance to displacement stopped the migration of sand. If the mats had not been present, the bulging would probably have been more general.

Figure 8. Island 63 revetted area underlaid with gravel bedding (range 123+00).

Figure 9. Island 63 bulged areas.

A sample of cloth adjacent to one of the bulges was removed during an author's visit to the site in 1969. Examination of the underside of the cloth revealed a cake of fines that may have prevented ready drainage from the cloth during falling stages of the river. The inability of the water to drain freely from the cloth could have produced the excess pore pressures that led to the movement of the underlying sand. As data given in Table 1 show, the cloth used (cloth B) had only 5.2 percent open area. A cloth with a greater open area could possibly have prevented such bulging.

The filter cloth appeared to be in good condition with the exception of a few isolated tears near the bulged areas. These tears were probably caused by debris from the river during high-water stages. The cloth in the bulged areas was stretched very tightly, but no fiber ruptures or rips at the factory-sewed seams were noted. Strength tests on samples of the cloth indicated no significant deterioration of the cloth.

Tests Made by Louisiana Department of Highways

The Louisiana Department of Highways, with some assistance from the New Orleans District, made full-scale field tests using cloth B and cloth Z beneath slope protection for a highway fill along the Gulf Coast (6). Figure 10 shows the test section at Holly Beach, Louisiana. The revetted area, 200 ft long, was constructed in January 1968 by using cellular concrete revetment blocks developed in Holland. Each block weighed approximately 14 lb and was about 8 by 8 by 4 in. The in-place revetment had about 30 percent open area obtained by 2-in. diameter holes in the blocks spaced on centers slightly less than 2 in. in both directions. Filter cloths were placed directly on a graded 1-on-3 slope, and the blocks were placed on the cloths. The soil along this stretch of beach is primarily fine sand with some silt and shell fragments. The elevation of the roadway was 7 to 8 ft above mean low water (called mean low gulf). Cloth B was used in constructing the westward 100 ft, and cloth Z was used for the other 100 ft.

In February 1969 a storm hit the area, and wave heights were well above the roadway elevation. The cloth B area failed, while the area in which cloth Z was used remained in place (Fig. 11). Cloth B was apparently lifted or floated out of position (dislodging the overlying block revetment) because water was not able to pass through fast enough to prevent hydrostatic pressures from developing beneath the cloth. Water apparently was able to pass readily through the more open weave of cloth Z. In February 1970 a similar storm hit the area, and the only damage was at the unprotected ends of the revetted area where cloth Z was used.

Samples of both cloths were obtained during an author's visit 1 week after the second storm. Strength tests indicated little if any deterioration of the cloths beneath the revetment. There had been considerable deterioration of both cloths exposed to sunlight since the first storm (1 year), and they could be torn by hand.

Figure 10. Louisiana Department of Highways test section (sand used as dry mortar).

Figure 11. Condition of Louisiana Department of Highways test section after storm (in-place revetment underlaid with cloth Z).

The highway department is satisfied with the performance of cloth Z and the block revetment. A 3-mile stretch of the beach has been revetted by using cloth Z and revetment blocks.

FIELD EXPOSURE TESTS

Cloths A and B have been subjected to field exposure tests at Treat Island, Maine, and at WES since 1964. Strength tests are performed on samples at 6-month intervals to determine the effects of exposure. The cloths at WES are enclosed in a laboratory building; at Treat Island one set of samples is protected from sunlight by an open-sided shed, and another set is covered with about 1 ft of sand. Both sets are under salt water part time because of tide fluctuations resulting in daily freeze-thaw cycles during the winter. There has been no apparent deterioration of either cloth since the tests were initiated.

CONCLUSIONS

The following conclusions were drawn from the results of this study.

1. In all but 2 cases, woven plastic filter cloths have satisfactorily replaced granular filter material. In the 2 cases where the performance of the cloths was not entirely satisfactory, the problem was attributed to the cloth not allowing free drainage. In both cases, it is believed that cloths C and G or similar cloths would have performed satisfactorily.
2. Nonwoven filter cloths or woven cloths with less than 4 percent open area should not be used where silt is present in sandy soils. Filtration tests on cloth G indicated that a cloth with an EOS equal to the No. 30 sieve and an open area of 36 percent would retain sands containing silt. Cloth G had the most open weave of any considered. Consequently, no laboratory or field data are available to provide guidance for the use of cloths having more open weaves.
3. When stones or rubble are to be dropped directly on the cloth, the minimum tensile strengths (ASTM Method D 1682) in the strongest and weakest directions should not be less than 350 and 200 lb respectively. Elongation at failure should not exceed 35 percent. The minimum burst strength (ASTM D 751-66T) should be 520 psi. When extreme care is used in placing stones or the cloth is used in applications not requiring high strengths or abrasion resistance, these strength requirements may be relaxed.
4. Cloths made of polypropylene, polyvinylidene chloride, and polyethylene fibers do not appear to deteriorate under most conditions. However, all of the cloths evaluated were affected to some degree by sunlight and consequently should be protected from direct sunlight in permanent installations.
5. When filter cloths are used to wrap collector pipes or in similar applications, backfill should consist of clean sands or gravels graded such that the 85 percent size of the backfill material is equal to or greater than the EOS of the cloth. When trenches are lined with filter cloth, the collector pipe should be separated from the cloth by at least 6 in. of granular filter material.
6. Cloths should be made of monofilament yarns, and the absorption of the cloth should not exceed 1 percent. These 2 requirements reduce the possibility of the fibers swelling and, thus, changing the EOS and percentage of open area.

REFERENCES

1. Barrett, R. J. Use of Plastic Filters in Coastal Structures. Proc. 10th Internat. Conf. on Coastal Engineering, Tokyo, Sept. 1966.
2. Calhoun, C. C., Jr. Investigation of Plastic Filter Cloths. U.S. Army Engineer Waterways Experiment Station, Vicksburg, Miss., Tech. Rept., in preparation.
3. Calhoun, C. C., Jr. Summary of Information From Questionnaires on Uses of Filter Cloths in the Corps of Engineers. U.S. Army Engineer Waterways Experiment Station, Vicksburg, Miss., Misc. Paper S-69-46, Oct. 1969.

4. Information provided by B. C. Beville, Soil Conservation Service, U.S. Department of Agriculture, Orlando, Florida.
5. Fairley, J. G., Easley, R. T., Bowman, J. H., and Littlejohn, B. J. Use of Plastic Filter Cloths in Revetment Bank Paving. U.S. Army Engineer District, Memphis, Potamology Investigation Rept. 21-4, June 1970.
6. Cox, A. L. Paving Block Study. Louisiana Department of Highways, Baton Rouge, Res. Proj. 68-6H(B), 1970.

RESPONSE OF CORRUGATED STEEL PIPE TO EXTERNAL SOIL PRESSURES

Reynold K. Watkins and Alma P. Moser,
Utah State University

Full-scale external load testing of buried corrugated steel pipes shows the structural performance limits of the soil-pipe system. The tests, sponsored by the American Iron and Steel Institute, indicate that the 3 most important factors influencing performance are the yield point strength of the pipe wall, the soil compressibility (determined primarily by soil density), and the ring flexibility of the pipe. The empirical relationship of these 3 factors is plotted on a graph from which it is possible to design buried corrugated steel pipes.

• SINCE corrugated steel pipes first appeared on the market about 70 years ago, their use as buried conduits has increased phenomenally. The structural success of these pipes is due to the flexibility of the pipe ring. As soil is placed over the pipe the ring is flattened; i.e., the ring is depressed vertically and expanded horizontally. The horizontal expansion develops lateral soil support on the sides, and this gives rigidity to the ring and strengthens it. The vertical depression of the ring relieves the ring of soil pressure concentrations and forces the soil to take part of the vertical load in arching action over the pipe. Thus the soil protects the pipe.

The discovery of this complementary soil-structure interaction has led to innumerable tests and continual observation. Four independent design criteria have evolved from these tests and observations (the Appendix contains a further discussion of these criteria): (a) excessive ring deflection (flattening of the pipe), (b) longitudinal seam strength, (c) ring compression strength (crushing or buckling of the pipe wall), and (d) handling strength (for shipping and installation) sometimes called flexibility factor.

All 4 design criteria have been used successfully. Proponents of each have provided a method of analysis and have suggested allowable limits. The first three are conservative enough so that, if design is within the limit specified for any one criterion, adequate performance is ensured. Most designers check more than one design criterion, however, and base design on the worst case. For the vast majority of all installations, such design is too conservative. However, a few exceptions suggest the need for reevaluation of design methods.

There are other reasons for reevaluation. These 4 design criteria do not include the interaction of 2 or more criteria. They are based on many assumed properties of materials that cannot be measured by the designer. One recourse is to pull a recommended value out of a graph or table based on other unmeasured properties. Soil properties are particularly troublesome. Consequently, they are often rounded up by guess or are abandoned within the comfortable confines of a large safety factor. This is really abandonment of the problem because soil is generally the most important factor in the soil-pipe interaction phenomenon. The allowable limits of design are unreasonably restrictive under some circumstances such as excellent backfill. Every user has to decide which design criteria to adopt. Often the appropriate criterion for design is unknown.

Sponsored by Committee on Subsurface Structures Design and presented at the 50th Annual Meeting.

For these reasons the 4 design criteria have been reevaluated within the past 3 years by the Federal Highway Administration, the American Association of State Highway Officials, and the American Iron and Steel Institute. With considerable cooperation and effort, design criteria, pertinent properties of materials, and design limits were agreed on. All 3 agencies have since published similar design procedures. In general the procedures are easy to use. However, they should be checked for precision and for design limits. Pertinent properties of materials should be verified and the significance of their influence ascertained—especially soil properties. The interaction of the design criteria should be determined. These are the objectives of this study. A test program at Utah State University was funded from 1967 to 1971 by the American Iron and Steel Institute to accomplish these objectives.

The study does not include live loads with minimum soil cover. It does not include longitudinal phenomena such as beam deflection or shearing stresses due to longitudinally nonuniform soil settlement.

TEST CELL

Basically the project comprises the testing to failure of full-scale corrugated steel pipes by applying vertical soil pressure. Sections of pipe 20 ft long and up to 5 ft in diameter are buried in soil within a large test cell (Fig. 1). The vertical soil pressure is applied by 50 hydraulic rams—5 on each of 10 load beams. The total load capacity is about 5 million lb. The maximum vertical soil stress at the level of the top of the test pipe is 20,000 lb/ft^2.

The height of soil cover over the top of the pipe is 1 pipe diameter. Consequently, failure is not a localized "punching through" of surface loads (like wheel loads).

The test cell is a horizontal cylinder of $\frac{5}{8}$-in. steel plate 22 ft long, 15 ft wide, and 18 ft high. The basic cross section is approximately elliptical with horizontal radius of curvature 3 times the vertical. This minimizes boundary effect. As an embankment of average soil is increased in height, the ratio of vertical to horizontal stress is roughly 3:1. The 3:1 stress ratio is maintained by the 3:1 ratio of radii in the steel shell. Moreover, the flexible plate does adjust to different stress ratios by changing curvature during loading. Tests on different pipe diameters from 1 to 5 ft prove that boundary effect is of secondary importance in determining ring strength. Even when combined with other secondary (extraneous) variables, the probable deviation is at most 10 percent and that only in loose soil. (Other variables include the nonuniformity of load under the hydraulic jacks and wedging out of soil on either end of the test cell.) Such a deviation is statistically insignificant compared with combined deviations in ring stiffness, yield point, soil density, and soil placement techniques. In field installations the deviations due to boundary effect and soil placement techniques are even greater (viz., trench wall slopes, trench wall compressibility, types of compactors, and proximity to pipe).

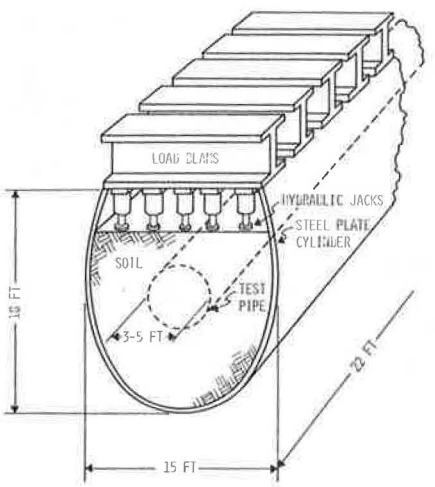

Figure 1. Test cell.

Test sections of pipe are buried as in average embankment installations. Embankment installation was selected over trench installation because ordinarily failure in an embankment occurs at less soil cover than does failure in a trench. Therefore the embankment tests are conservative for design. Tested in the series were 130 sections of pipe.

Probably the worst soil that could be selected for testing is liquid (viscous mud). This was not considered in these tests because (a) the phenomenon is understood [the design of cylinders subjected to external fluid pressure is classical (1)], and (b) for most installations "liquid" soil is not acceptable as a fill. For example, clay would be avoided even though placed dry (dry side of op-

timum moisture content) if it could become saturated later. Organic material (humus or peat) is not to be included as soil in this report.

The next worst soil that could be selected for testing is highly compressible soil. Such was selected for these tests. It is basically fine sand with 18 percent silt, a trace of clay, and a small fraction of sand. The 100 percent dense unit weight is 130 lb/ft^3. (Density is based on modified AASHO T-180.) It bulks easily and can be placed as loosely as 65 percent standard density. When loose it is highly compressible. If used as backfill in field installations, it should be carefully compacted. Placement techniques such as washing into place or end dumping are not adequate for this soil. Because of the high compressibility when loose, it provides a broad range of soil compressibility for testing purposes.

Figure 2. Loading the cell.

TEST PROCEDURE

The pipe to be tested was instrumented with several fluid-filled pressure gages around the circumference to measure soil pressure against the pipe during the test. A soil bedding was prepared, and the pipe was located in the cell. Soil was then carefully compacted about the pipe in approximately 1-ft lifts (Fig. 2). If loose soil was desired, no compaction was employed. If medium dense soil was required, a Wacker vibroplate made 1 pass over each lift. If dense soil was required, compaction was by Wacker rammer compactors at optimum moisture content (Fig. 3). In-place density tests were conducted by the sand displacement method in several of the lifts.

After the cell was loaded with soil, steel plates were placed on the top of the soil. The beams were then lowered and locked into place (Fig. 4). The hydraulic rams

Figure 3. Technique for compacting the backfill in 1-ft lifts.

Figure 4. Loading beams being lowered into position where they are pinned before load is applied to cell (top), and test cell loaded and ready for test to begin (bottom).

exerted force on the steel plates. This procedure prevented penetration of the hydraulic rams into the soil and produced a more uniform loading.

A profile instrument was mounted inside the pipe to determine the ring profile at any time during the test. During each test the following readings were noted at various intervals: (a) hydraulic ram pressure—this was later converted to vertical soil pressure, (b) pressure readings from pressure gages around pipe circumference, (c) vertical ring deflection, (d) horizontal ring deflection, and (e) ring profile. In addition to these readings any pipe distress noted by technicians inside the pipe was recorded. Also, photographs of most of the tests were made by using both elapsed time photography and still shots.

Most of the pipes tested were in diameters of 3, 4, and 5 ft. Corrugation depths of 1, 0.5, and 0.25 in. were tested. Both annular and helical corrugations were tested. The seams of the annular pipes were of 2 types: spot-welded and riveted. The helical pipes had a lock seam joint.

RESULTS OF TESTS

The most significant results of the tests are shown in Figure 5. The ordinate is apparent ring compression strength f_c. It is defined as the apparent ring compression stress at performance limit; i.e.,

$$f_c = PD/2A \text{ at performance limit} \qquad (1)$$

where (Fig. 6)

P = apparent vertical soil pressure, i.e., calculated pressure at the level of the top of the pipe if no pipe were in place,
D = nominal diameter of the pipe, and
A = cross-sectional area of the pipe wall per unit length of pipe.

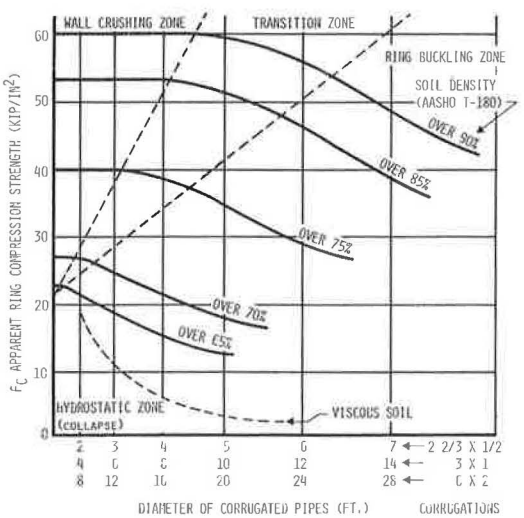

Figure 5. Apparent ring compression strength as a function of ring flexibility and soil compressibility (density) based on performance limit of incipient ring failure (probable deviation, i.e., 50 percent uncertainty, is about half the spacing between curves; curves apply to corrugated steel pipes with yield point of 40 ksi).

Performance limit is ring deformation beyond which the soil-pipe system does not perform adequately. It is discussed in the Appendix.

To design the pipe ring, one can employ the well-known, universal design criterion STRESS < STRENGTH, i.e.,

$$PD/2A = f_c/N \qquad (2)$$

where

P = apparent vertical soil pressure, (i.e., calculated pressure at the level of the top of the pipe if no pipe were in place) that compromises dead load DL and live load LL, i.e., P = DL + LL;
DL = γH or unit weight of soil γ times the height of fill H over the top of the pipe;
LL = vertical soil pressure at the level of the top of the pipe due to surface loads;
f_c = apparent ring compression strength that can be simply picked off the plots (Fig. 5); and
N = safety factor.

The ordinates f_c shown in Figure 5 are values of apparent ring compression strength

to be used in design. The abscissas shown in Figure 5 are values of ring flexibility of the pipe. Ring flexibility is determined almost entirely by the depth of corrugation and the nominal diameter as shown. The parameter distinguishing the various curves is soil density in percentage of modified AASHO T-180. Soil compressibility is the single most important soil property. Soil density is the single most important factor determining compressibility. In fact, other soil properties become secondary (insignificant) within the average deviations of soil density and boundary conditions (trench, zone of compaction, and bedding) resulting from present-day installation techniques.

The data shown in Figure 5 are based on a performance limit referred to as incipient ring failure. Incipient ring failure is defined as a ring deformation beyond which the ring would continue to deform (to collapse) if loads on it were not relieved by soil-arching action. Actually incipient ring failure is not complete failure of the soil-pipe system. The pipe does not collapse. Any increase in external pressure is supported by the soil in arching action. Incipient ring failure is recognized by completely developed plastic hinges on the sides of the pipe or by reversal of curvature of the wall or by seam separation. The Appendix contains a further discussion.

The minimum specified yield strength of culvert steel is 33,000 lb/in.^{2} with values being about 40,000 lb/in.^{2} (40 ksi) for these tests. Figure 5 shows a maximum apparent ring compression strength higher than the 40 ksi yield point. Actually the well-compacted soil is supporting part of the vertical pressure in arching action (a low-grade masonry arch). As the pipe ring begins to be distressed, it deforms and relieves itself of part of the external pressure so actual stress in the pipe wall does not exceed yield point. The ring compression strength (ordinate) shown in Figure 5 is called apparent for this reason.

When the soil is relatively incompressible (densely compacted), the apparent ring compression strength is essentially constant depending on yield point strength or longitudinal joint strength or (more probably) the interaction of both. In Figure 5 this is shown as the wall-crushing zone.

When the soil is relatively compressible (loose or poorly compacted), the apparent ring compression strength is reduced significantly because of pressure concentrations on the ring and because of ring deflection that causes flexural stress in addition to compression stress in the wall. Figure 5 shows that strength envelopes drop down as soil density decreases.

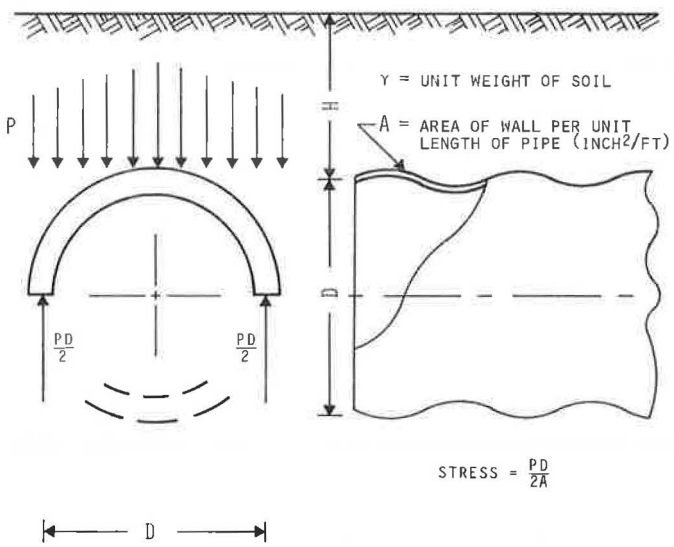

Figure 6. Free body diagram of pipe ring with vertical soil pressure.

It is noteworthy that the strength envelopes dip down to the right with increasing ring flexibility. This is due to the increased sensitivity of the very flexible ring to nonuniform soil density. If the soil could be placed particle by particle, the strength envelopes would not dip down so much (especially in well-compacted soil). However, present soil-placement techniques result in nonhomogeneous soil that causes pressure spots and precipitates wall-buckling in the very flexible rings. This is shown as the ring-buckling zone.

STRUCTURAL DESIGN OF PIPE RING

Suppose that a 48-in. diameter $2\frac{2}{3}$- by $\frac{1}{2}$-in. corrugated steel pipe is to be installed under 120 ft of soil embankment. The soil about the pipe is to be compacted to 90 percent modified density (found to have a unit weight of about 120 lb/ft^3). Determine the pipe wall thickness (gage) if the performance limit is defined as incipient ring failure (Fig. 5). Suppose that H20 loading will pass over the surface. If control of the installation is dubious, a safety factor of N = 2 will be assumed.

The apparent vertical soil pressure on the pipe ring is

$$P = DL + LL = 14.4 \text{ kip/ft}^{-2}$$

where

DL = γH = 120 lb/ft^{-3} x 120 ft, and
LL = negligible (2).

The apparent ring compression stress is

$$PD/2A = \left[14.4 \text{ kips } (4.0 \text{ ft})\right]/ft^2 2A = 28.8 \text{ kips/A ft}$$

The apparent ring compression strength is (based on 40 ksi yield point)

$$f_c = 60 \text{ kips/in.}^{-2}$$

which is the ordinate to the strength envelope shown in Figure 5 corresponding to soil density of 90 percent and a pipe diameter of 4.0 ft in a $2\frac{2}{3}$ by $\frac{1}{2}$ corrugation. (Where the yield point is something other than 40 ksi, the apparent ring compression strength f_c would be modified proportionally.) Equating stress to strength divided by safety factor yields

$$PD/2A = f_c/N$$

or

$$28.8 \text{ kips/A ft} = 60 \text{ kips/2 in.}^2$$

Solving for the area yields A = 0.96 $in.^2/ft$. One should use 12-gage steel that has an area of 1.356 $in.^2/ft$ (3).

A check on ring deflection would predict a ring deflection of less than 3 percent at a soil density of 90 percent (4).

The ring flexibility factor (handling factor) is adequate.

CONCLUSIONS

The most pertinent criteria for the structural design of the soil-ring system for buried corrugated steel pipes are included in the empirical strength envelopes shown in Figure 5. Design is simply the equating of stress to allowable strength (design limit), i.e., $PD/2A = f_c/N$.

The stress PD/2A is apparent ring compression stress in the pipe wall; i.e., it is based on a vertical soil pressure P at the level of the top of the pipe if no pipe were in place. f_c/N is the design limit. N is an appropriate safety factor. The apparent strength

f_c is apparent ring compression strength; i.e., it is treated as ring compression stress at failure. Actually f_c includes more than just ring compression. It takes into account the soil-arching action in dense soil and the soil pressure concentrations. It also takes into account ring deflection in compressible soil and wall-buckling of very flexible pipes. It accounts for the formation of plastic hinges and seam failures.

In general the soil is the most important factor in determining f_c. The single most important soil property is soil compressibility, which is basically a function of soil density. Density is the most basic soil property or index for relating the performance of different soil types.

The second most important factor in determining f_c is the yield point of the steel. This is usually within fairly narrow limits (33 to 40 ksi).

The third factor is ring stiffness.

All other factors are of lesser importance and for most installations are secondary and not significant compared to soil density, yield point of steel, and ring stiffness. The total range of influence of secondary factors is less than the probable deviation of the 3 important factors.

A reasonable performance limit of buried corrugated steel pipes for most installations is incipient ring failure. It is defined as that ring deformation beyond which the ring would continue to deform if external loads on it were not relieved by arching action of the soil. If this performance limit is used, the arching action of soil becomes an additional safety factor. Thus protection against collapse is ensured.

The data shown in Figure 5 apply to all types of soil that can be compacted and held at a specified density. This would exclude expansive soils such as humus and highly expansive clay. Clay may be more compressible when saturated than when dry. If wet clay were conceivably used as backfill, the lower curve shown in Figure 5 could be helpful as a conservative limit for design. The dotted hydrostatic curve applies to liquid (viscous) soil. Saturated clay with any shearing strength will fall above the hydrostatic curve. Ordinarily if clay has been placed at a density well above critical void ratio (85 percent density), it is so impervious that saturation is too slow to be a problem (if saturation can proceed at all). If saturation proceeds slowly enough, soil cohesion develops and decreases compressibility enough to offset the increase of compressibility due to the water. In other words, the compressibility of densely compacted, confined clay is usually not increased as moisture moves into it if the load is constant.

After the ring is designed by use of curves shown in Figure 5, the ring deflection may be checked if there is any question about excessive ring deflection. The ring flexibility factor (handling factor) should be checked if there is any question.

Seam strength seems to be independent of the type of seam used in these tests. Welded, riveted, and lock seam seams were tested. All performed adequately. It is recommended that welded and riveted longitudinal seams not be placed in the 10 and 2 o'clock positions in the pipe if design is near performance limit. This recommendation is made because riveted or welded seams in these positions can trigger premature reversal of curvature. However, the loss of strength due to improper seam placement was observed to be less than 10 percent.

REFERENCES

1. Timoshenko, S. Strength of Materials, Part II, 3rd Ed. D. Van Nostrand, 1956, pp. 186-193.
2. Handbook of Drainage and Construction Products. Armco Drainage and Metal Products, Inc., 1955, p. 22.
3. Handbook of Steel Drainage and Highway Construction Products. American Iron and Steel Institute, New York, 1967, pp. 17, 21, and 250.
4. Welded Steel Water Pipe Manual. Steel Plate Fabricators Association, Inc., 1970, p. 24.

Appendix

CRITERIA USED TO DESIGN BURIED CORRUGATED STEEL PIPES

Four independent criteria used in the past to design buried corrugated steel pipes grew out of a need for design criteria and represent 4 structural limitations in corrugated steel pipes.

1. Excessive ring deflection (flattening of the pipe) in some installations led to research at Iowa State University that resulted in the development of the Iowa ring deflection formula (5).
2. The strength of longitudinal seams proved to be important in design. The soil pressure on the pipe (2) determines the ring compression that can be equated to the seam strength (3) reduced by an appropriate safety factor.
3. The ring compression stress in large pipes may not necessarily exceed the seam strength, yet it can be high enough to cause elastic buckling of the pipe wall (6). This has led to a method of design based on reversal of curvature of the ring.
4. A pipe must be handled during transport to the job, and it must withstand distorting pressures during backfilling. This consideration requires a reasonably stiff pipe as quantified by a handling and installation factor called a ring flexibility factor (3).

PERFORMANCE LIMITS

The performance limit of a buried corrugated steel pipe ring is deformation—that deformation of the ring beyond which the system can no longer perform the purpose for which it was designed. If an unacceptable hump or dip or crack develops in the soil surface above the pipe, performance limit is exceeded. If the flow characteristics of the pipe are reduced below designed values because of ring deformation, performance limit is exceeded. The final definition of performance limit must be left up to the design engineer.

For most installations the definition of performance limit is incipient ring failure as shown in Figure 5. Incipient ring failure is defined as some deformation of the ring beyond which the ring would continue to deform (to collapse) if loads on it were not relieved by arching action of the soil. This is an arbitrary performance limit. It does not mean collapse. The proposed strength envelopes shown in Figure 5 become a design chart for this performance limit. The strength envelope for dense soil exceeds the yield point for steel because part of the vertical soil pressure is supported by the soil in arching action. An additional safety factor is "built in" because the ring does not collapse even though it is deformed to incipient ring failure.

The performance limit for buried corrugated steel pipes is not a single phenomenon, but the interaction of a number of phenomena. For example, performance limit is not simply crushing of the wall or buckling of the wall or shearing of the longitudinal seam or ring deflection. Each of these influences one another, and all are interrelated to varying degrees under varying circumstances. As might be anticipated, the crushing strength of the wall is less if the ring deflection is large. This is due to flexural stresses. A longitudinal seam in one panel causes a stress concentration in the wall of the adjacent panel and triggers wall-crushing. Of course, as wall-crushing develops, wall-buckling is initiated, and buckling near seams causes seam failure—truly an interaction phenomenon.

In every case, performance limit is a ring deformation, observable inside the pipe. The probable deviation in observing performance limits may be as much as 10 percent of vertical soil pressure—especially near critical void ratio. The following are some deformations identified as performance limits in these tests.

Wall-Crushing

When the pipe is buried in densely compacted soil (denser than critical void ratio), wall-crushing is often the first indication that performance limit has been reached. Slight dimpling of the corrugations is the first visual indication of distress. Dimpling is not a performance limit, but dimpling portends the location of general wall-crushing

(Fig. 7). This crushing usually occurs between 10 and 2 o'clock in the ring. Deep corrugations dimple as soon as or sooner than shallow corrugations, but general wall-crushing shows up at equal or slightly higher pressures. In general, wall-crushing develops as shown in Figure 8. It starts with a dimpling of the corrugations and progresses into an accordion effect.

Reversal of Curvature

As the load increases, a section of the ring may tend to flatten and then reverse curvature (Fig. 9). There are 2 general types of reversal of curvature. In the case of very loose soil (density less than critical void ratio), as the soil is compressed downward the pipe tends to form an ellipse but, in so doing, high flexural stresses develop at the sides. These stresses combined with some ring compression cause plastic hinges. If this deformation is carried to the extreme, the top of the pipe comes down in a reversal of curvature and ultimately a third plastic hinge forms in the top center.

The other type of reversal occurs in dense soil and may be referred to as localized buckling. This is not confined to top center. It usually forms between 10 and 2 o'clock, but not necessarily so. Occasionally the reversal occurs in the bottom between 5 and 7 o'clock (Fig. 10). None has been seen in the sides between about 2 and 5 o'clock or 7 and 10 o'clock.

Performance limit for deep corrugations tends to be plastic hinges at the sides rather than reversed curvature. For shallow corrugation, plastic hinges at the sides form only if the soil is very compressible; otherwise, performance limit is reversal of curvature. The difference is insignificant in light of uncertainties in soil placement, density, or boundaries.

Seam Separation

Seam separation is complex shearing, tearing, pulling through, and bearing all at once. There is no question about identifying seam separation; the question is usually what triggers seam separation. For example, in the case of the helical

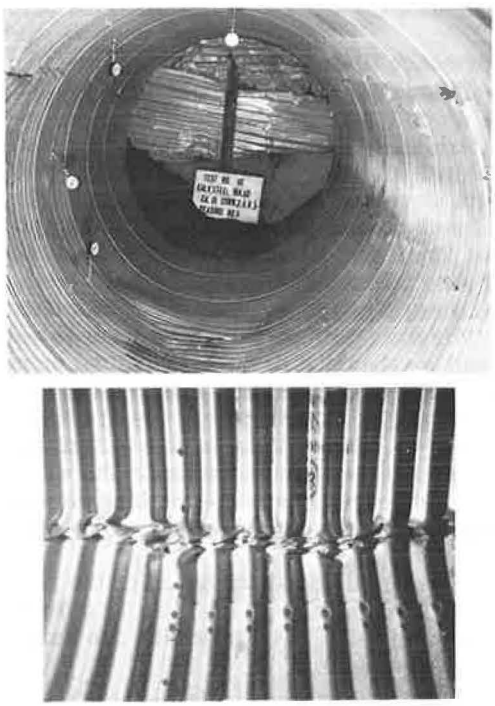

Figure 7. General wall-crushing at 10 and 2 o'clock in test with dense soil where tendency to wall-crushing is visible at 4 o'clock (top) and wall-crushing at 2 o'clock is shown in close-up (bottom), but integrity as a pipe is still maintained.

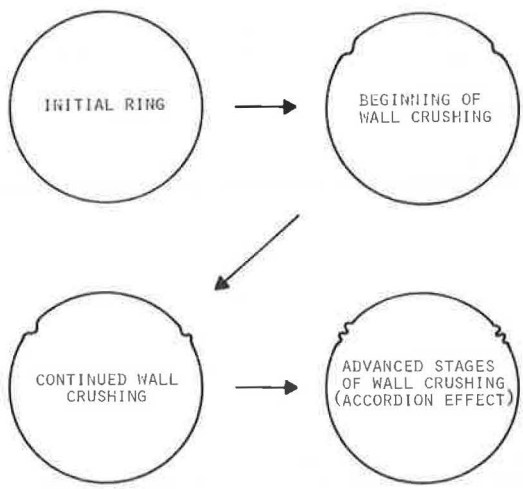

Figure 8. Mechanism of wall-crushing.

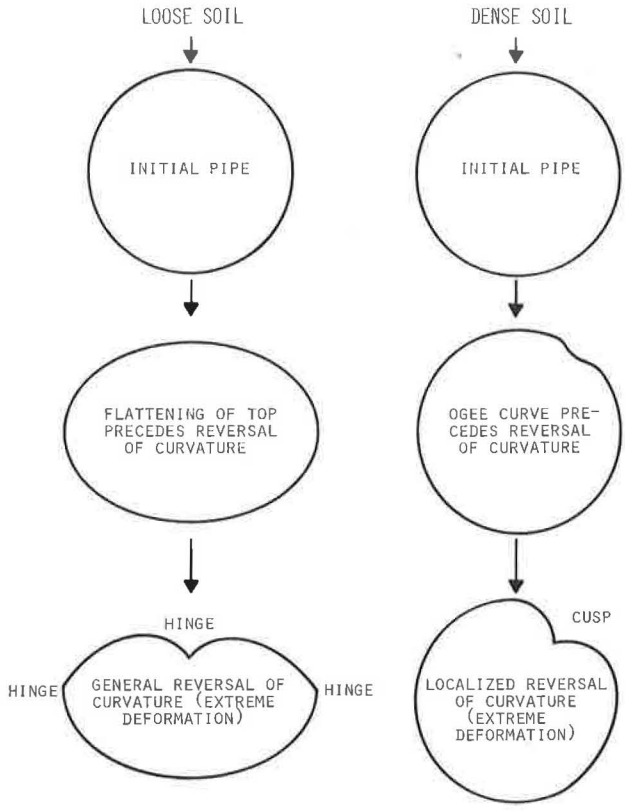

Figure 9. Comparison of types of reversal of curvature observed in dense and loose soil.

Figure 10. Pipe wall buckled at invert in dense soil (this is exceptional, for buckling is usually between 10 and 2 o'clock).

lock seam when a reversal of curvature commences, and more especially as it develops into a cusp, the seam at the cusp tends to open. All of the standard seams tested performed adequately. Differences were insignificant.

In all cases, it is important to note that dimpling of the crests of the corrugations is not a performance limit. Neither is slipping of joints. These should be accepted as stress relievers.

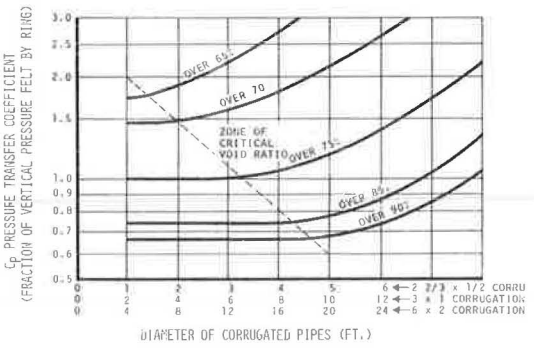

Figure 11. Test values of pressure transfer coefficient C_p as a function of soil density, diameter, and corrugation configuration.

PRESSURE TRANSFER COEFFICIENT

Figure 5 can be redrawn in the form shown in Figure 11. The basic difference is in the definition of apparent ring compression stress and strength. Figure 11 shows that the strength is the nominal yield point strength of the steel (such as 33 ksi). The stress is $C_p(PD/2A)$ where C_p is the pressure transfer coefficient. C_p is read from Figure 11. Design proceeds as before; i.e., stress = strength/N. This design method has one advantage in that the nominal yield point of steel can vary. For Figure 5, the nominal yield point of steel is fixed at 40 ksi. For extreme ranges of yield point, Figure 11 should be checked empirically.

References

5. Spangler, M. G. Soil Engineering. Internat. Textbook Co., 1960.
6. Corrugated Metal Pipe Culverts. Bureau of Public Roads, U. S. Department of Commerce, 1966, pp. 6-7.

Discussion

M. G. Spangler, Engineering Research Institute, Iowa State University

When laboratory procedures are employed to study the performance of a field prototype structure, it is essential that the experimental specimen be mounted and loaded in such a manner and in such an environment that its action, in all respects, will be analogous to the normal action of its counterpart under service conditions. It is the opinion of this writer that the Utah tests, described by Watkins and Moser, fail to comply with this essential criterion, and the reported results are, therefore, applicable only to those specific pipe specimens that were used in the tests. The results cannot be generalized and validly applied to the vast majority of installations of corrugated steel pipes under normal service conditions. Any similarity between the structural action of the Utah test pipes and that of actual pipes under earth embankments is purely coincidental.

Normally a buried flexible pipe is bedded on soil of some degree of compressibility. Soil fill is then placed on each side of the pipe up to its top, after which a soil embankment is constructed up to a finished grade. The basic structural action of the pipe is as follows: As the side fills are placed, the active lateral earth pressures cause a limited amount of negative pipe deflection; that is, the horizontal diameter decreases and the vertical diameter increases. When the side fills reach the horizontal plane through the top of the pipe, called the critical plane, additional increments of fill cause the pipe to deform positively, the horizontal diameter increasing and the vertical diameter decreasing. As the horizontal diameter increases, the sides of the pipe push

outward against the side fills, and this movement mobilizes the passive resistance pressure of the soil. These passive pressures, acting on each side of the pipe, very greatly influence the deformation or change in shape of the pipe and the magnitude and character of stresses in the pipe wall. An essential characteristic of the installation of this type of structure is that the interaction between the soil and the pipe be free and uninhibited by extraneous forces or unnatural barriers to the operation of the flexible character of the pipe. The pipe should "float free" in its surrounding soil environment.

In the Utah tests, corrugated steel pipes were artificially loaded in a cell consisting of heavy steel plates located 1 pipe diameter out from each side of the pipe. These plates were backed up by concrete retaining walls that contributed to the rigidity of the sides of the cell. There is little doubt in this writer's mind that confinement of the pipes between these side walls served to inhibit the normal flexible action characteristics of corrugated steel pipe under an earth embankment. It is as though a 60-in. flexible culvert pipe were installed in a canyon with vertical rock side walls only 15 ft apart. Such an installation certainly would not qualify as typical of the vast majority of corrugated steel pipe culverts in highway or railway construction.

In addition to the lateral restraining influence of the steel plate and concrete side walls of the load cell, the pipes were further restrained in a vertical direction by the action of hydraulic jacks reacting against heavy steel beams that extended transversely across the top of the cell and that were anchored to the steel plates of the side walls. The vertical loads from the hydraulic rams were transmitted to the soil backfill surface, 1 diameter above the top of the pipe, through steel plates. It is doubtful whether such a load system would adequately simulate the load of an actual soil embankment. Furthermore, because of the concave configuration of the steel plates, it is probable that the vertical upward reactions of the cross beams caused horizontal components of force to be directed toward the specimen pipes. All in all, it appears that the pipes were encased in a straitjacket that prevented their normal action as flexible structures in which pipe deflections bring about redistribution of stresses and deformations within the soil. Such interaction and redistribution are the hallmarks of flexible pipe action, and they contribute greatly to the efficiency of this type of structure.

Another circumstance that polarizes and restricts the applicability of the test results is the kind of soil with which the pipe was surrounded in the test cell. Only one soil type was used, a "fine sand with about 18 percent silt, a slight fraction of sand, and a trace of clay." Such a soil, when compacted, would be very stiff and strain resistant. It would contribute to the rigidity of the pipe environment that prevailed during the tests.

The authors show a free body diagram of the top half of a vertically loaded corrugated steel pipe (Fig. 6). This free body diagram is incomplete. When a statically indeterminate structure is cut on any section, the stresses acting on the section are a thrust, a moment, and a shear, as shown in Figure 12b. Equations for these stresses around the periphery of a corrugated metal pipe are given at the end of this discussion. The radial shear is a finite stress but is of minor magnitude and can be neglected in consideration of the action of the pipe, but the bending moment is very real and cannot be ignored. It would appear that in the construction of their free-body diagram the authors have fallen into the same error as the proponents of White and Layer's compression ring theory (8), in which bending moment in the pipe wall is completely ignored and left out of consideration. The authors give an expression for stress in the pipe wall in the form

$$\sigma = pD/2A \qquad (3)$$

where

σ = stress in pipe wall,
p = unit load on pipe,

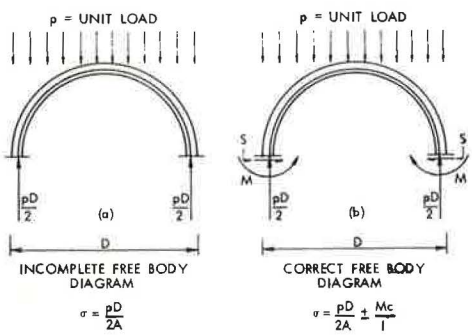

Figure 12. Free body diagrams of pipe.

D = diameter of pipe, and
A = cross-sectional area of pipe wall.

The correct expression for stress is

$$\sigma = pD/2A \pm Mc/I \quad (4)$$

where

M = bending moment in pipe wall,
c = distance from neutral axis to outer fiber, and
I = moment of inertia of cross section through pipe wall.

The validity of the principle of combined direct stress and bending stress is well documented by the strain measurements made by Scheer and Willett (9) in connection with the reconstruction of the Wolf Creek culvert.

It is important to take into account the bending moment in a flexible pipe for 2 principal reasons. First, it is associated with deflection of a pipe. Anyone who has walked through a corrugated steel pipe and observed the deformation of the pipe in relation to its original shape will recognize that the pipe wall is subjected to bending moment. Also it is important in connection with the design of bolted longitudinal seams. Such seams are subjected to a combination of tangential thrust and moment. The thrust causes stress in bolts or rivets at the seam in single shear, while the moment generates a prying action that may throw some of the fasteners into direct tension, so that the stress in the bolts is a combination of shear and tension. The present widespread practice of designing a bolted seam on the basis of its strength in single shear alone is workable only because of the application of a high factor of safety that masks the effect of combined shear and tension. But sometimes this procedure is not successful, as witness the extensive seam failures of the Wolf Creek culvert in Montana (10).

Bending moment in the pipe wall causes outer fiber stresses at the peaks of the corrugations, and these may very readily exceed the yield stress of the metal, even at moderate pipe deflections. The writer agrees with the authors that this circumstance is not detrimental to the performance of the pipe, unless, of course, the stress increases to the ultimate. The regions of such overstress are limited to short sections of the pipe perimeter at the top, bottom, and 2 sides. The plastic strains in these regions serve only to augment the deflection of the pipe. This, in turn, augments the development of passive resistance pressures and contributes to the overall strength of the pipe-soil system. It is also important to note that the load on a buried conduit is a one-shot affair that does not fluctuate widely, except possibly when the earth cover is very shallow and a substantial part of the load is attributable to surface traffic.

The authors devote considerable space to a discussion of performance limits for corrugated steel pipe, and the importance of this subject is obvious. Much of their discussion appears to be based on the performance of the experimental pipes of the Utah tests. The writer believes that the place to look for evidence on which to base design limits is in the field, by examination of the performance of actual pipes in service under actual soil embankments. Some field observations have revealed 2 major types of phenomena that contribute to failure of this kind of structure, although the term "failure" has not been defined completely or satisfactorily. These phenomena are (a) excessive deflection of the pipe ring, or (b) distress in longitudinal seams either by failure of the bolt fasteners or by failure of the pipe metal due to bending moment stress in the vicinity of a seam, or (c) both of these. A secondary type of distress may develop at transverse joints when adjacent rings deflect differentially.

Photographs of corrugated steel pipes in actual service are shown in Figures 13, 14, 15, and 16. Deflections in these pipes were excessive. Figures 17, 18, and 19 show excessive distress at the longitudinal seams, due both to bolt failure and to tension failure of the pipe metal adjacent to a seam. In the case of another pipe in which a seam failure was observed, many of the bolts pulled apart; whether they did so by shear or tension or a combination of these stresses could not be determined. In this case, the seam failures were relatively short in length and the pipe retained its essentially circular shape. The separated plates were jacked back together and welded. These

Figure 13. Complete collapse of 96-in. pipe.

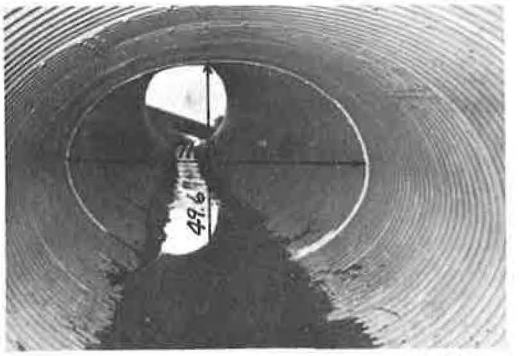

Figure 14. Excessive deflection of 60-in. pipe.

Figure 15. Excessive deflection of 84-in. storm sewer pipe.

Figure 16. Failure of transverse joint in pipe shown in Figure 15.

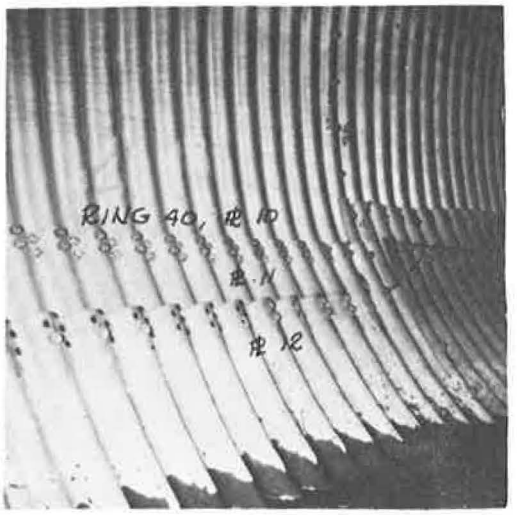

Figure 17. Longitudinal seam failure and circumferential deformation.

Figure 18. Failure of transverse joint due to differential deformation of adjacent rings.

repairs were satisfactory from a structural standpoint but, of course, the spelter coating in the vicinity of the welds was ruined.

The authors place considerable emphasis on the phenomenon of wall-crushing. In their tests it began with a "dimpling" of the wall, usually at 10 and 2 o'clock, then proceeded to an advanced stage of an accordion-like folding effect. The writer has neither seen nor heard of a similar phenomenon in the case of a structure under field loading. It is the writer's opinion that this type of effect was primarily induced by the unnatural and excessive confinement of the pipe test specimens provided by the shape and rigidity of the side walls of the load cell, by the hydraulic jacks, and by the unyielding type of soil backfill. Such confinement and restraint inhibited ring deflection and greatly increased tangential thrust that led to the crushing phenomenon.

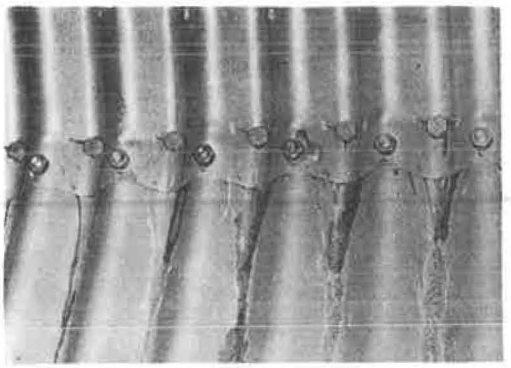

Figure 19. Tension failure due to bending moment at longitudinal seam.

The authors introduce a factor called the "pressure transfer coefficient" designated by the symbol, C_p. This coefficient is multiplied by the weight of a soil column above the horizontal plane through the top of the pipe in order to obtain the load on the pipe. It is a purely empirical factor, whose values have been determined from the test results with a single soil type in several states of density. The experimental results are shown in Figure 11, which is purported to be a widely applicable design diagram.

It is the writer's opinion that the Marston Theory (5, ch. 24; 11) of loads on buried conduits provides a more appropriate means of determining the earth load on a buried pipeline, regardless of whether it is a rigid or flexible type. Marston developed a theoretically sound method of evaluating the load transfer by arch action from or to the column of soil above the pipe, to or from the columns of soil immediately adjacent thereto. As shown in Figure 20, if the side columns of soil settle less than the interior column, that is, if the top of the pipe moves downward more than the critical plane, a part of the weight of the interior column is transferred by arch action to the exterior columns, and the load on the pipe is less than the weight of the interior column. If the reverse situation prevails, that is, if the critical plane settles more than the top of the pipe, as shown in Figure 21, an inverted arch action takes place, and additional load

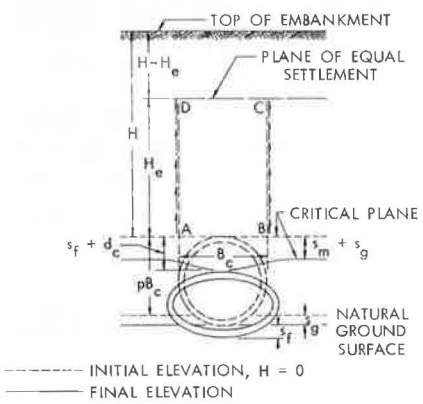

Figure 20. Negative settlement ratio for incomplete ditch condition.

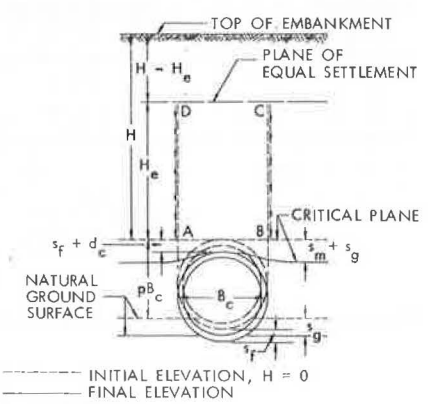

Figure 21. Positive settlement ratio for incomplete projection condition.

is transferred to the interior column and to the pipe. A neutral or transition case occurs when the critical plane and the top of the pipe settle downward the same amount, as shown in Figure 22. In this case no arch action develops and the load on the pipe is equal to the weight of the interior column.

The Marston load equation is

$$W_c = C_c w B_c^2 \tag{5}$$

where

W_c = load on conduit per unit of length,
C_c = calculation coefficient,
w = unit weight of soil, and
B_c = outside width of conduit.

The value of the coefficient C_c is a function of the ratio of the height of embankment to the width of the conduit, H/B_c, and of the product of the settlement ratio times the projection ratio. The projection ratio is equal to the distance from the natural ground surface to the critical plane, divided by B_c, as indicated in Figures 20, 21, and 22. It can be determined from the geometry of a proposed pipe installation. Values of C_c may be taken from data shown in Figure 23.

The settlement ratio is equal to the difference between settlement of the top of the conduit and the adjacent critical plane, divided by the compression strain of the pB_c column of soil. It is indicated by the formula

$$r_{sd} = \left[(s_g + s_m) - (s_f + d_c)\right] / s_m \tag{6}$$

where

r_{sd} = settlement ratio,
s_m = compression strain of columns of soil pB_c,
s_g = settlement of the natural ground surface adjacent to the conduit,
$(s_m + s_g)$ = settlement of the critical plane,

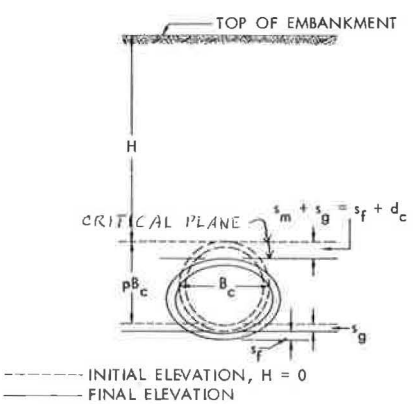

Figure 22. Zero settlement ratio for equal settlements.

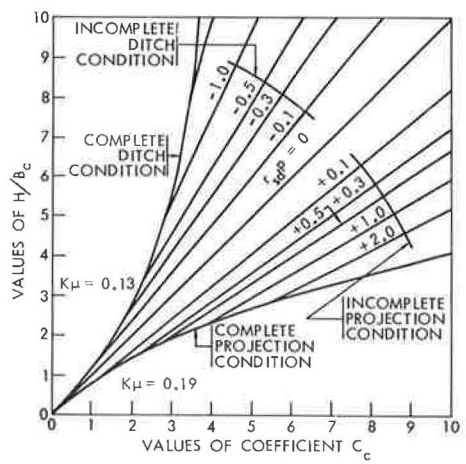

Values of C_c in terms of H/B_c

Incomplete Projection Condition Kμ = 0.19		Incomplete Ditch Condition Kμ = 0.13	
r_{sdP}	Equation	r_{sdP}	Equation
+ 0.1	$C_c = 1.23H/B_c - 0.02$	- 0.1	$C_c = 0.82H/B_c + 0.05$
+ 0.3	$C_c = 1.39H/B_c - 0.05$	- 0.3	$C_c = 0.69H/B_c + 0.11$
+ 0.5	$C_c = 1.50H/B_c - 0.07$	- 0.5	$C_c = 0.61H/B_c + 0.20$
+ 0.7	$C_c = 1.59H/B_c - 0.09$	- 0.7	$C_c = 0.55H/B_c + 0.25$
+ 1.0	$C_c = 1.69H/B_c - 0.12$	- 1.0	$C_c = 0.47H/B_c + 0.40$
+ 2.0	$C_c = 1.93H/B_c - 0.17$		

Figure 23. Diagram for coefficient calculation.

s_f = settlement of the conduit foundation,
d_c = shortening of the vertical height of the conduit, and
$(s_f + d_c)$ = settlement of the top of the conduit.

Examination of Eq. 5 and Figure 23 reveals that, when r_{sd} is negative, the load on the pipe is less than the weight of the overlying column of soil; when it is positive, the load is greater than the weight of the soil column; and when it is zero, the load is equal to this weight.

Although the settlement ratio is completely rational in the development of the Marston Theory, it cannot be evaluated for a particular culvert in advance of construction without extensive soil tests and computations, which are expensive and impractical. It is, therefore, considered to be a semi-empirical constant, usable values of which can best be determined by observation of the settlements and environmental characteristics of actual conduits. In this respect it is similar to many such semi-empirical constants that are prevalent in engineering practice, as, for example, the coefficient of roughness in the Manning Formula for hydraulic flow. A very few field measurements (11) of the settlement ratio for flexible conduit installation have been made. Those few indicate support for the currently widespread practice of designing flexible culverts to carry the weight of the overlying column of soil, that is, assuming that the settlement ratio is equal to zero. Many more field measurements are needed before the determination of a design load on this type of conduit can be considered to be on a reliable basis.

When the load to which a flexible conduit will be subjected in service has been determined, it is possible to estimate the probable deflection of the pipe and stresses in the pipe wall by means of the Iowa formula and the associated stress formulas (1, 5). The Iowa formula is

$$\Delta X = D_1 \left[(KW_c r^3)/(EI + 0.061\, E' r^3)\right] \qquad (7)$$

where

ΔX = horizontal deflection (vertical deflection is essentially the same),
D_1 = deflection lag factor,
W_c = load on pipe per unit length,
K = bedding width factor,
r = radius of pipe,
E = modulus of elasticity of pipe material,
I = moment of inertia of cross section of pipe wall,
E' = er, modulus of soil reaction, and
e = modulus of passive resistance of soil.

The deflection lag factor is an empirical quantity that was introduced into the deflection equation as a result of observations of the fact that pipe deflection sometimes continues to develop for a substantial period of time after the maximum load is applied. It results from a yielding of the soil at the sides of the pipe in response to continuing pressure between the pipe and the soil. Values of this factor are related to the strain-resistant characteristics of the side fill soil. For loose soil the lag factor is relatively high. For dense well-graded soil it is essentially unity and can be ignored.

Although Watkins, the principal author of the paper, played a major role in the refinement and revision of the Iowa formula in 1957 (12, 13), he has since repudiated it. In a document dated February 21, 1970, he stated (14): "In fact, I don't accept the Iowa Formula as an adequate method for predicting deflection of pipes...because the Iowa Formula has not predicted precisely the deflection in pipes in the field and generally speaking the Iowa Formula has predicted more deflection than has been measured...." Presumably he has field data on which this repudiation is based, but the writer has not seen it. The extent to which the statement is true merely reflects the state of uncertainty relative to design values of E' and D_1, coupled with the desire of most designers to be conservative in a situation in which specific information is scarce. The writer does not share the author's lack of confidence in the deflection formula, when appropriate

values of the various factors are employed, although it is known that some people in the corrugated steel pipe industry agree with his statement.

When the Iowa Formula was developed, field experiments with flexible pipes under actual embankments indicated the validity of the concept of a modulus of soil reaction, and they yielded some specific values of this factor for a very limited number of soils. Since publication of the equation, its application to actual situations (9) has revealed that this modulus varies over a very wide range—from as little as 234 psi to as much as 8,000 psi, a 34-fold variation. The soil properties that influence this factor are somewhat obscure although qualitatively it is certain that texture and density characteristics are of prime importance. Probably moisture content is also influential.

Several investigators have attempted to determine the modulus of soil reaction E' by direct laboratory measurements, but without success. Spangler and Donovan (15) tried in 1957. Watkins and Nielsen (16) later developed the Modpares device (acronym for modulus of passive resistance) for this purpose in 1964. Nielsen (17) developed a correlation between modulus of soil reaction and soil properties, particularly the CBR, but this correlation has not been widely tested. The writer's conclusion from these attempts is that E', like the settlement ratio, should be treated as a semi-empirical constant.

The writer's appraisal of the current situation with respect to the design of flexible culvert pipes is that we have available theoretically sound procedures for estimating loads and predicting deflections and stresses in a proposed structure by means of the Marston Theory, Spangler's Iowa Formula, and associated stress equations. The practical application of these theories is hampered at the present time by lack of reliable values of certain semi-empirical constants, such as the settlement ratio, the deflection lag factor, and the modulus of soil reaction.

The best way and, in fact, the only reliable way to obtain usable values of these constants is to mount a massive program of study and measurement of a large number of actual flexible pipe conduits in the field at the time they are being constructed and subsequent thereto. It is recommended that the American Iron and Steel Institute, the Federal Highway Administration, the Corps of Engineers, the Aluminum Pipe Industry, the various state highway departments, and other interested parties undertake such a program. The data for each installation should include—in addition to the height of fill, the size of pipe, the gage of metal, and the type, depth, and spacing of corrugations—(a) the pipe bedding; (b) the projection ratio; (c) a complete description of the soil, particularly its texture, density, and moisture content; (d) settlements of the top of the conduit; (e) settlements of the critical plane and the natural ground surface; (f) deflections of the pipe both during construction and for a period of time after completion; (g) load on the pipe either reliably estimated or measured; and (h) all additional pertinent data that may become available during and after construction. With a complete record of the environment and performance of a large number of individual installations, encompassing many soil types at various densities, good reliable values of the semi-empirical constants needed for design of this type of structure will become available.

References

7. Spangler, M. G. The Structural Design of Flexible Pipe Culverts. Eng. Research Institute, Iowa State Univ., Bull. 153, 1941.
8. White, H. L., and Layer, J. P. The Corrugated Metal Conduit as a Compression Ring. HRB Proc., Vol. 39, 1960, pp. 389-397.
9. Scheer, A. C., and Willett, G. A., Jr. Rebuilt Wolf Creek Culvert Behavior. Highway Research Record 262, 1969, pp. 1-13.
10. Spangler, M. G. General Discussion of Kraft, A. N., and Eagle, H. L., Design Features of an 18.5-Foot Diameter Culvert Installation in Montana and Data on Subsequent Failure, and Macadam, J. N., Research on Bolt Failures in Wolf Creek Structural Plate Pipe, Highway Research Record 144, 1966, pp. 42-50.
11. Spangler, M. G. Field Measurements of the Settlement Ratios of Various Highway Culverts. Eng. Research Institute, Iowa State Univ., Bull. 170, 1950.
12. Watkins, R. K. Characteristics of the Modulus of Passive Resistance of Soil. Iowa State Univ., PhD thesis, 1957.

13. Watkins, R. K., and Spangler, M. G. Some Characteristics of the Modulus of Passive Resistance of Soil: A Study in Similitude. HRB Proc., Vol. 37, 1958, pp. 576-583.
14. Watkins, R. K. Deposition in the Action of Sanford Construction Company Versus Kaiser Aluminum and Chemical Sales, Inc. U.S. District Court, Eastern District of Kentucky, Feb. 21, 1970.
15. Spangler, M. G., and Donovan, J. C. Application of the Modulus of Passive Resistance of Soil in the Design of Flexible Pipe Culverts. HRB Proc., Vol. 36, 1957, pp. 371-381.
16. Watkins, R. K., and Nielsen, F. D. Development and Use of the Modpares Device. Jour. Pipeline Div., Proc. ASCE, Jan. 1964.
17. Nielsen, F. D., Bhandhausavee, C., and Yeb, K. Determination of Modulus of Soil Reaction From Standard Soil Tests. Highway Research Record 284, 1969, pp. 1-12.

Appendix

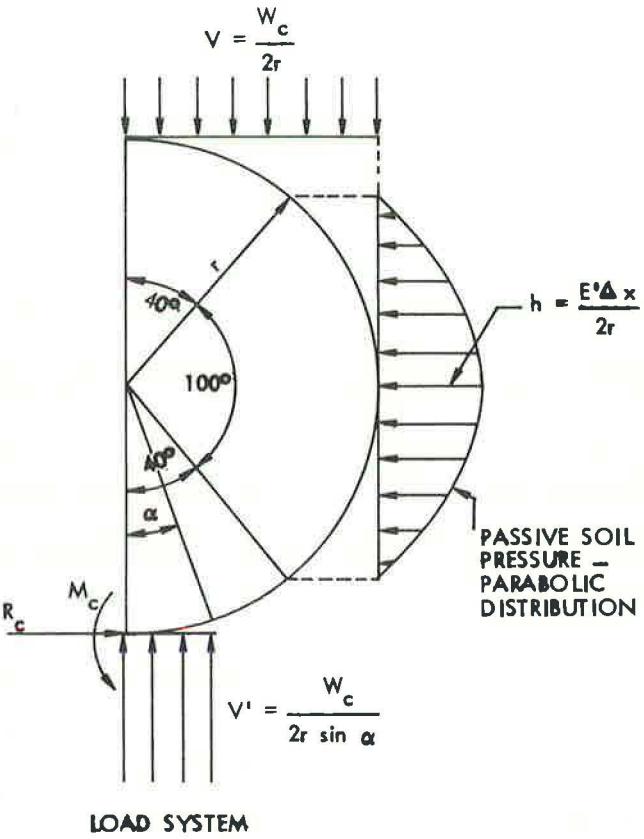

LOAD SYSTEM

Deflection Formula

$$\Delta x = D_1 \frac{KW_c r^3}{EI + .061E'r^3}$$

α	K
0	0.110
35^{o}	0.100
60^{o}	0.090

Moment and thrust at bottom of pipe due to horizontal load:

$$M_c = -0.166\ hr^2 \qquad R_c = 0.511\ hr$$

Moment and thrust at bottom of pipe due to vertical load:

$$M_c = AW_c r \qquad R_c = BW_c$$

α	A	B	sin α
0	0.294	0.053	0
15	0.234	0.050	0.259
30	0.189	0.040	0.500
45	0.157	0.026	0.707
60	0.138	0.014	0.866

Moment, thrust and shear due to vertical load:

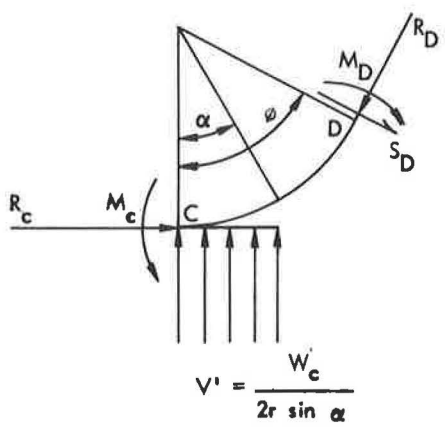

$$0 \leq \phi \leq \alpha$$

$$M_D = W_c r \left[A + B\,(1 - \cos\phi) - 0.250\,\frac{\sin^2\phi}{\sin\alpha} \right]$$

$$R_D = W_c \left(0.500\,\frac{\sin^2\phi}{\sin\alpha} - B\cos\phi \right)$$

$$S_D = W_c \left(0.500\,\frac{\sin\phi\cos\phi}{\sin\alpha} - B\sin\phi \right)$$

$$\alpha \leq \phi \leq 90^\circ$$

$$M_D = W_c r \left[A + B(1 - \cos\phi) - 0.50\sin\phi + 0.25\sin\alpha \right]$$

$$R_D = W_c \left(0.500\sin\phi + B\cos\phi \right)$$

$$S_D = W_c \left(0.500\cos\phi - B\sin\phi \right)$$

$$90^\circ \leq \phi \leq 180^\circ$$

$$M_D = W_c r \left[A + B(1 - \cos\phi) - 0.25\,(1 + \sin^2\phi - \sin\alpha) \right]$$

$$R_D = W_c \left(0.50\sin^2\phi + B\cos\phi \right)$$

$$S_D = W_c \left(0.50\sin\phi\cos\phi - B\sin\phi \right)$$

Moment, thrust and shear due to horizontal load:

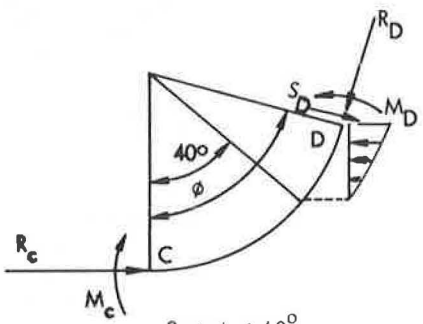

$$0 \leq \phi \leq 40^\circ$$

$$M_D = hr^2(0.345 - 0.511 \cos \phi)$$

$$R_D = 0.511 \, hr \cos \phi$$

$$S_D = 0.511 \, hr \sin \phi$$

$$40^\circ \leq \phi \leq 140^\circ$$

$$M_D = hr^2(0.199 - 0.500 \cos^2\phi + 0.143 \cos^4\phi)$$

$$R_D = hr(\cos^2\phi - 0.568 \cos^4\phi)$$

$$S_D = hr(\sin \phi \cos \phi - 0.568 \sin \phi \cos^3\phi)$$

$$140^\circ \leq \phi \leq 180^\circ$$

$$M_D = hr^2(0.345 + 0.511 \cos \phi)$$

$$R_D = - 0.511 \, hr \cos \phi$$

$$S_D = 0.511 \, hr \sin \phi$$

Combine stresses due to vertical and horizontal loads algebraically.

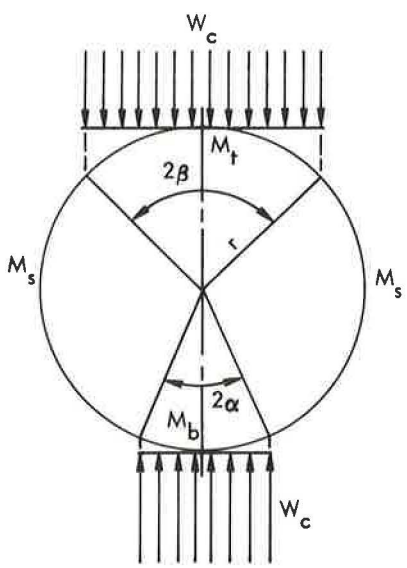

MOMENTS: $M = KW_c r$

DEFLECTIONS: $\Delta = K \dfrac{W_c r^3}{EI}$

USE: K_b FOR MOMENT AT BOTTOM
K_t FOR MOMENT AT TOP
K_s FOR MOMENT AT SIDES
K_x FOR HORIZONTAL DEFLECTION
K_y FOR VERTICAL DEFLECTION

2β, deg.	2α, deg.	K_b	K_t	K_s (neg.)	K_x	K_y
	0	0.318	0.318	0.182	0.137	0.149
	30	0.259	0.317	0.180	0.135	0.146
	60	0.213	0.312	0.175	0.130	0.138
0	90	0.182	0.305	0.168	0.122	0.129
	120	0.162	0.299	0.161	0.116	0.122
	150	0.153	0.295	0.156	0.111	0.117
	180	0.150	0.294	0.153	0.110	0.116
	0	0.317	0.259	0.180	0.135	0.146
	30	0.257	0.257	0.178	0.133	0.143
	60	0.211	0.252	0.173	0.127	0.135
30	90	0.180	0.246	0.166	0.120	0.127
	120	0.160	0.240	0.159	0.114	0.119
	150	0.151	0.236	0.154	0.109	0.115
	180	0.148	0.235	0.152	0.108	0.113
	0	0.312	0.213	0.175	0.129	0.138
	30	0.252	0.211	0.173	0.127	0.135
	60	0.207	0.207	0.168	0.122	0.127
60	90	0.175	0.201	0.161	0.115	0.118
	120	0.156	0.194	0.154	0.109	0.111
	150	0.146	0.190	0.149	0.104	0.107
	180	0.143	0.189	0.147	0.103	0.105
	0	0.306	0.182	0.168	0.122	0.129
	30	0.246	0.180	0.166	0.120	0.127
	60	0.201	0.175	0.161	0.115	0.118
90	90	0.169	0.169	0.154	0.108	0.110
	120	0.150	0.163	0.147	0.101	0.103
	150	0.140	0.158	0.142	0.097	0.098
	180	0.137	0.157	0.140	0.096	0.096
	0	0.299	0.162	0.161	0.116	0.122
	30	0.240	0.160	0.159	0.114	0.119
	60	0.194	0.156	0.154	0.109	0.111
120	90	0.163	0.150	0.147	0.101	0.103
	120	0.143	0.143	0.140	0.095	0.096
	150	0.134	0.139	0.135	0.091	0.091
	180	0.131	0.138	0.133	0.089	0.089

2β, deg.	2α, deg.	K_b	K_t	K_s (neg.)	K_x	K_y
	0	0.295	0.153	0.156	0.111	0.117
	30	0.236	0.151	0.154	0.109	0.115
	60	0.190	0.146	0.149	0.104	0.107
150	90	0.158	0.140	0.142	0.097	0.098
	120	0.139	0.134	0.135	0.091	0.091
	150	0.129	0.129	0.129	0.086	0.086
	180	0.126	0.128	0.128	0.085	0.085
	0	0.294	0.150	0.153	0.110	0.116
	30	0.235	0.148	0.152	0.108	0.113
	60	0.189	0.143	0.147	0.103	0.105
180	90	0.157	0.137	0.140	0.096	0.096
	120	0.138	0.131	0.133	0.089	0.089
	150	0.128	0.126	0.127	0.085	0.085
	180	0.125	0.125	0.125	0.083	0.083

Richard A. Parmelee, Northwestern University

The basis and keystone of the highly simplified method for the design of corrugated steel pipe as presented by the authors is the apparent ring compression strength f_c. The values of this empirical parameter were obtained from full-scale tests utilizing 1 type of soil and 130 pipe sections ranging in size from 3- to 5-ft diameters, and for 3 different corrugation configurations. These f_c values are shown in Figure 5 and are related to the curves shown in Figure 11.

Because these curves assume such a major role in the application of the proposed design method, the writer would like to inquire about the rationale of their construction. The validity of the curves is strongly dependent on the distribution of the 130 data points from the test results. However, in the absence of a graphical display or a discussion and statistical description of the dispersion of these points, the implications and significance of the curves shown in Figures 5 and 11 become suspect. The proper significance of the curves could be easily evaluated by the reader if the authors would present information concerning the distribution of the data points with respect to soil densities, corrugation configurations, and pipe diameters.

For purposes of this discussion the essential features shown in Figures 5 and 11 have been reproduced and are shown in Figures 24 and 25 respectively. Each figure has been subdivided into 4 zones as noted along the top of the figure. The upper bounds for zones I, II, and III are determined on the basis of the scale value for a 5-ft diameter pipe for each of the 3 corrugation configurations tested. The significance of these bounds is that they correspond to the maximum diameter of pipe tested in the investigation. Thus, it appears that no test data were obtained for establishing the shape of the design curves in zone IV. Consequently, these curved portions of the diagrams are shown as dashed lines in Figures 24 and 25.

Below the abscissa in the 2 figures are bar scales with tick marks indicating the 3 diameters of the test pipe (3, 4, and 5 ft) for each of the 3 corrugation configurations studied. The scale for the test pipe having the 6 by 2 corrugation extends over only a small portion of the diameter scale of zone I. In contrast, the bar scales for the test pipe having 3 by 1 and $2\frac{2}{3}$ by $\frac{1}{2}$ corrugations cover almost the entire range of zones II and III respectively. Thus, the basis for establishing the shape of the design curve within zones I, II, and III is dependent on only 1 corrugation configuration; no overlapping of test data for different corrugations was possible. The authors state, "It is noteworthy that the strength envelopes dip down to the right with increasing flexibility." Figures 24 and 25 show that the greatest amount of "dipping" occurs in the dashed curves in zone IV.

The authors also remark, "Corrugation depths of 1, 0.5, and 0.25 in. were tested." A knowledge of the distribution of the 130 test pipes with respect to corrugation configuration and diameter is of extreme importance. This is especially true for the case of the $2\frac{2}{3}$ by $\frac{1}{2}$ corrugation because these data are used to establish the behavior of the curves in zone III. This 1 zone occupies the major portion of the diagram representing regions for which test data were obtained. Consequently, this zone serves the unique function of establishing the basis for the dramatic changes in the slopes of the design curves and possibly justifying the extrapolation of the curves to larger pipe diameters.

The writer would like to inquire as to the statistical basis of the design curves; i.e., What are the correlation coefficient, standard deviation, and the standard error of the estimate of the f_c curves shown in Figure 5?

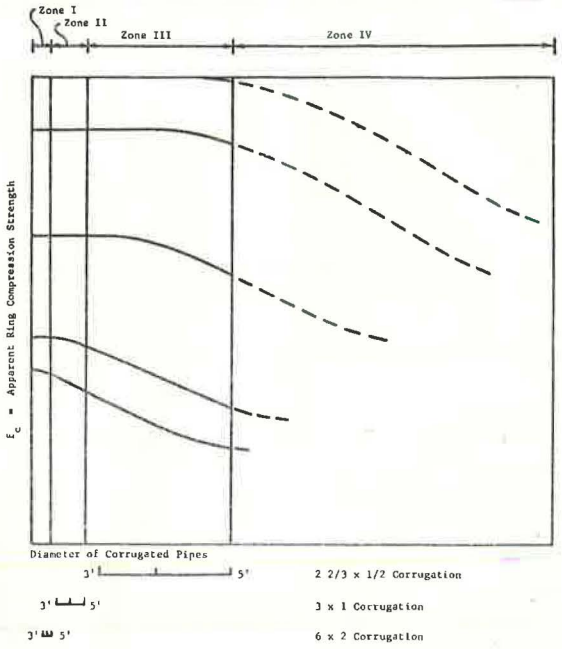

Figure 24. Apparent ring compression strength from Figure 5.

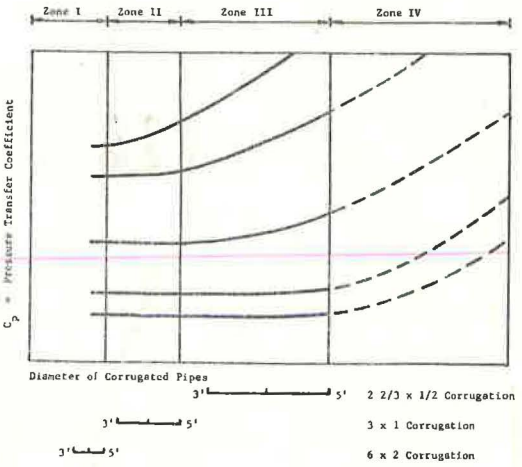

Figure 25. Pressure transfer coefficient from Figure 11.

AUTHORS' CLOSURE

The basic method proposed for designing corrugated steel pipes is the method of apparent ring compression strength. Empirical ring compression strength must exceed the calculated ring compression stress. The method is widely used and understood. It applies to standard culvert steel (33,000 to 40,000-psi yield point) and so does not raise the academic question concerning performance of conduits of much higher or much lower yield points.

A more general design method, suggested in the last section of the Appendix, is based on yield point strength. In this case the ring compression stress is modified by a pressure transfer coefficient. Both methods are simple to use. When corrugated steel culverts of extremely high or extremely low yield point are manufactured, additional charts can be prepared to provide the apparent ring compression strength.

As the paper indicates, the apparent ring compression strength provides automatic correction for flexural stress in the wall, relative compressibility of the soil and pipe, and effect of seams in standard corrugated steel pipes.

The test cell was designed to duplicate field conditions. The elliptical shape of the cell was selected to maintain soil stresses of P vertical and P/3 horizontal. The cell was calibrated by placing soil pressure gages at several locations in the soil and then loading the cell. The calibration gave vertical soil pressure anywhere in the cell as a function of the applied load. Using the calibration data, we presented the apparent ring compression strength envelopes as a function of the pressure at the top of the pipe if no pipe were in place.

The first tests were run without placing steel loading plates on top of the soil. Some penetration resulted, so plates were introduced. However, the load at the performance limit was not significantly affected by the use or absence of loading plates.

The concrete retaining walls were constructed only to hold the flexible cell in its approximate elliptical shape during soil placement. The flexible cell is drawn away from the concrete retaining walls during pressure loading of the test cell. Actual tests to determine the boundary effect of the cell on pipes of different diameters show that boundary effect exists but is not significant compared with other pertinent variables. The most conservative (lowest) strength envelope for various diameters is plotted for each soil density. The conservative test cell boundaries are adequate when one contemplates field boundary conditions. In the field, how compressible is the bedding?

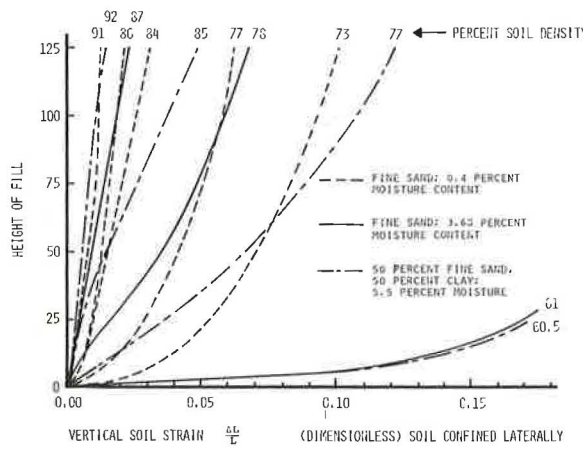

Figure 26. Typical soil compression diagram for different soil types at different densities (tests were modified consolidation tests).

How uniform is the trench cross section? How homogeneous is the boundary soil? How uniform is the fill soil?

In the selection of test pipes, the very flexible rings were achieved by special $2\frac{2}{3}$ by $\frac{1}{4}$ corrugations (up to 5 ft diameter) that extend the ring flexibility values out to the equivalence of a 10-ft diameter pipe in the standard $2\frac{2}{3}$ by $\frac{1}{2}$ corrugation. Similarity is ensured. In this way the full plots are based on actual test data.

The test soil was selected because of the broad range of densities to which it can be compacted. It was found that the most important soil property in the performance of buried flexible conduits is soil compressibility, E′. A better term is soil stiffness. Soil stiffness is affected mostly by soil density. Figure 26 shows a few typical vertical compression diagrams for different soil densities. The 2 most important observations from this figure are that (a) soil density is more important than any other variable (including soil type) in determining the soil stiffness E′ (slope of secant to some curve at some given height of fill) and that (b) the diversity of compression diagrams points out the reality that soil is complex, and different soils do not perform exactly the same. Many variables (soil friction angle, Poisson's ratio, and moisture content in sand) must be handled as secondary soil properties. Fortunately the total range of variation of these secondary soil properties is less significant (has less effect on performance) than the probable deviation due to soil density and soil placement techniques. Moreover, even though the soil is important in buried conduit performance, it is only 1 of 2 components in the system. The conduit also influences performance and contributes to the standard deviation.

Granted that soil stiffness E′ is the most important soil property, soil stiffness is not quickly and easily determined. On the other hand, soil density is understood. It can be determined rapidly by standard techniques in the field as a control during the placement of backfill. Greater sophistication is probably not justified under the variability of common installation techniques. In the future it may become possible to select and place the soil with such homogeniety that E′ and even additional soil properties will become significant.

For soil placed at density greater than critical void ratio, and excluding wet soil with a substantial fraction of fines (such as viscous soil), soil density is the most important criterion of soil stiffness E′. Any exceptions to the density criterion would be a very special type of soil. For example, a spongy soil (high organic content) would be more compressible (less stiff) than granular soil at the same percentage of density because of rebound. However, highly organic soil would be suspect as backfill. If used, a special test would be advisable. Viscous soil (mud) is another exception, but a conduit in viscous soil would be analyzed by classical theories for collapse.

The Marston-Spangler method of ring design is based on many empirical observations (settlement ratio, bedding angle, lag factor, plane of equal settlement, projection ratio, and modulus of passive resistance). Because of the difficulty of obtaining some of the empirical values, the Marston-Spangler method does not lend itself to easily understood and usable design. All of these empirical variables are really functions of more basic variables such as soil stiffness (soil density), ring stiffness, yield point, and soil placement techniques. So why not use the more basic variables—especially when they are measurable?

In the future as the soil properties as well as conduit materials are controlled within close tolerances, highly theoretical computer methods for analysis will take over. However, if performance limit is deformation, the soil does not perform as an elastic medium. Shearing planes develop, and for analysis the inclusion of friction angle and soil cohesion is required. The precise analyses of the future must include Poisson's ratio and the anisotropy and nonhomogeniety that result from soil compaction. Essential also will be the effect of time lag in soil consolidation and the trench or embankment boundary conditions. Near the conduit, where compaction is so difficult, the effect of compaction is most critical. Installations of the future may well include a special compressible backpacking about the conduit.

Until soil control and placement techniques justify such precision, the statistical, empirical design procedure proposed here is the most realistic approach.